

THE INFECTION DYNAMICS, CO-INFECTION, MULTI-GENE PHYLOGENY, AND
MOLECULAR SCREENING OF *PLASMODIUM CAPRAE* INFECTION IN GOATS AND
MOSQUITO SPECIES



A Dissertation Submitted in Partial Fulfillment of the Requirements
for the Degree of Doctor of Philosophy in Veterinary Science and technology

FACULTY OF VETERINARY SCIENCE

Chulalongkorn University

Academic Year 2022

Copyright of Chulalongkorn University

พลวัตของการติดเชื้อการติดเชื้อร่วม มัลติอินไฟโลจินีและการตรวจหาเชื้อ
พลาสมาเดียมคาปริโนแพะและไนยุง



วิทยานิพนธ์นี้เป็นส่วนหนึ่งของการศึกษาตามหลักสูตรปริญญาวิทยาศาสตรดุษฎีบัณฑิต
สาขาวิชาวิทยาศาสตร์ทางการสัตวแพทย์และเทคโนโลยี ไม่สังกัดภาควิชา/เทียบเท่า
คณะสัตวแพทยศาสตร์ จุฬาลงกรณ์มหาวิทยาลัย
ปีการศึกษา 2565
ลิขสิทธิ์ของจุฬาลงกรณ์มหาวิทยาลัย

Thesis Title THE INFECTION DYNAMICS, CO-INFECTION, MULTI-GENE
PHYLOGENY, AND MOLECULAR SCREENING OF *PLASMODIUM*
CAPRAE INFECTION IN GOATS AND MOSQUITO SPECIES

By Miss Hoang Lan Anh Nguyen

Field of Study Veterinary Science and technology

Thesis Advisor Associate Professor Dr. MORAKOT KAEWTHAMASORN, Ph.D.

Thesis Co Advisor Associate Professor Dr. Masahito Asada, Ph.D.

Accepted by the FACULTY OF VETERINARY SCIENCE, Chulalongkorn University in Partial
Fulfillment of the Requirement for the Doctor of Philosophy

..... Dean of the FACULTY OF VETERINARY
SCIENCE
(Professor Dr. SANIPA SURADHAT, Ph.D.)

DISSERTATION COMMITTEE

..... Chairman
(Assistant Professor Dr. Saruda Tiwananthagorn, Ph.D.)

..... Thesis Advisor
(Associate Professor Dr. MORAKOT KAEWTHAMASORN, Ph.D.)

..... Thesis Co-Advisor
(Associate Professor Dr. Masahito Asada, Ph.D.)

..... CHULALONGKORN UNIVERSITY Examiner
(Assistant Professor Dr. SITTIPORN PATTARADILOKRAT, Ph.D.)

..... Examiner
(Associate Professor Dr. SONTAYA TIAWSIRISUP, Ph.D.)

..... Examiner
(Associate Professor Dr. NOPADON PIRARAT, Ph.D.)

หวง ลาน อัน เหงียน : พลวัตของการติดเชื้อการติดเชื้อร่วม มัลติอินโฟโลจีนีและการตรวจหาเชื้อ
พลาสมอดีียมคาปรีในแพะและในยุง. (THE INFECTION DYNAMICS, CO-INFECTION, MULTI-GENE
PHYLOGENY, AND MOLECULAR SCREENING OF *PLASMODIUM CAPRAE* INFECTION IN GOATS AND
MOSQUITO SPECIES) อ.ที่ปรึกษาหลัก : มรกต แก้วธรรมสอน, อ.ที่ปรึกษาร่วม : มาฮาอีโตะ อาซาฮา

เชื้อปรสิต *Plasmodium caprae* เป็นสาเหตุของโรคมาลาเรีย โดยมีสัตว์เท่ากับเป็นโฮสต์ และมีรายงานการแพร่ระบาดในแพะ ยังได้รับความสนใจศึกษาไม่มากนัก ยกเว้นการศึกษาบางส่วนเกี่ยวกับความชุกและการวิเคราะห์ไมโทคอนเดรียจีโนม การศึกษานี้จึงมีวัตถุประสงค์เพื่อศึกษาพลวัตการติดเชื้อตามธรรมชาติของ *P. caprae* และยุงพาหะนำโรค นอกจากนี้ การวิเคราะห์จีโนมโดยอาศัยยีนจากนิวเคลียสของเชื้อ *P. caprae* เพื่อเปรียบเทียบกับเชื้อปรสิตในอันดับ Haemosporida ที่เกี่ยวข้องอื่น ๆ ยังได้ดำเนินการเพื่อให้ได้ความเข้าใจที่ลึกซึ้งยิ่งขึ้นเกี่ยวกับประวัติวิวัฒนาการและที่มาของเชื้อปรสิตกลุ่มดังกล่าว โดยทำการเก็บตัวอย่างเลือดแพะทั้งหมด 423 ตัวอย่างในช่วงฤดูฝนระหว่างปี พ.ศ. 2561 ถึง พ.ศ. 2564 เพื่อประเมินสถานะการติดเชื้อมาลาเรีย นอกจากนี้ ระหว่างปี พ.ศ. 2563 - พ.ศ. 2564 ยังทำการจับยุงก้นปล่อง 1,019 ตัว และยุงที่ไม่ใช่ยุงก้นปล่อง 133 ตัว เพื่อระบุสายพันธุ์ สถานะการเป็นพาหะของมาลาเรีย และการวิเคราะห์จีโนมของเชื้อปรสิต *P. caprae* ได้ตรวจคัดกรองโดยใช้วิธี PCR โดยกำหนดเป้าหมายยีน *cytochrome b (cytb)* ในขณะที่ยีนจากนิวเคลียสได้ถูกเพิ่มปริมาณโดยใช้ Polymerase Chain Reaction (PCR) ยุงได้ถูกจำแนกทางสัณฐานวิทยาภายใต้กล้อง stereo และทำการยืนยันด้วยวิธี PCR และการจัดลำดับของหน่วยย่อย *cytochrome c oxidase subunit 1 (cox1)*, *cytochrome c oxidase subunit 2 (cox2)* และ internal transcribed spacer 2 (ITS2) เชื้อปรสิตที่พบในเลือดนั้นต่ำเพียง 4,510 สำเนา DNA ต่อไมโครลิตรของเลือด และคงอยู่จนถึงวันที่ 15 ของการสังเกตการณ์ เชื้อ *P. caprae* ที่ทำการศึกษานี้ถูกจัดวิวัฒนาการไว้ใน clade เดียวกับปรสิตมาลาเรียในสัตว์เคี้ยวเอื้องที่มีกบเท้าอื่น ๆ และมีบรรพบุรุษร่วมกับ *Polychromophilus* ที่พบในค้างคาว ในส่วนของยุงก้นปล่องนั้น มีการพบ 9 ชนิดที่แตกต่างกันในฟาร์มแพะ ซึ่งเป็นของกลุ่ม *Hircanus*, *Barbirostris*, *Subpictus*, *Funestus*, *Tessellatus* และ *Annularis* พบว่า กลุ่ม *Subpictus (An. subpictus)* และ *Funestus (An. aconitus)* ตรวจพบ DNA ของเชื้อ *P. caprae* การวิเคราะห์แหล่งที่มาของเลือดในยุง พบว่า แหล่งเลือดมาจากโค กระบือ คน สุนัข และแพะ โครงสร้างทางพันธุกรรมของประชากรของยุงชี้ว่ามีความผันแปรทางพันธุกรรมในสายพันธุ์ที่โดดเด่นส่วนใหญ่มีอยู่ในระหว่างหมู่ประชากรของยุงพบค่า F_{ST} ต่ำถึงปานกลางบ่งชี้ว่ามีการไหลของยีนเกิดขึ้นในหมู่ *An. peditaeniatus*, *An. subpictus*, *An. vagus* และ *An. aconitus* ทั้งที่ยุงเหล่านี้มีระยะห่างทางภูมิศาสตร์ระหว่างจังหวัดทางภาคเหนือและภาคตะวันตก การศึกษานี้เป็นรายงานฉบับแรกเกี่ยวกับการวิเคราะห์ยีนจากนิวเคลียสของเชื้อมาลาเรียในแพะและยุงพาหะนำโรคที่อาจจะเป็นได้ การถ่ายทอดเชื้อ *P. caprae* ในประเทศไทย

สาขาวิชา	วิทยาศาสตร์ทางการสัตวแพทย์และเทคโนโลยี	ลายมือชื่อนิสิต
ปีการศึกษา	2565	ลายมือชื่อ อ.ที่ปรึกษาหลัก
		ลายมือชื่อ อ.ที่ปรึกษาร่วม

6278804231 : MAJOR VETERINARY SCIENCE AND TECHNOLOGY

KEYWORD: malaria mosquito natural infection Plasmodium caprae ungulate

Hoang Lan Anh Nguyen : THE INFECTION DYNAMICS, CO-INFECTION, MULTI-GENE PHYLOGENY, AND MOLECULAR SCREENING OF *PLASMODIUM CAPRAE* INFECTION IN GOATS AND MOSQUITO SPECIES.
 Advisor: Assoc. Prof. Dr. MORAKOT KAEWTHAMASORN, Ph.D. Co-advisor: Assoc. Prof. Dr. Masahito Asada, Ph.D.

Ungulate malaria parasites, including *Plasmodium caprae* that infects the domestic goats, have received little attention. There are only few studies about the prevalence and mitochondrial genome analyses. This study, therefore, aimed to investigate the natural infection dynamics of *P. caprae* and its mosquito vectors. Besides, genome analyses based on nuclear genes of *P. caprae* and other related haemosporidian parasites were also carried out to obtain an in depth understanding about their evolutionary history and origin. A total of 423 goat blood samples were collected during rainy seasons from 2018 to 2021 to assess the malaria infection status. In addition, 1,019 anopheline and 133 non-anopheline mosquitoes were also captured between 2020 and 2021 for species identification, malaria-carrying status and genome analyses. The parasite *P. caprae* was screened using nested PCR targeting *cytochrome b (cytb)* gene, whereas four nuclear genes were amplified using touch down nested PCR. The mosquitoes were morphologically identified under the stereomicroscope, followed by PCR and sequencing of *cytochrome c oxidase subunit 1 (cox1)*, *cytochrome c oxidase subunit 2 (cox2)* and internal transcribed spacer 2 (ITS2). The parasite load was as low as 4,510 DNA copies per microliter of blood and maintained until day 15 of observation. The phylogeny based on multiple nuclear genes revealed that *P. caprae* was placed in the ungulate malaria parasite clade and formed a sister group with the bat parasite *Polychromophilus*. Regarding the mosquitoes, nine distinct species were recorded in the goat farm, belonging to Hyrcanus, Barbirostris, Subpictus, Funestus, Tessellatus, and Annularis groups. The Subpictus (*An. subpictus*) and Funestus (*An. aconitus*) groups were found to carry the *P. caprae*'s DNA by molecular method. The analysis of blood meal sources in the engorged mosquitoes showed that the blood sources came from either cattle, human, dog or goat. Two mosquito species of *An. subpictus* and *An. peditaeniatus* were found to carry the goat blood. The population genetic structure of the mosquitoes suggested that genetic variations in four dominant species have mostly existed within populations rather than among populations. Low to moderate F_{ST} indicated that gene flow has occurred among *An. peditaeniatus*, *An. subpictus*, *An. vagus*, and *An. aconitus* mosquito populations without geographic distance between northern and western provinces. This study is the first report about the multiple nuclear genes analyses and possible mosquito vectors of *P. caprae* in Thailand.

Field of Study:	Veterinary Science and technology	Student's Signature
Academic Year:	2022	Advisor's Signature
		Co-advisor's Signature

ACKNOWLEDGEMENTS

First and foremost, my deepest appreciation and gratitude go to my advisor Assoc. Prof. Dr. Morakot Kaewthamasorn and my co-advisor Assoc. Prof. Dr. Masahito Asada for the enthusiastic and patient guidance throughout this study as well as further research motivation in the future. I have learned a lot from their insight and advice.

I am so thankful to Assist. Prof. Winai Kaewlamun and his team in School of Agricultural Resources, Chulalongkorn University for the invaluable help in collecting blood and mosquito samples. Without their kind assistance, this study would not have been possible.

I would like to express my sincere appreciation to all my dissertation committee members, Dr. Saruda Tiwananthagorn, Dr. Sittiporn Pattaradilokrat, Dr. Sonthaya Tiawsirisup, and Dr. Nopadon Pirarat for their valuable comments and suggestions.

Next, I also want to thank all my friends, who helped and shared ups and downs in my study and life for the last three years. Especial thanks to all my lab mates for their optimistic thinking, encouragement, and academic assistance during my lab and paper works.

My graduate study would have been impossible without the financial support from the Second Century Fund, Chulalongkorn University, and the 90th Anniversary of Chulalongkorn University Scholarship for research funding.

Most of all, I would like to express my utmost gratefulness and appreciation to my beloved parents and older brother for always being beside me during difficult times, giving me unending moral support, guidance, and encouragement throughout my life.

Finally, I would like to thank Lord for letting me overcome all difficulties, sorrows, ups and downs.

Hoang Lan Anh Nguyen

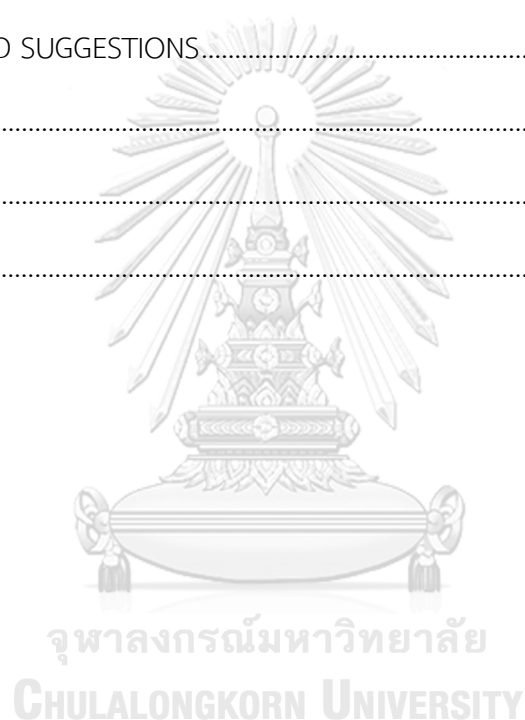
TABLE OF CONTENTS

	Page
.....	iii
ABSTRACT (THAI).....	iii
.....	iv
ABSTRACT (ENGLISH).....	iv
ACKNOWLEDGEMENTS.....	v
TABLE OF CONTENTS.....	vi
LIST OF TABLES.....	x
LIST OF FIGURES.....	xi
CHAPTER 1.....	15
INTRODUCTION.....	15
Objectives of the Study.....	18
Hypotheses.....	18
CHAPTER 2.....	19
LITERATURE REVIEW.....	19
2.1 Goat and malaria in goat.....	19
2.2 Life cycle of <i>Plasmodium</i> species.....	21
2.3 Clinical symptoms of malaria.....	22
2.4 Phylogeny of malaria parasites.....	23
2.5 Mosquito vector.....	26
CHAPTER 3.....	28
MATERIALS AND METHODS.....	28

3.1 Experiment 1: Natural infection of <i>Plasmodium caprae</i> and its co-infection....	28
3.1.1 Sample size determination.....	28
3.1.2 Blood sample collection.....	29
3.1.3 Infection dynamics of <i>P. caprae</i> and co-infection with other protozoa parasites.....	30
3.1.4 Quantitative measurement of <i>P. caprae</i> based on microscopic examination and real-time PCR methods.....	30
3.1.5 Statistical analysis.....	31
3.2 Experiment 2: Multigene analysis of <i>Plasmodium caprae</i> and its related genera	35
3.2.1 Primer design for nuclear genes of <i>P. caprae</i>	35
3.2.2 DNA amplification of <i>P. caprae</i> nuclear genes.....	37
3.2.3 DNA cloning and sequencing.....	37
3.2.4 Data analysis.....	38
3.3 Experiment 3: Mosquito composition and identification of the possible mosquito vector of <i>P. caprae</i> from goat farms.....	48
3.3.1 Mosquito collection.....	48
3.3.2 Morphological identification, dissection, and DNA extraction.....	48
3.3.3 Mosquito species identification and <i>Plasmodium</i> detection by molecular method.....	50
3.3.4 Blood meal source analysis in mosquito.....	51
3.3.5 DNA sequencing and data analysis.....	51
3.4 Ethical statements.....	51
CHAPTER 4.....	59
RESULTS.....	59

4.1 Experiment 1: Natural infection of <i>Plasmodium caprae</i> and its co-infections ..	59
4.1.1 Goats' gender, age, and pregnancy status.....	59
4.1.2 Natural infection of <i>P. caprae</i> and its clinical outcomes.....	59
4.1.3 Co-infection of goat with other protozoa parasites.....	61
4.1.4 Association between season and malaria infection rate.....	61
4.2 Experiment 2: Multi-gene analysis of <i>Plasmodium caprae</i> and its related genera	62
4.2.1 <i>Plasmodium</i> identification based on nuclear genes	62
4.2.2 Molecular phylogeny of <i>Plasmodium caprae</i> based on four concatenated nuclear genes.....	63
4.2.3 Molecular phylogeny of <i>Plasmodium caprae</i> based on concatenated <i>cox1</i> , <i>cytb</i> , <i>clpC</i> , and four nuclear genes.....	67
4.3 Experiment 3: Mosquito composition and identification of the possible mosquito vector of <i>P. caprae</i> from goat farms.....	69
4.3.1 Mosquito species composition collected from goat farms based on morphological and molecular identifications.....	69
4.3.2 Molecular detection and phylogenetic analysis of <i>P. caprae</i> from mosquito samples	73
4.3.3 Molecular determination of the source of host blood meal in anopheline mosquito.....	77
4.3.4 Intraspecific and interspecific variations of dominant mosquito species..	78
4.3.5 Population genetic structure of the four dominant mosquito species.....	81
4.3.6 Haplotype network of the four dominant mosquito species	83
4.3.7 Phylogenetic analysis of anopheline mosquitoes collected from goat farms	85
CHAPTER 5	90

DISCUSSION	90
5.1 Experiment 1: Natural infection of <i>Plasmodium caprae</i> and its co-infections ..	90
5.2 Experiment 2: Multigene analysis of <i>Plasmodium caprae</i> and its related genera	92
5.3 Experiment 3: Mosquito composition and identification of the possible mosquito vector of <i>P. caprae</i> from goat farms	96
CHAPTER 6	104
CONCLUSIONS AND SUGGESTIONS.....	104
REFERENCES.....	106
APPENDIX.....	116
VITA.....	119



LIST OF TABLES

	Page
Table 1. Primers and PCR conditions to monitor the course of natural infection of <i>P. caprae</i> and its co-infections	32
Table 2. Primer sequences for nuclear gene amplification and touchdown PCR conditions	40
Table 3. Primer sequences for identification of mosquito species, <i>Plasmodium</i> spp. detection, blood meal analysis, and PCR conditions.....	53
Table 4. Association between season and malaria infection rate.....	62
Table 5. BLASTN searches for <i>Plasmodium caprae</i> based on four nuclear genes.	63
Table 6. Number of anopheline mosquitoes collected in the present study according to gonotrophic status.....	70
Table 7. Overview of search results using <i>cox1</i> , <i>cox2</i> and ITS2 sequences in the BOLD and GenBank database.....	71
Table 8. Minimum infection rates (MIR) of <i>P. caprae</i> in collected mosquitoes.....	73
Table 9. Host blood meal source of female anopheline mosquitoes collected from goat farms in Thailand.....	77
Table 10. Genetic diversity indices and neutrality test values of <i>cox1</i> , <i>cox2</i> , and concatenated sequences within and among the four dominant anopheline mosquitoes in the present study.	80
Table 11. Analysis of molecular variance (AMOVA), Wright's fixation index and gene flow based on the <i>cox1</i> , <i>cox2</i> and concatenated sequences within and between the four dominant anopheline mosquitoes found in the present study.	82

LIST OF FIGURES

	Page
Figure 1. The life cycle of Plasmodium in human (Merrick, 2021).....	22
Figure 2. Global distribution of 34 dominant malaria vector mosquito species (Sinka et al., 2012).....	27
Figure 3. Sequence alignment and primer design for <i>P. caprae</i> nuclear gene amplifications. All sequences referred to <i>P. odocoilei</i> and were aligned with orthologous genes available in the PlasmoDB and NCBI databases. (a) ETIF2: MF508338_ <i>P. odocoilei</i> , (b) Sec24a: MF775866_ <i>P. odocoilei</i> , (c) RuvB: MF775893_ <i>P. odocoilei</i> , (d) RDR: MF508492_ <i>P. odocoilei</i> . The <i>P. odocoilei</i> sequences were used as the basis for primer design. The outer primer sequences of <i>P. odocoilei</i> were highlighted in yellow, and the inner primer sequences of <i>P. odocoilei</i> were highlighted in light blue. Degenerate outer and inner primers were indicated by blue and black arrows, respectively. The mismatch nucleotides are highlighted in red.	36
Figure 4. Malaria parasite's copy number in goat blood as measured by qPCR during the observation period in naturally infected goat ID THGoat20-101 in Nan Province. 61	61
Figure 5. Body temperature of malaria in naturally infected goat ID THGoat20-101 in Nan Province during observation period.....	61
Figure 6. Bayesian posterior probabilities and Maximum likelihood bootstrap values from analysis of four concatenated nuclear genes (a). Consensus cladogram of the analysis using Bayesian inference (b). Consensus cladogram of analysis using Maximum likelihood (c). The non-haemosporidian parasite (<i>Theileria orientalis</i>) as an outgroup was displayed. Taxa recovered in this study were highlighted in red letters. The length (2.0) indicated the number of substitutions per site.....	65
Figure 7. Phylogenetic trees of four concatenated nuclear genes based on nucleotides. Bayesian inference (a) and Maximum likelihood (b). Bayesian posterior probabilities and bootstrap values were shown at the nodes. All trees were rooted with <i>Cryptosporidium</i> as an outgroup. The concatenated sequence of <i>P. caprae</i>	

obtained from this study is colored red. The length (2.0) indicated the number of substitutions per site. 66

Figure 8. Phylogenetic trees of four concatenated nuclear genes based on codons. Bayesian inference (a) Maximum likelihood (b). Bayesian posterior probabilities and bootstrap values were shown at the nodes. All trees were rooted with *Cryptosporidium* as an outgroup. The concatenated sequence of *P. caprae* obtained from this study is colored red. The length (2.0) indicated the number of substitutions per site. 66

Figure 9. Phylogenetic trees of four concatenated nuclear genes based on amino acids. Bayesian inference (a) and Maximum likelihood (b). Bayesian posterior probabilities and bootstrap values were shown at the nodes. All trees were rooted with *Cryptosporidium* as an outgroup. The concatenated sequence of *P. caprae* obtained from this study is colored red. The length (2.0) indicated the number of substitutions per site. 67

Figure 10. Consensus tree based on BI and ML analyzes using concatenated nucleotides (4,044 bp) of two mtDNA (*cox1*, *cytb*), one apDNA (*clpC*) and four novel nuDNA genes (ETIF2, Sec24a, RuvB and RDR). Bayesian posterior probabilities (BPP) and Maximum likelihood bootstrap values (BV) more than 0.5/58 were given at the nodes. A bootstrap value less than 50 was presented as '-'. The length (0.2) indicated the number of substitutions per site. The sequence of the goat malaria parasite *P. caprae* obtained from this study is highlighted in red. The icons in black represented the animal hosts of haemosporidian parasites. 68

Figure 11. Chart illustrating the percentage and number of mosquitoes collected according to morphological identification. Percentages of each genus collected by the CDC light trap at goat farms (a). Anopheline mosquitoes collected from goat farms by mouth aspirator according to the species in this study (b). 70

Figure 12. Phylogenic position of *Plasmodium caprae* that infects *Anopheles* mosquitoes in this study. Phylogenetic tree inferred by BI based on the partial *cytb* gene (632 bp). All sequences were rooted with *Haemoproteus columbae*. Bayesian

posterior probabilities values (≥ 0.60) were given in the nodes. The *P. caprae* sequences obtained in this study were highlighted in red and reference sequences retrieved from the GenBank database in black. The length (0.03) indicated the number of substitutions per site. 75

Figure 13. Phylogenic position of *Plasmodium caprae* obtained in this study. The phylogenetic tree was constructed using partial *cox1* gene (231 bp) (a). Phylogenetic tree was constructed using partial 18S rRNA gene (335 bp) (b). The length (0.02) indicated the number of substitutions per site..... 77

Figure 14. TCS network of the concatenated *cox1* and *cox2* sequences of the dominant mosquito species collected from four provinces in Thailand. The brown, green, purple, and blue shadows indicated four different mosquito species, *An. peditaeniatus*, *An. subpictus*, *An. vagus*, and *An. aconitus*, respectively. Each haplotype was represented by a cycle, and the size of the cycle was proportional to the number of individuals in each haplotype. The number of nucleotide differences between haplotypes was presented by lines indicating mutations from the common haplotype. The colors of four provinces were annotated in the box. 84

Figure 15. Consensus phylogenetic tree of *Anopheles* spp. based on the *cox1* gene using the BI and ML method. The posterior probability and the bootstrap value were shown at the nodes. Bootstrap values less than 50 were presented as “-”. The reference taxa retrieved from GenBank were in black, the color codes were from the present study. The subgenus *Anopheles* and *Cellia* was highlighted in blue and yellow shadows, respectively..... 86

Figure 16. The BI and ML methods were used to construct a consensus phylogenetic tree of *Anopheles* spp. based on the *cox2* gene. Posterior probability and bootstrap values were presented at the nodes. Bootstrap values less than 50 were denoted by a “-”. The GenBank reference taxa were in black and the color codes are from the current study. *Anopheles* and *Cellia* subgenera were highlighted in blue and yellow shadow, respectively..... 87

Figure 17. Consensus phylogenetic tree of *Anopheles* spp. based on concatenated *cox1* and *cox2* sequences (954 bp) using the BI and ML method. The posterior probability and the bootstrap value were shown at the nodes. Bootstrap values less than 50 are presented as “-”. The GenBank accession numbers and the reference species names were given in black. Blue, pink, green, purple, red, and orange represent the Hyrcanus, Barbirostris, Tessellatus, Subpictus, Annularis groups, and Aconitus subgroup, respectively. The subgenus *Anopheles* and *Cellia* was highlighted in blue and yellow shadows, respectively. Accession numbers in brackets represented for *cox1* and *cox2* sequences, respectively..... 88

Figure 18. Consensus phylogenetic tree of anopheline mosquitoes in the genera *Anopheles* and *Cellia* of the present study based on the ITS2 region using the BI and ML methods. The subgenus *Anopheles* and *Cellia* was in light blue and yellow shades, respectively. The reference taxa retrieved from GenBank were in black, and taxa in colors were from the present study..... 89

CHAPTER 1

INTRODUCTION

Aside from the main livestock animals such as pigs, cattle, and chickens, goats play an important role in providing food and other commodities to people, particularly the Muslim population. Goats have significantly contributed to food and economic profits for several decades (Khamseekhiew and Pompei, 2016). According to The American Goat Federation, when compared to other red meats, goat meat is leaner than meat from other domestic animals in terms of nutritional value. Goat meat has less calories, saturated fat, and cholesterol, but more protein and iron than beef, pork, lamb, and chicken. Furthermore, goat meat is favored by many religions and cultures, including the Muslim and Hindu communities (Dhanda et al., 2003). In addition, goat milk is easier to digest than cow milk and it can be also utilized to make cheese or soft, mild body soap. In addition to food-providing benefits, goat manure is a great source of fertilizer for farmers. Although goats bring great benefits to human society, they are also known to harbor many diseases such as babesiosis, theileriosis, and malaria that resulted in considerable economic losses.

Malaria, a mosquito-borne disease, is one of the world's most important parasitic infections. It is caused by *Plasmodium* spp., which belongs to the phylum Apicomplexa. Malaria in humans is one of the most serious and lethal diseases. People living in endemic areas such as tropical and subtropical countries are prone to malaria and infected people usually show fever, chills, muscle aches, headache, vomiting, and diarrhea (CDC, 2019). Malaria has primarily occurred in humans and most deaths are caused by *Plasmodium falciparum*, while *P. vivax*, *P. ovale*, and *P. malariae* generally result in a milder form of malaria (Caraballo and King, 2014). In addition to human-

infecting species, *Plasmodium* species that are capable of infecting ungulates were reported in duiker antelope (*P. cephalophi*) (Bruce et al., 1913), water buffalo (*P. bubalis*) (Sheather, 1919), African marshbuck (*P. limnotragi*) (van den Berghe, 1937), domestic goat (*P. caprae*) (de Mello and Paes, 1923), mouse deer (*P. traguli*) (Garnham and Edeson, 1962), white-tailed deer (*P. odocoilei*) (Garnham and Kuttler, 1980), and pampas deer (*P. odocoilei*) (Asada et al., 2018).

Mosquitoes are insects that belong to the order Diptera and the family Culicidae. They are common and abundant in humid, warm tropical regions such as Africa, South America, and Asia. The mosquito has positive and negative effects on humans and the environment. From a beneficial point of view, mosquito larvae provide food for fish and other aquatic species. The mosquito larvae eat tiny organic matter in the water and help recycle it. The adult mosquito pollinates flowers and is a food source for insect-eating animals such as birds, bats, frogs, and dragonflies. However, the negative effects outweigh their benefits. Mosquitoes are known to carry and transmit a variety of infectious diseases, including West Nile virus, Chikungunya virus, Zika virus, Japanese encephalitis virus, yellow fever, dengue fever, and malaria, not only in humans but also in livestock (Fang, 2010). Malaria in goats, caused by *Plasmodium caprae*, was first discovered in Angola (de Mello et al., 1923). Recently, DNA isolation was used to characterize the parasite from a goat blood sample in Zambia. Later, *P. caprae* was shown to be globally distributed, ranging from Sudan and Kenya in Africa, Iran in West Asia, to Myanmar and Thailand in Southeast Asia (Templeton et al., 2016a, Kaewthamasorn et al., 2018). However, there was only one nucleotide substitution in the whole mitochondrial DNA sequence (5,987 bp) between Asian and African isolates (Kaewthamasorn et al., 2018). Ungulate malaria parasites are

relatively understudied, as there would be many challenges developing and working with complete genome and nuclear gene markers; approximately one to four genes located on mitochondria or apicoplast are used to study molecular phylogenetics and evolution (Perkins, 2014).

Borner et al. (2016) analyzed the deep-level phylogenetic relationship using twenty-one nuclear genes of haemosporidian parasites but there was no taxon originating from *Plasmodium* in ungulates. Their analyzes revealed highly congruent topologies between the nuclear genes and the dataset of concatenated nuclear gene, mitochondrial and apicoplast (Borner et al., 2016). Until recently, there has been a few investigations about ungulate malaria parasites. A previous study showed that haemosporidian parasites were split into two divergent clades. The first clade consisted of the genus *Plasmodium*, which was paraphyletic with *Hepatocystis*. The second clade was *Plasmodium* of mammal hosts, which was associated with *Anopheles* mosquito vectors (Martinsen et al., 2008). Due to the lack of taxon sampling, host switching events and diversification in ungulate malaria parasites remain unknown. Recently, another study on ungulate reported that *Plasmodium* sequences detected in pampas deer in South America were grouped in the same clade with *Plasmodium* spp. in white-tailed deer in North America but solely based on mitochondrial and apicoplast (Asada et al., 2018). Nuclear genes have evolved in a more complex manner than mitochondrial genes, which are only inherited from the mother. Molecular information on nuclear genes of ungulate malaria parasites in general and *P. caprae* in specific remains unknown.

Therefore, in the present study, our objective was to investigate the infection dynamics, genome and characteristics of the malaria parasite in goats based on the

four nuclear genes, as well as determine the species diversity of mosquito vectors collected in goat farms in six districts in four provinces of Thailand including Nan, Kanchanaburi, Ratchaburi, and Phetchaburi. Molecular detection and genetic characterization of ungulate malaria parasites and mosquitoes could provide new knowledge on the goat host and their mosquito vectors.

Objectives of the Study

1. To observe the infection dynamics of *Plasmodium caprae* and its clinical outcomes in goat.
2. To analyze the phylogenetic position of *Plasmodium caprae* based on its nuclear genes.
3. Assess the diversity of mosquito species from goat farms and to identify potential vectors of the *Plasmodium caprae* malaria parasite.

Keywords (Thai): มาลาเรีย ยุง การติดเชื้อตามธรรมชาติ พลาสโมเดียม คาปรี สัตว์กีบคู่

Keywords (English): malaria, mosquito, natural infection, *Plasmodium caprae*, ungulate

Hypotheses

1. The infection dynamic of *Plasmodium caprae* in goats has a unique pattern and could be predictable.
2. *Plasmodium caprae* has a close relationship with the other known *Plasmodium* in ungulates.
3. Potential vectors for malaria transmission in goats might be the same species as vectors for the other ungulate malaria parasites.

CHAPTER 2

LITERATURE REVIEW

2.1 Goat and malaria in goat

Goat (*Capra hircus*) is a domesticated animal and one of the most prolific ruminants in tropical and subtropical areas, especially in Southeast Asia and Africa. The goat is highly adaptable to harsh living conditions because it is tolerant to heat stress, can maintain the balance between metabolic and environmental heats, and live in poor quality feed (Dhanda et al., 2003). Based on the results of previous research studies, unusual characteristics, including high respiration and sweating rate, water conservation capability, constant cardiac output, and heart rate, make goat become an exclusive animal compared to other ruminants and farm animals (Robertshaw, 1968, Quartermain and Broadbent, 1974, Feistkorn et al., 1983). Therefore, the goat is well adapted to mountainous, desert, and tropical regions where other livestock animals would not flourish (Amills et al., 2017). As stated by the Food and Agriculture Organization (FAO, 2021) statistics, the number of goats raised in Thailand has slightly increased from 465,014 heads in 2017 to 478,559 heads in 2019 due to a rise in demand for goat meat and milk. There are three main types in the goat population consisting of fiber goat (e.g., Angora, Cashmere), dairy goat (e.g., Saanen, Toggenburg, Nubian), and meat goat (e.g., Boer, Spanish). In Thailand, meat goat is predominant with more than 90% of the population, less than 10% of the goat population is raised for milk production (Nakavisut and Anothaisinthawee, 2014). There are two local goat breeds and nine exotic ones in Thailand. The Northern Native Thai goats are known as 'Bangala', having a large but thin body, long pendulous ears and a straight face, while the other found in Southern Thailand, called 'Katjang', is small in size with short

upright ears. Five breeds of dairy goats comprise Saanen, Alpine, Toggenburg, Shami, and Laoshan. Saanen is raised in the central and southern regions, known as the most popular among dairy goats owing to its high milk production (Nakavisut et al., 2014). Although local goat breeds are smaller than exotic breeds, they are highly adaptable to a harsh environment and tolerant of tropical parasites and diseases. Other dominant characteristics of local breeds are prolificacy with nonseasonal breeding, multiple births, low heritability rate, high litter size but low meat and milk production in comparison with exotic breeds. Hence, cross-breeding between local and exotic breeds would improve body conditions, increased resistance to diseases, and improve meat and milk productivity (Anothaisinthawee et al., 2010).

Plasmodiidae is one of the four families in the Order Haemosporida, Class Aconoidasida, Phylum Apicomplexa, which is an intraerythrocytic parasitic alveolate in mammals. Plasmodiidae comprises the genus *Plasmodium*, which is known to cause malaria in both humans and a wide range of animals. Ungulate malaria is found in both domestic and wild even-toed hoofed mammals. In domestic animals such as water buffaloes, malaria is caused by *Plasmodium bubalis* and was first observed by Sheather in India (1919) (Sheather, 1919), and was followed by many researchers (Rao, 1938, Shastri et al., 1985). Other Haemosporida parasites of wild ungulates have been described including *Plasmodium traguli* and *Hepatocystis fieldi* in the Asian mouse-deer (Garnham et al., 1980), a *Hepatocystis* parasite in the hippopotamus (Garnham, 2007), *Plasmodium limnotragi* in the African marshbuck (van den Berghe, 1937), and *Plasmodium caprae* in African goats (de Mello et al., 1923). The ungulate malaria parasite is globally distributed, from North and South America to Africa and Asia. *Plasmodium odocoilei* was detected in white-tailed deer in North America (Guggisberg

et al., 2018). In another study, South American pampas deer was shown to harbor *Plasmodium* spp. that was closely related to *P. odocoilei* clade 2 from North American white-tailed deer (Asada et al., 2018). Another species of *Plasmodium*, presumably *P. caprae*, was found in domestic goats from Sudan and Kenya in Africa, Iran in West Asia, Myanmar and Thailand in Southeast Asia (Kaewthamasom et al., 2018). *Plasmodium cephalophi* and *Plasmodium brucei* were detected in duiker antelope (*Sylvicapra grimmia*) in Central Africa (Boundenga et al., 2016).

2.2 Life cycle of *Plasmodium* species

Most *Plasmodium* species have a similar life cycle that requires vertebrate (animal) and invertebrate (mosquito) hosts. The brief life cycle of *Plasmodium* species is illustrated in **Figure 2**. First of all, the sporozoites are inoculated into the host by the bite of an infected *Anopheles* mosquito. Two stages occur, including the preerythrocytic liver stage and erythrocytic stage. Among *Plasmodium* species, only *P. vivax* and *P. ovale* infect hepatocytes and stay dormant in the liver for up to 9 months known as “hypnozoites” (Merrick, 2021). Sporozoites invade host hepatocytes, and then develop into merozoites. After release from the liver, merozoites enter the bloodstream and invade erythrocytes, where they become a ring-shaped and a larger form called trophozoites. Trophozoites then mature into schizonts, which divide several times to produce new merozoites. The new merozoites released from the ruptured erythrocytes enter the bloodstream then most of them infect new erythrocytes to continue their replication while some differentiate into male and female gametocytes. These gametocytes are then taken up by another mosquito via blood meal. In the mosquito, the gametocytes move to the mosquito’s midgut and

form the zygote through the fertilization between male and female gametes. The zygotes then transform into motile and elongated ookinetes that pass through the gut wall of the mosquito where they develop into oocysts. The oocysts divide and produce sporozoites which migrate to the salivary gland of the mosquito and are inoculated into a new host and start the cycle over again (Venugopal et al., 2020).

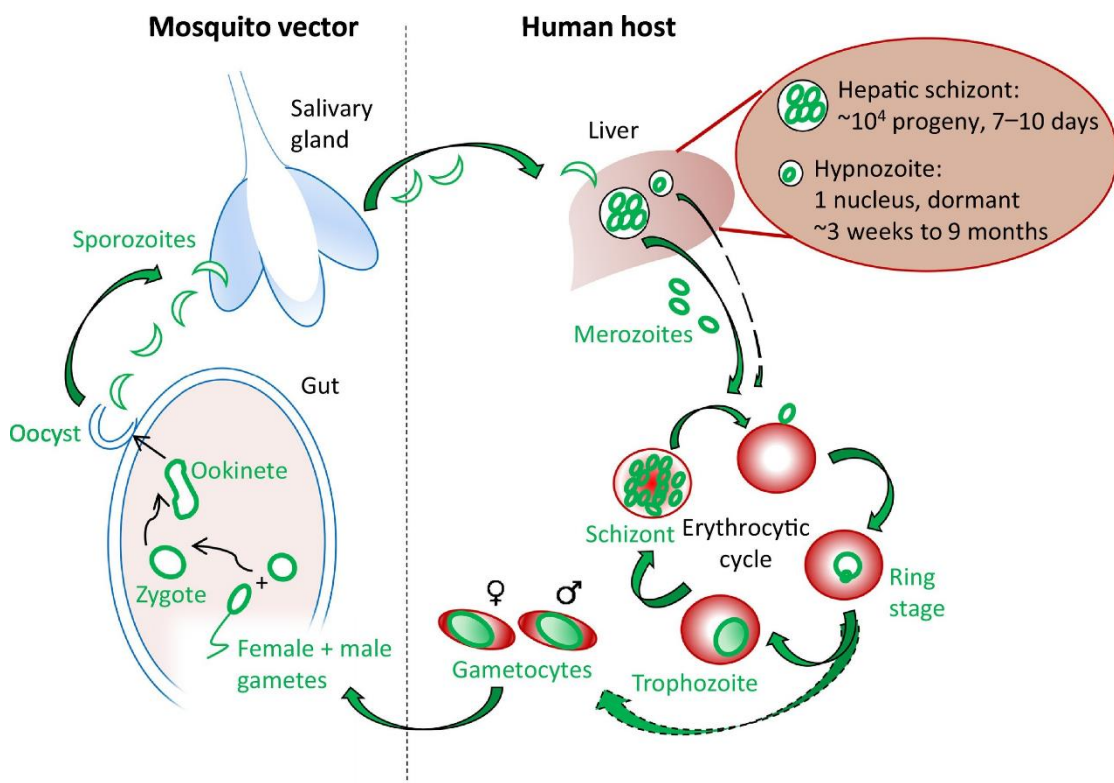


Figure 1. The life cycle of *Plasmodium* in human (Merrick, 2021)

2.3 Clinical symptoms of malaria

The clinical signs of malaria in humans include three consecutive stages, starting with shivering and feeling cold, then fever, headache, muscle pain, dry skin, and nausea. After the fever stops, sweating follows. Physical manifestations, including anemia, jaundice, hepatomegaly, and splenomegaly, were well reported in malaria infected patients (McKenzie et al., 2002). Compared to other studies, little was known

about the clinical manifestations of ungulate malaria parasites. A previous study revealed that *P. bubalis* infection in buffalo causes fever (39.4 – 40.6°C) for 1-2 days, followed by a mild fever course lasting up to two weeks, and then natural recovery (Sheather, 1919). In some cases, however, they are accompanied by diarrhea, and the disease can be more severe and fatal. Pathological changes are believed to be similar to those seen in human malaria, but further research is required. Buffalo malaria manifestations include anorexia, lacrimation, hemoglobinemia, hemoglobinuria, dullness, and loss of body weight (Shinde et al., 2005). Until now, no reports have been any reports about clinical signs in malaria-infected goats, with the exception of one description, which showed that a goat (*Capra aegagrus hircus*) was infected with *Laverania caprae* (now named *Plasmodium caprae*) in Angola in 1923, having a submandibular abscess with bacterial infection but without anemia (de Mello et al., 1923). Knowledge on the incubation period, duration of disease, and goat immune response to malaria parasite has been all poorly understood.

2.4 Phylogeny of malaria parasites

In the past, morphology and life history traits including storage of malaria hemozoin pigment and schizogony in the blood were traditionally used to study the evolutionary characters and history of the parasite. However, they are uninformative characters for understanding the evolutionary relationship and comparison among *Plasmodium* species (Perkins and Schall, 2002). Hence, later, there were many research studies on the phylogenetic analysis of haemosporidian parasites by a single or multi-gene molecular approach. In 1994, a phylogeny study based on *SSU rRNA* gene sequences confirmed that *P. falciparum* and avian malaria parasites share a

moderately recent avian progenitor but are distantly related to human malaria parasites, *P. vivax*, and *P. malariae* (Escalante and Ayala, 1994). In contrast, recovery of haemosporidian phylogeny depended on *cytochrome b* gene sequences among four genera (*Plasmodium*, *Haemoproteus*, *Hepatocystis*, and *Leucocytozoon*) showed that *P. falciparum* was not derived from an avian malarial ancestor. Moreover, it has a close relationship with its sister species *P. reichenowi* in chimpanzees but is distantly related to haemosporidian parasites of all other mammals (Perkins et al., 2002). In addition, *Plasmodium* is paraphyletic with regard to two other genera, *Hepatocystis* and *Haemoproteus* (Perkins et al., 2002). Another study conducted by Hagner et al. (2007) revealed that the avian malaria parasite split into three distinct lineages as same as the parasites in lizards, and did not form a monophyletic lineage as discovered by Perkins and Schall (2002) based on the *cytb* gene (Hagner et al., 2007). The avian and lizard parasites appear to be paraphyletic, since the three lineages do not overlap. On the other hand, *clpC* and *18S rRNA* gene sequences do not provide sufficient phylogenetic information to make robust conclusions on the position of various haemosporidian species (Hagner et al., 2007). Among the published studies, no data from ungulate malaria parasites have been included using single gene analysis.

The phylogeny employing multigene analysis placed the genus *Haemoproteus* into two divergent clades, while the genus *Plasmodium* was paraphyletic regarding *Hepatocystis*, a group of parasites with different morphology and life-history traits. Besides, *Plasmodium* species fell into two major clades, one containing *Plasmodium* parasites in mammals and the others in birds and lizards. *Leucocytozoon* was found to be more distantly related group with other three parasites *Plasmodium*, *Haemoproteus*, and *Hepatocystis*. Therefore, it was considered as the sister clade to

the other genera and used as outgroup taxa (Martinsen et al., 2008). Subsequently, to resolve the unstable outgroup taxa, Outlaw and Ricklefs (2011) reconstructed the outgroup-free phylogenetic tree using relaxed molecular clocks. Their results suggested that the malaria parasites and avian *Plasmodium* are related to the avian parasite *Leucocytozoon* and *Haemoproteus*, implying that the life history has modified and evolved (Outlaw and Ricklefs, 2011). According to the previous single and multigene analysis of haemosporidia phylogeny, no ungulate malaria parasites were not phylogenetically studied until 2016. Templeton et al. have first described the phylogenetic tree of malaria parasites of even-toed ungulate including *P. bubalis* in water buffaloes and *P. caprae* in domestic goats, using concatenated sequences of mitochondrial and apicoplast (Templeton et al., 2016a). However, the relationship between ungulate *Plasmodium* (*P. bubalis* in water buffaloes, *P. odocoilei* in white-tailed deer, and *P. caprae* in domestic goats) and *Polychromophilus* has remained obscure (Templeton et al., 2016b). The phylogeny of ungulate malaria parasites is relatively understudied as there would be many challenges in developing and working with complete genome and nuclear gene markers; approximately one to four genes located in mitochondria or apicoplast are used to study molecular phylogenetics and evolution (Perkins, 2014). The evolutionary study of hemopridian blood parasites revealed by a multigene method (mitochondrial, apicoplast, and nuclear genes) obtained a more robust and reliable topology and position of ungulate *Plasmodium* species within the order Haemosporida (Borner et al., 2016). Until now, only one study reported the evolutionary relationship between ungulate malaria parasites and other hemosporidia based on combined sequences between mitochondrial and apicoplast genes (Templeton et al., 2016a). In detail, two types (Type I and Type II) of *P. bubalis* were

described in water buffalo, while Type III *P. caprae* were isolated solely from Zambia goat. It was concluded that Type II *P. bubalis* had a closer relationship with Type III *P. caprae* than it was with Type I *P. bubalis* based on phylogenetic inference of the whole mitochondrial genome (Templeton et al., 2016a). However, the relationship between ungulate *Plasmodium* and *Polychromophilus* remains unclear and needs further investigation. Therefore, the multigene analysis using nuclear genes is expected to reveal a precise and a clearer position of the ungulate *Plasmodium* taxa within haemosporidian parasites.

2.5 Mosquito vector

The mosquito is widely distributed in temperate and tropical regions around the world. Human malaria parasites are transmitted by mosquitoes of the genus *Anopheles*. There are approximately 460 recognized mosquito species (Harbach, 2011). Among them, about 70 species are responsible for human malaria transmission, while 34 species are considered dominant vector species/species complexes, having the capability to pose a public health concern (Sinka et al., 2012). The main mosquito vectors for human malaria transmission on each continent are shown in **Figure 2**. In addition to the anopheline mosquito species illustrated in **Figure 2**, *Anopheles umbrosus*, *An. vagus*, and *An. philippinensis* have been incriminated as vectors of malaria in human. Some studies revealed that the *Plasmodium* parasites in ungulate mammals could be transmitted by an anopheline mosquito (Boundenga et al., 2016, Martinsen et al., 2016). Martinsen et al. (2016) isolated the *Plasmodium* species from the salivary glands of *An. punctipennis* and DNA sequence analysis confirmed the parasite as *Plasmodium odocoilei*, which was in agreement with the malaria parasite

from white-tailed deer in North America (Martinsen et al., 2016). Although many research studies on the mosquito vector for human malaria transmission were carried out due to community health considerations, the mosquito vectors responsible for ungulate malaria remain obscure.

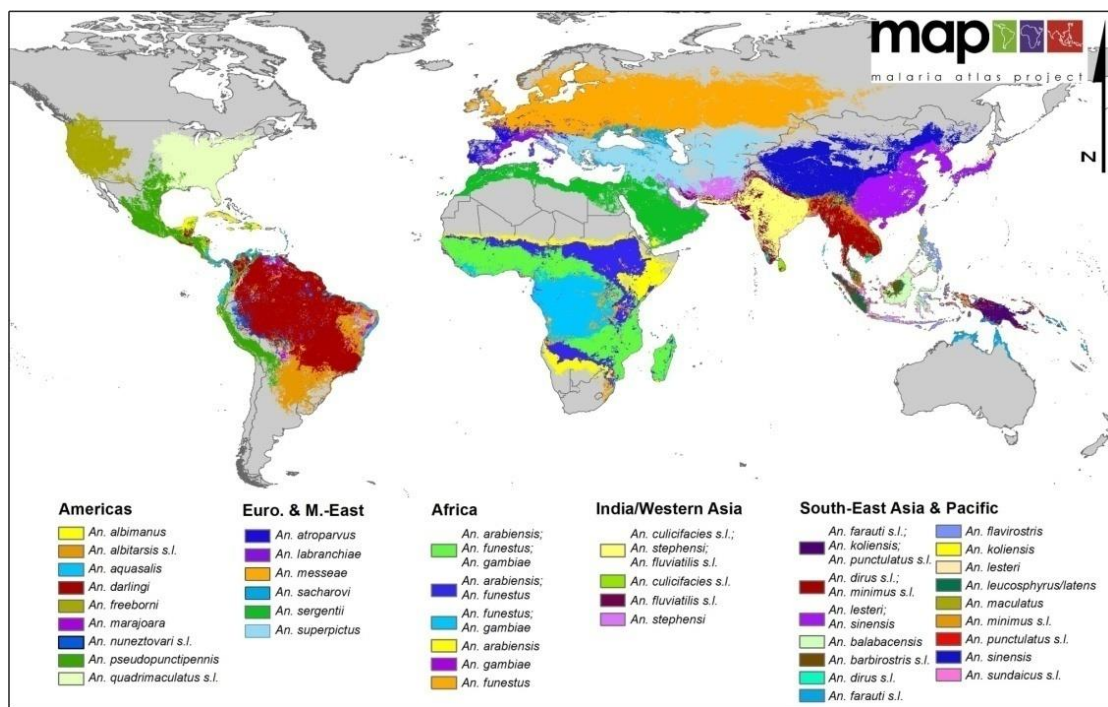


Figure 2. Global distribution of 34 dominant malaria vector mosquito species (Sinka et al., 2012).

CHAPTER 3

MATERIALS AND METHODS

3.1 Experiment 1: Natural infection of *Plasmodium caprae* and its co-infection

3.1.1 Sample size determination

According to statistics from the Food and Agriculture Organization (FAO, 2021) statistics, the number of goats raised in Thailand is 478,559 heads throughout the country, mainly by smallholders. In this study, goat blood samples were collected through cross-sectional and longitudinal studies to examine the prevalence of malaria in Thai goats during the rainy season. Blood samples were collected from 18 goat farms in three provinces of Thailand, including Kanchanaburi in 2020 (three farms), 2021 (three farms) and 2022 (two farms), Nan in 2020 (five farms) and 2021 (three farms), and Phetchaburi in 2021 (two farms). At each sampling site, the blood samples were collected once each rainy season depending on the consent and social situation. The estimated sample size was calculated using the following formula:

$$n = N * X / (X + N - 1), \text{ where } X = Z_{\alpha/2}^2 * p * (1-p) / \text{MOE}^2$$

In which n is the estimated sample size, $Z_{\alpha/2}$ represents the critical value of the normal distribution at $\alpha/2$ (confidence level of 95%, α is 0.05 and the critical value (Z) is 1.96), MOE abbreviates for the margin of error, p is the expected sample proportion of goat population, and N is the population size (Daniel, 1999). Therefore, the estimated sample size in this study was calculated as follows:

$$X = Z_{\alpha/2}^2 * p * (1-p) / MOE^2$$

$$X = 1.96^2 \times 0.5 \times (1-0.5) / 0.05^2$$

$$\Rightarrow X = 384.16$$

$$n = N * X / (X + N - 1)$$

$$n = 478,559 \times 384.16 / (384.16 + 478,559 - 1)$$

$$\Rightarrow n = 384$$

3.1.2 Blood sample collection

A total of 423 blood samples were collected from the jugular vein of goats from three provinces of Thailand. The goat was restrained by a human then the volume of 8 ml of blood was withdrawn and kept in BD Vacutainer® containing 1.5 ml of anticoagulant Acid Citrate Dextrose Solution (ACD) (BD Franklin Lakes, NJ, USA) and brought to the laboratory of the Faculty of Veterinary Science, Chulalongkorn University. A thin blood smear was conducted on site right after the blood collection, air dried, and then kept in the slide box for further staining. Genomic DNA was extracted from 1.5 ml of whole blood using a NucleoSpin® Blood extraction kit (Macherry-Nagel, Germany) following the manufacturer's protocol. This gDNA was stored at -20°C for later use.

3.1.3 Infection dynamics of *P. caprae* and co-infection with other protozoa parasites

All the blood samples were screened for *P. caprae* infection using universal primers targeting the *cytb* gene of haemosporidian parasites (Perkins et al., 2002, Templeton et al., 2016a). The *P. caprae* positive samples were further tested for co-infections with other blood pathogens that comprise anaplasmosis, theileriosis, and babesiosis. The primers used are described in detail in **Table 1**. Samples with co-infection with the other pathogens of interest were confirmed by DNA sequencing accordingly. Natural malaria-infected goats confirmed by the molecular method were followed up for 14 consecutive days. During this time, several parameters were monitored, including body temperature, appetite status, and clinical signs. One ml of blood was collected daily and kept in an ACD solution for further analysis.

3.1.4 Quantitative measurement of *P. caprae* based on microscopic examination and real-time PCR methods

Blood samples collected during the 14-day observation was quantitatively evaluated using both microscopic examination and real-time PCR. On the one hand, a thin blood smear was made on site, air-dried, and kept in a slide box until staining. The slides were fixed in methanol for 3 minutes and then stained with 10% Giemsa solution (v/v) for 40 minutes. After staining, slides every single day were observed every day under the light microscope (Olympus CX31, Tokyo, Japan) with a 1,000-time magnification to monitor each stage of parasite development. For the determination of parasitemia, a minimum of 2,000 red blood cells (RBCs) should be counted (WHO, 2015). Parasite levels were determined as a percentage of the number of infected red

blood cells in a total number of red blood cells counted. There has been very little published information about the morphology of *P. caprae* so far except for one study (Kaewthamasorn et al., 2018). However, several *Plasmodium* morphologies from other ungulates consisting of *P. bubalis* (Sheather, 1919, Templeton et al., 2016a), and *P. odocoilei* (Martinsen et al., 2016) were reported. Any suspected photos of *P. caprae* (early, late, trophozoite, schizont, microgamete, and macrogamete) were captured and documented. A negative blood smear was double checked to make sure the true negative result. On the other hand, the number of parasite's DNA copies was determined using real-time PCR (Applied Biosystems® Quant Studio™ Thermo Fisher Scientific, USA) after being checked with nested PCR as *Plasmodium*-positive. Real-time PCR was performed using SYBR® Green PCR Master Mix and primers targeting the *cytochrome oxidase subunit 1 (cox1)* gene. Primer sequences and the optimal real-time PCR condition are presented in **Table 1**.

3.1.5 Statistical analysis

Statistical analysis was conducted using SPSS version 22 software. For the cross-sectional study, the number of positive samples was reported as the prevalence of malaria in goats as well as its co-infections. The Chi-square test was used to assess the impact of rainy and dry seasons on the infection rate with a confidence interval of 95%. Fisher's exact test was used for the small expected frequency (less than 5). $P < 0.05$ was considered statistically significant.

Table 1. Primers and PCR conditions to monitor the course of natural infection of *P. caprae* and its co-infections

Parasite	Primer name	Primer sequence (5' - 3')	Expected size (bp)	PCR condition	Reference
<i>P. caprae</i> (<i>cytb</i>)	DW2	TAATGCCTAGAGGTATTCCTGATTATCCAG	1,256	94 °C: 2 min;	(Perkins et
	DW4	TGTTTGCTTGGGAGCTGTAATCATAATGTG		40 cycles: 98°C: 10 sec, 62°C: 3 min; 68°C: 5 min	al., 2002)
<i>Anaplasma</i>	NCYBINF	TAAGAGAATTATGGAGTGGATGGTG	822	94°C: 2 min;	(Templeton
	NCYBINR	CTTGTGGTAATTGACATCCAATCC		40 cycles: 98°C: 10 sec, 62°C: 3 min; 68°C: 5 min	et al., 2016a)
<i>marginale</i> (<i>msp2</i>)	MSP2F	ATGAGTGCTGTAAGTAATAGGAAGC	1,266	94°C: 5 min;	(Junsiri et al.,
	MSP2R	CTAGAAGGCAAAACCTAACACCCCAACTC		40 cycles: 98°C: 10 sec, 60°C: 30 sec; 68°C: 1 min 68°C: 5 min	2020)

Note: The letters in bold indicate amplification steps including denaturation, annealing, and extension in a number of 40 cycles.

Table 1 (cont). Primers and PCR conditions to monitor the course of natural infection of *P. caprae* and its co-infections

Parasite (Target gene)	Primer name	Primer sequence (5' – 3')	Expected size (bp)	PCR condition	Reference
<i>Anaplasma</i>	Abovis_groELFWD	TGAAGAGCCTTTGGCTGCTG	852	94°C: 5 min;	(Aung et al, 2022)
<i>bovis</i> (<i>groEL</i>)	Abovis_groELREV	CTCTCTATACTTGCAGAGCGGC		40 cycles: 98°C: 10 sec, 56°C: 30 sec; 68°C: 1 min 68°C: 5 min	
<i>Anaplasma</i>	Aovi_MSP5IF	CCACCTCCGAAGTTGCGAGC	777	94°C: 5 min;	(Aung et al, 2022)
<i>ovis</i> (<i>msp5</i>)	Aovi_MSP5IR	GCGCAAAACATGTTAAAGCCCATG		40 cycles: 98°C: 10 sec, 56°C: 30 sec; 68°C: 45 sec 68°C: 5 min	

Note: The letters in bold indicate amplification steps including denaturation, annealing, and extension in a number of 40 cycles.

Table 1 (cont). Primers and PCR conditions to monitor the course of natural infection of *P. caprae* and its co-infections

<i>P. caprae</i>	PiroPlasmoCoxIFout	GWRRWGGWACWGGATGGAC	708–717	94°C: 2 min;	(Tu et al., 2021)
<i>Babesia</i>	PiroPlasmoCoxIRout	CWAYDARHACWCCAGTWTGACCWCC		40 cycles: 94°C: 15 sec, 52°C: 30 sec,	
spp.,				68°C: 25 sec	
<i>Theileria</i>				68°C: 7 min	
<i>luwenshuni</i>	PcapraeCoxIFinn	CCTTTAAGTACATCTTTAATGTCCTTAT	664	94°C: 5 min;	(Tu et al., 2021)
(<i>cox1</i>)		CTCCAG		40 cycles: 98°C: 10 sec, 56°C: 30 sec;	
	PcapraeCoxIRinn	CAAAAGTAAATGTACATATAAATAATA		68°C: 45 sec	
		ATGCTAATAAAGATG		68°C: 5 min	
	BabeCoxIFinn	ATGAGTGGTGCTAATTTTGTGTTACT	555		
		TTTGG			
	BabeCoxIRinn	TTTACAACAATAAGAAATAGCCATC			
	TluweCoxIFinn	CTATAGGTTACGTTATAGATAGAATTC	320		
		TTCCAAC			
	TluweCoxIRinn	CAAACATCCCAATAAAGCGATAGAGGC			

3.2 Experiment 2: Multigene analysis of *Plasmodium caprae* and its related genera

3.2.1 Primer design for nuclear genes of *P. caprae*

The primers were adapted from previous successful amplifications of 21 nuclear genes from haemosporidian species (Borner et al., 2016), as well as nuclear DNA sequences available in the Plasmodium database (PlasmoDB) and the National Center for Biotechnology Information (NCBI). At least four nuclear protein-coding genes comprising the gamma subunit of eukaryotic translation initiation factor 2 (ETIF2), protein transport protein (Sec24a), RuvB-like helicase 3 (RuvB) and ribonucleoside-diphosphate reductase – large subunit (RDR) were amplified and underwent sequencing. For each gene, two pairs of degenerate primers were designed based on *Plasmodium odocoilei* and the other conserved sequences that have a close relationship with *P. caprae* and are available in the PlasmoDB and NCBI databases, as illustrated in **Figure 3**. *Plasmodium odocoilei* sequences were used as the primary sequences for primer design, with the outer primers highlighted in yellow while inner primers are in blue. The remaining nuclear genes were also amplified if they were successful in gaining more informative data. Nucleotide sequence alignment was conducted using the online tool Multiple Sequence Alignment Clustal Omega (<https://www.ebi.ac.uk/Tools/msa/clustalo/>). Conserved nucleotide regions were manually chosen that have similar melting temperatures and high CG content. Oligonucleotide degenerate primers were synthesized by Pacific Science, Thailand (<http://www.pacificscience.co.th/>).

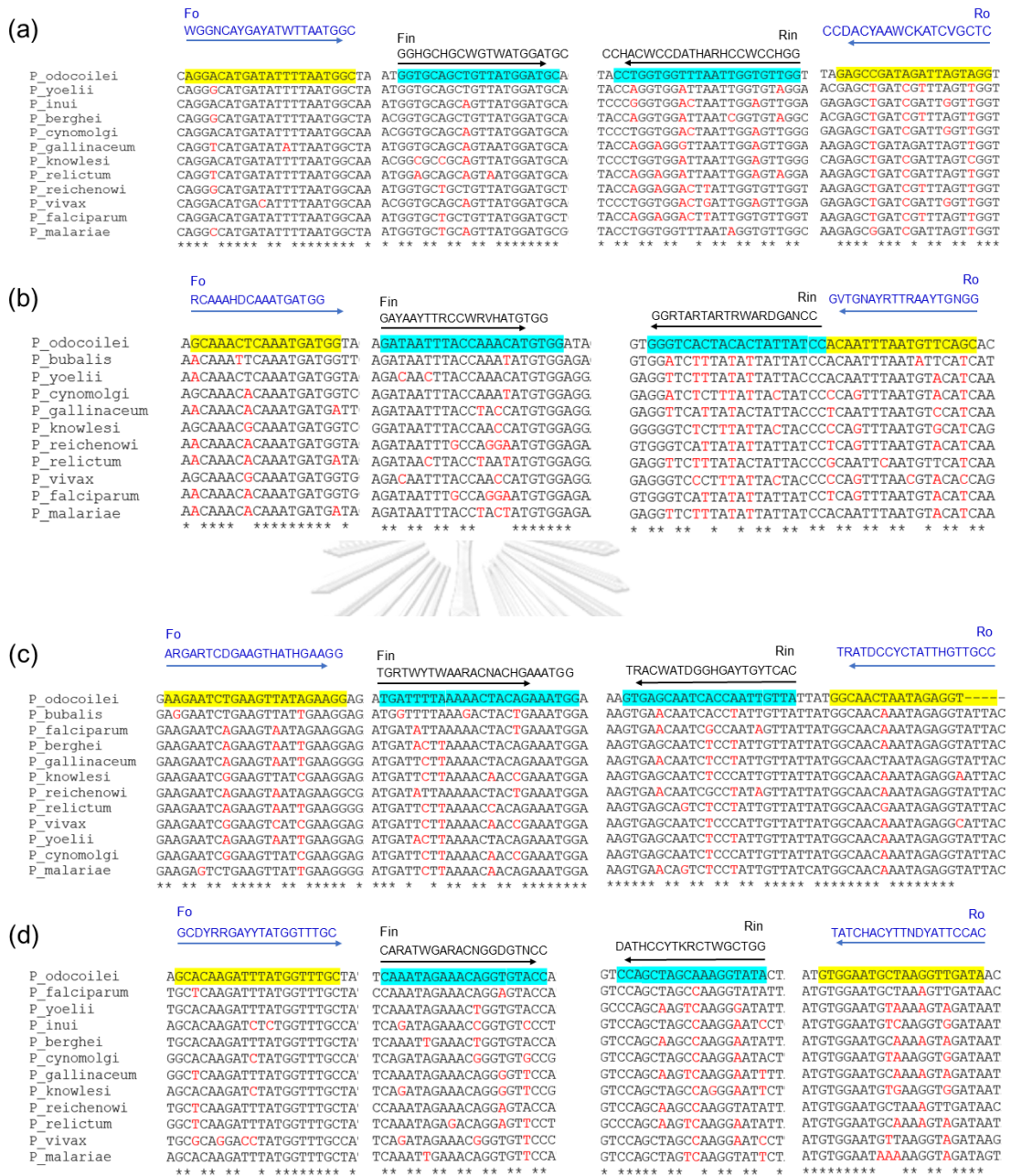


Figure 3. Sequence alignment and primer design for *P. caprae* nuclear gene amplifications. All sequences referred to *P. odocoilei* and were aligned with orthologous genes available in the PlasmoDB and NCBI databases. (a) ETIF2: MF508338_ *P. odocoilei*, (b) Sec24a: MF775866_ *P. odocoilei*, (c) RuvB: MF775893_ *P. odocoilei*, (d) RDR: MF508492_ *P. odocoilei*. The *P. odocoilei* sequences were used as the basis for primer design. The outer primer sequences of *P. odocoilei* are

highlighted in yellow, and the inner primer sequences of *P. odocoilei* were highlighted in light blue. Degenerate outer and inner primers were indicated by blue and black arrows, respectively. The mismatch nucleotides are highlighted in red.

3.2.2 DNA amplification of *P. caprae* nuclear genes

Nested touchdown PCR amplifications were carried out using the KOD Fx Neo (Toyobo, Japan) for both primary and nested rounds with a volume of 12.5 μ l. For primary PCR amplification, one μ l of genomic DNA from *P. caprae*-positive goat blood was used to amplify with outer primers as presented in **Table 2**. The amplicon sizes of the outer primers ranged from 536 to 657 bp. For nested rounds, two μ l of the primary PCR product without dilution was used to amplify with inner primers and then reamplified the third time with the same inner primers. The amplicon sizes of the inner primers ranged between 410 and 578 bp. The primer sets and the touchdown PCR conditions are described in detail in **Table 2**. According to a previous study, malaria in goats showed extremely low parasitemia (Kaewthamasorn et al., 2018); therefore, many *P. caprae positive* blood samples collected from different goats were combined, followed by DNA extraction to increase the amount of parasite DNA. This gDNA was used as a template for the amplification of four nuclear genes. The sterile distilled water was used as a no template negative control.

3.2.3 DNA cloning and sequencing

The expected PCR amplicons of each target nuclear gene were cut from 1.5% agarose gel and purified using NucleoSpin® Gel and PCR clean-up kit (Macherey-Nagel, Germany). The addition of A-overhang was performed using gel purification product

with Target Clone™-Plus (Toyobo, Japan) before being ligated into pTA2 plasmid vector according to the manufacturer's protocol. Then this plasmid vector that harbors the target nuclear gene was transformed into the DH5 α *E. coli*, followed by incubated at 37 ° C for 18 hours. Single white colonies were chosen and the successful insertion of the nuclear gene of interest was verified with universal primers M13. Successfully, plasmid-containing *E. coli* cells were continuously proliferated with LB broth in the shaking incubator at 37 ° C, 225 rpm for 18 hours. The plasmid DNA was then extracted using NucleoSpin® Plasmid QuickPure (Macherey-Nagel, Germany) and sent for sequencing with universal primers M13-20 and M13-48 at Pacific Science and U2Bio, Thailand.

3.2.4 Data analysis

Sequencing results were manually edited, and ambiguous parts were trimmed in BioEdit software version 7.0.5.3 (Hall, 1999). Primer regions were removed from the sequences. The final sequences were blasted and compared to the reference sequences available in the GenBank database using the BLASTN tool that is freely accessible at (<https://blast.ncbi.nlm.nih.gov/Blast.cgi>) with default settings. The sequences obtained from this study were deposited in the GenBank database. Analysis of nucleotide sequences between obtained sequences and other *Plasmodium* spp. was performed, and the phylogeny of *Plasmodium* genera was constructed. Reference sequences from other *Plasmodium* and haemosporidian parasites of four target nuclear genes were retrieved from the PlasmoDB and NCBI databases. The DNA sequences of mitochondrial, apicoplast and nuclear genes were concatenated using MEGA-X software version 10.0.4 available online at <https://www.megasoftware.net/>

(Kumar et al., 2018). To find the best-fit partitioning schemes and nucleotide substitution models for multigene analysis, partition finder version 2 was employed that can be accessed at <http://www.robertlanfear.com/partitionfinder/> (Lanfear et al., 2012). The phylogenetic tree was constructed using Maximum Likelihood in the IQ-TREE 1.6.12 software, which can be downloaded from <http://www.iqtree.org/> (Minh et al., 2020). Another method, Bayesian inference, was also utilized to construct the phylogenetic tree in MrBayes 3.2.7 software, which is freely accessible at <http://nbisweden.github.io/MrBayes/index.html> (Huelsenbeck and Ronquist, 2001). The tree file was visualized and decorated with Figtree 1.4.3 software, which is available at <http://tree.bio.ed.ac.uk/software/figtree/>. The haplotype and genetic diversity were determined in DNaSP version 6.10.04 (Rozas et al., 2017). The haplotype network was created using median joining and TCS methods in the Population Analysis with reticulate trees (PopART) (Leigh and Bryant, 2015). Genetic differentiation (F_{ST}) and analysis of molecular variance (AMOVA) of dominant mosquito species were performed in Arlequin version 3.5.2.2, and significance was determined using a default setting of 1,023 permutations (Excoffier et al., 2005). $F_{ST} > 0.25$ indicates significant genetic differentiation, 0.15 to 0.25 indicates moderate differentiation, and $F_{ST} < 0.05$ indicates minimal differentiation (Wright, 1978). The levels of gene flow as measured by the number of migrants (N_m) were calculated based on F_{ST} following the previous formula (Hudson et al., 1992). $N_m > 1$ indicates high gene flow, N_m between 0.25 and 0.99 indicates intermediate gene flow, and $N_m < 0.25$ indicates low gene flow (Govindaraju, 2009).

Table 2. Primer sequences for nuclear gene amplification and touchdown PCR conditions

Parasite (Target gene)	Primer name	Primer sequence (5' -3')	Expected size (bp)	Expected Touchdown PCR condition	Reference
<i>P. caprae</i>	MF508338_ETIF2	WGGNCAYGAYATWTTAATGGC	657	94°C: 5 min	This study
(<i>ETIF2</i>)	_Fout	CCDACYYAAWCKATCVGCTC		10 cycles: 98°C: 10 sec, 50°C: 30 sec; 68°C: 40 sec	
	MF508338_ETIF2			10 cycles: 98°C: 10 sec, 48°C: 30 sec; 68°C: 40 sec	
	_Rout			10 cycles: 98°C: 10 sec, 46°C: 30 sec; 68°C: 40 sec	
				5 cycles: 98°C: 10 sec, 44°C: 30 sec; 68°C: 40 sec	
				5 cycles: 98°C: 10 sec, 42°C: 30 sec; 68°C: 40 sec	
				68°C: 5 min	

Note: The letters in bold indicate amplification steps including denaturation, annealing, and extension in a number of N cycles.

Primer ending name: Fout: outer forward, Rout: outer reverse, Fin: inner forward, Rin: inner reverse

Table 2 (cont). Primer sequences for nuclear gene amplification and touchdown PCR conditions

Parasite (Target gene)	Primer name	Primer sequence (5' -3')	Expected size (bp)	Touchdown PCR condition	Reference
<i>P. caprae</i>	MF508338_ETIF2	GGHGCHGCWGTWATGGATGC	578	94°C: 5 min	This study
(<i>ETIF2</i>)	_Fin	CCHACWCCDATHARHCCWCCHGG		10 cycles: 98°C: 10 sec, 54°C: 30 sec; 68°C: 35 sec	
	MF508338_ETIF2			10 cycles: 98°C: 10 sec, 52°C: 30 sec; 68°C: 35 sec	
	_Rin			10 cycles: 98°C: 10 sec, 50°C: 30 sec; 68°C: 35 sec	
				5 cycles: 98°C: 10 sec, 48°C: 30 sec; 68°C: 35 sec	
				5 cycles: 98°C: 10 sec, 46°C: 30 sec; 68°C: 35 sec	
				68°C: 5 min	

Note: The letters in bold indicate amplification steps including denaturation, annealing, and extension in a number of N cycles.

Primer ending name: *Fout*: outer reverse, *Rout*: outer reverse, *Fin*: inner forward, *Rin*: inner reverse.

Table 2 (cont). Primer sequences for nuclear gene amplification and touchdown PCR conditions

Parasite (Target gene)	Primer name	Primer sequence (5'–3')	Expected size (bp)	Expected Touchdown PCR condition	Reference
<i>P. caprae</i>	MF775866_Sec24a	RCAAHIDCAAATGATGG	536	94°C: 5 min	This study
(Sec24a)	_ Fout			10 cycles: 98°C: 10 sec, 46°C: 30 sec; 68°C: 35 sec	
	MF775866_Sec24a	GVTGNAYRTTAAAYTGNGG		10 cycles: 98°C: 10 sec, 44°C: 30 sec; 68°C: 35 sec	
	_ Rout			10 cycles: 98°C: 10 sec, 42°C: 30 sec; 68°C: 35 sec	
				5 cycles: 98°C: 10 sec, 40°C: 30 sec; 68°C: 35 sec	
				5 cycles: 98°C: 10 sec, 38°C: 30 sec; 68°C: 35 sec	
				68°C: 5 min	

Note: The letters in bold indicate amplification steps including denaturation, annealing, and extension in a number of N cycles.

Primer ending name: Fout: outer forward, Rout: outer reverse, Fin: inner forward, Rin: inner reverse.

Table 2 (cont). Primer sequences for nuclear gene amplification and touchdown PCR conditions

Parasite (Target gene)	Primer name	Primer sequence (5'–3')	Expected size (bp)	Touchdown PCR condition	Reference
<i>P. caprae</i>	MF775866_Sec24a	GAYAAYTTTRCCWRVHATGTGG	410	94°C: 5 min	This study
(Sec24a)	_ Fin			10 cycles: 98°C: 10 sec, 46°C: 30 sec; 68°C: 25 sec	
	MF775866_Sec24a	GRTARTARWARDGANCC		10 cycles: 98°C: 10 sec, 44°C: 30 sec; 68°C: 25 sec	
	_ Rin			10 cycles: 98°C: 10 sec, 42°C: 30 sec; 68°C: 25 sec	
				5 cycles: 98°C: 10 sec, 40°C: 30 sec; 68°C: 25 sec	
				5 cycles: 98°C: 10 sec, 38°C: 30 sec; 68°C: 25 sec	
				68°C: 5 min	

Note: The letters in bold indicate amplification steps including denaturation, annealing, and extension in a number of N cycles.

Primer ending name: Fout: outer forward, Rout: outer reverse, Fin: inner forward, Rin: inner reverse.

Table 2 (cont). Primer sequences for nuclear gene amplification and touchdown PCR conditions

Parasite (Target gene)	Primer name	Primer sequence (5'-3')	Expected size (bp)	Touchdown PCR condition	Reference
<i>P. caprae</i>	MF775893_RuvB	ARGARTCDGAGGATHGAAGG	609	94°C: 5 min	This study
(<i>RuvB</i>)	_Fout	TRATDCCYCTATTGTTGCC		10 cycles: 98°C: 10 sec, 48°C: 30 sec; 68°C: 40 sec	
	MF775893_RuvB			10 cycles: 98°C: 10 sec, 46°C: 30 sec; 68°C: 40 sec	
	_Rout			10 cycles: 98°C: 10 sec, 44°C: 30 sec; 68°C: 40 sec	
				5 cycles: 98°C: 10 sec, 42°C: 30 sec; 68°C: 40 sec	
				5 cycles: 98°C: 10 sec, 40°C: 30 sec; 68°C: 40 sec	
				68°C: 5 min	

Note: The letters in bold indicate amplification steps including denaturation, annealing, and extension in a number of N cycles.

Primer ending name: Fout: outer forward, Rout: outer reverse, Fin: inner forward, Rin: inner reverse.

Table 2 (cont). Primer sequences for nuclear gene amplification and touchdown PCR conditions

Parasite (Target gene)	Primer name	Primer sequence (5' -3')	Expected size (bp)	Touchdown PCR condition	Reference
<i>P. caprae</i>	MF775893_RuvB	TGRTWYTWAARACNACHGAAATGG	492	94°C: 5 min	This study
(<i>RuvB</i>)	_Fin	TRACWATDGGHGAYTGTCAC		10 cycles: 98°C: 10 sec, 48°C: 30 sec; 68°C: 30 sec	
				10 cycles: 98°C: 10 sec, 46°C: 30 sec; 68°C: 30 sec	
	MF775893_RuvB			10 cycles: 98°C: 10 sec, 44°C: 30 sec; 68°C: 30 sec	
	_Rin			5 cycles: 98°C: 10 sec, 42°C: 30 sec; 68°C: 30 sec	
				5 cycles: 98°C: 10 sec, 40°C: 30 sec; 68°C: 30 sec	
				68°C: 5 min	

Note: The letters in bold indicate amplification steps including denaturation, annealing, and extension in a number of N cycles.

Primer ending name: Fout: outer forward, Rout: outer reverse, Fin: inner forward, Rin: inner reverse.

Table 2 (cont). Primer sequences for nuclear gene amplification and touchdown PCR conditions

Parasite (Target gene)	Primer name	Primer sequence (5'-3')	Expected size (bp)	Touchdown PCR condition	Reference
<i>P. caprae</i>	MF508492_RDR	GCDYRRGAYTATGGTTTGC	577	94°C: 5 min	This study
(RDR)	_Fout	DATHCCYTKRCTWGCTGG		10 cycles: 98°C: 10 sec, 50°C: 30 sec; 68°C: 35 sec	
	MF508492_RDR			10 cycles: 98°C: 10 sec, 48°C: 30 sec; 68°C: 35 sec	
	_Rin			10 cycles: 98°C: 10 sec, 46°C: 30 sec; 68°C: 35 sec	
				5 cycles: 98°C: 10 sec, 44°C: 30 sec; 68°C: 35 sec	
				5 cycles: 98°C: 10 sec, 42°C: 30 sec; 68°C: 35 sec	
				68°C: 5 min	

Note: The letters in bold indicate amplification steps including denaturation, annealing, and extension in a number of N cycles.

Primer ending name: Fout: outer forward, Rout: outer reverse, Fin: inner forward, Rin: inner reverse.

Table 2 (cont). Primer sequences for nuclear gene amplification and touchdown PCR conditions

Parasite (Target gene)	Primer name	Primer sequence (5'-3')	Expected size (bp)	Touchdown PCR condition	Reference
<i>P. caprae</i>	MF508492_RDR	CARATWGARACNGGDTNCC	510	94°C: 5 min	This study
(<i>RDR</i>)	_Fin	DATHCCYTKRCTWGCTGG		10 cycles: 98°C: 10 sec, 50°C: 30 sec; 68°C: 30 sec	
	MF508492_RDR			10 cycles: 98°C: 10 sec, 48°C: 30 sec; 68°C: 30 sec	
	_Rin			10 cycles: 98°C: 10 sec, 46°C: 30 sec; 68°C: 30 sec	
				5 cycles: 98°C: 10 sec, 44°C: 30 sec; 68°C: 30 sec	
				5 cycles: 98°C: 10 sec, 42°C: 30 sec; 68°C: 30 sec	
				68°C: 5 min	

Note: The letters in bold indicate amplification steps including denaturation, annealing, and extension in a number of N cycles.

Primer ending name: Fout: outer forward, Rout: outer reverse, Fin: inner forward, Rin: inner reverse.

3.3 Experiment 3: Mosquito composition and identification of the possible mosquito vector of *P. caprae* from goat farms

3.3.1 Mosquito collection

The mosquitoes were collected by two methods: CDC light trap and mouth aspirator. For the first method, the CDC light traps were mounted at a height of approximately 1.5 meters above the ground near the corner of the goat stable. The traps were set up from 6:00 pm to 6:00 am the next day. The collected mosquitoes were initially screened under a stereomicroscope to separate the anopheline and non-anopheline mosquitoes. Non-anopheline mosquitoes were kept in 70% ethanol. The second method, the mouth aspirator, needs a mosquito net and human power to work. The mosquito net was placed around the goat stable. Anopheline and other mosquitoes were collected using a mouth aspirator and then separated into unfed and blood-fed mosquito cups. The time to collect mosquitoes by mouth aspirator was from 7:00 pm to midnight (Ariey et al., 2020).

3.3.2 Morphological identification, dissection, and DNA extraction

The collected anopheline mosquitoes were identified as a group or species using a stereomicroscope based on the pictorial identification key (Rattanarithikul et al., 2006). For some groups that have a species complex, the mosquitoes were identified at the group level only. The gonotrophic status (unfed, blood fed, half-gravid and gravid) of all anopheline mosquitoes was determined using a stereomicroscope according to the blood digestion stage and ovarian development determination guidelines. The unfed mosquitoes were determined to have no blood abdomen, while the blood fed ones were partially or fully engorged with red blood. The dark red color

of blood covering 3-4 segments and the ovaries / eggs covering the rest of the mosquito abdomen were assigned as half-gravid, whereas the gravid mosquitoes were absent from blood and the ovaries/eggs covering almost all of the abdomen (Williams and Pinto, 2012). Then the anopheline mosquitoes were dissected to separate the midgut (body part) and salivary glands (head and thorax parts). DNA samples were extracted from the head and thorax parts of the mosquito, while the remaining body part of the unfed mosquito was kept in 70% alcohol and stored at -20 ° C for later use. The abdomen part of the blood-fed mosquitoes was individually extracted DNA for blood meal screening and analysis. The head and thorax parts of anopheline mosquitoes were pooled according to species, collection site, and gonotrophic status, while nonanopheline mosquitoes were pooled according to genus without any dissection. DNA extraction was carried out using NucleoSpin Tissue (Macherey-Nagel, Germany) according to the manufacturer's protocol. In the last step, genomic DNA was eluted twice with elution buffer. The first elution solution was used for the screening of *P. caprae*, while the second one was used for mosquito species confirmation. After obtaining the preliminary result of *P. caprae*-positive mosquito species by molecular method, more mosquitoes were collected, examined, and dissected the salivary gland then stained with mercurochrome dye to screen for the presence of sporozoites under the microscope. Any salivary gland that harbors the sporozoites was re-stained with Giemsa solution and the images were captured. DNA samples from abdomen part were subjected to blood meal analysis using primers and protocols described by Kent et al. (Kent and Norris, 2005).

3.3.3 Mosquito species identification and *Plasmodium* detection by molecular method

The mosquito species were identified by molecular method targeting the *cox1*, *cox2* genes, and the ITS2 region. The primers targeting the ITS2 region were described in a previous publication (Beebe and Saul, 1995) while the primers targeting the *cox1* and *cox2* genes were from a related study (Nugraheni et al., 2022). Mosquitoes were also tested for the presence of *Plasmodium* spp. using three different sets of primers targeting *cox1*, *cytb*, and *18S rRNA* genes. The primers used for mosquito species confirmation and *P. caprae* detection are described in **Table 3**. Conventional PCR was applied for the confirmation of mosquito species, but nested PCR was required for the detection of *P. caprae* because the parasitemia in the goat blood was extremely low based on our previous results (Kaewthamasorn et al., 2018). All PCR amplifications were performed on an Axygen® MaxyGene Thermal Cycler (Life Science, USA). Gel electrophoresis was set at 100 volts, 400 mA, and run for 40 minutes in 1.5% agarose gel stained with ethidium bromide. The result was evaluated under a UV transilluminator. The minimum infection rate (MIR) was determined for each mosquito species in which *Plasmodium* DNA was found in an attempt to assess the infection rate of positive mosquitoes. It was assumed that a mosquito pool had at least one infected mosquito if *Plasmodium* DNA was found. As a result, MIR was calculated using the previously mentioned formula: (number of positive pools/total number of mosquitoes studied) x 100 (Ventim et al., 2012). The MIR was estimated using the Wilson confidence interval method for binomial proportions with a 95% confidence interval (CI).

3.3.4 Blood meal source analysis in mosquito

Engorged mosquitoes were separated the blood-containing abdomen from the head and thorax, then extracted DNA for PCR amplification. The primers used to determine the source of blood meal in the abdomen were from previous study (**Table 3**). Nested multiplex PCR targeting the *cytochrome b* gene was used for amplification, consisting of the first round for general identification of mammalian blood, and nested round using the specific primers for human, cattle, pig, dog, and goat blood (Kent et al., 2005).

3.3.5 DNA sequencing and data analysis

The PCR products of mosquito species were bidirectionally sequenced using the same primers as conventional PCR. If the mosquito showed any expected amplicon with *Plasmodium* spp., the PCR product was sequenced to determine the exact species of *Plasmodium*. The DNA sequences were manually trimmed, edited in BioEdit, and further analyzed in DnaSP6 software to find out the number of haplotypes, and several parameters for the genetic diversity of mosquitoes. A haplotype network using concatenated genes was created using the TCS method in Population Analysis with Reticulate Trees (PopART) (Leigh et al., 2015). The overall prevalence and infection rate of *P. caprae* found in mosquitoes were analyzed using the Wilson confidence interval to estimate the proportion.

3.4 Ethical statements

This study has been approved by the Institutional Biosafety Committee and the Institutional Animal Care and Use Committee of the Faculty of Veterinary Science,

Chulalongkorn University (IBC No. 2031037; IACUC No. 2031083). All experiments were carried out according to university guidelines and regulations, as well as biosafety policies.



Table 3. Primer sequences for identification of mosquito species, *Plasmodium* spp. detection, blood meal analysis, and PCR conditions

Parasite (Target gene)	Primer name	Primer sequence (5'-3')	Expected size (bp)	PCR condition	Reference
<i>Anopheles</i> spp. (cox1)	AnplCox1-F	GGATCCCTTCAGCCATTTAATCGCG	1,585	94°C: 5 min	(Nugraheni et al., 2022)
	AnplCox1-R	TCGAGCTTAAATTCATTGGCACTAATCTGCC		40 cycles: 98°C: 10 sec, 56°C: 30 sec; 68°C: 1 min 40 sec 68°C: 5 min	
<i>Anopheles</i> spp. (cox2)	AnplCox2-F	GGATCCAGATTAGTGCAATGAATTAAGC	792	94°C: 5 min	(Nugraheni et al., 2022)
	AnplCox2-R	CTGCAGGATTTAAGAGATCATTACTTGC		40 cycles: 98°C: 10 sec, 58°C: 30 sec; 68°C: 50 sec 68°C: 5 min	

Note: The letters in bold indicate amplification steps in 40 cycles that included denaturation, annealing, and extension.

Table 3 (cont). Primer sequences for identification of mosquito species, *Plasmodium* spp. detection, blood meal analysis, and PCR conditions

Parasite (Target gene)	Primer name	Primer sequence (5'-3')	Expected size (bp)	PCR condition	Reference
<i>Anopheles</i> spp.	ITS2A	TGTGAACTGCAGGACACAT	450 – 1,500	94°C: 5 min	(Beebe et al.,
(ITS2)	ITS2B	TATGCTTAAATTCAGGGGGT		40 cycles: 98°C: 10 sec, 54°C: 30 sec; 68°C: 1 min 30 sec 68°C: 5 min	1995)

Note: The letters in bold indicate amplification steps in 40 cycles that included denaturation, annealing, and extension.

Table 3 (cont). Primer sequences for identification of mosquito species, *Plasmodium* spp. detection, blood meal analysis, and PCR conditions

Parasite (Target gene)	Primer name	Primer sequence (5'-3')	Expected size (bp)	PCR condition	Reference
<i>P. caprae</i>	Cox1_PbubF	GTACATTTACTTTTGGTGTAC	616	94°C: 5 min	(Nugraheni et
(<i>cox1</i>)	Cox1_PbubR	CCATCCACTCCATAAATCTC		40 cycles: 98°C: 10 sec, 50°C: 30 sec; 68°C: 40 sec	al., 2022)
	PbuCox1-F3-2	ATTATGTAATTGCACATTTCCATTITG	283	94°C: 5 min	(Nugraheni et
	PbuCox1-4B3	CCAAATAAAGTCATTGTWGAACC		40 cycles: 98°C: 10 sec, 60°C: 30 sec; 68°C: 20 sec	al., 2022)
				68°C: 5 min	

Note: The letters in bold indicate amplification steps in 40 cycles that included denaturation, annealing, and extension.

Table 3 (cont). Primer sequences for identification of mosquito species, *Plasmodium* spp. detection, blood meal analysis, and PCR conditions

Parasite (Target gene)	Primer name	Primer sequence (5'-3')	Expect size (bp)	PCR condition	Reference
<i>P. caprae</i>	DW2 (outer)	TAATGCCTAGACGTATTCCTGATTATCCAG	1,256	94°C: 5 min	(Perkins et al.,
(<i>cytb</i>)	DW4 (outer)	TGTTTGCTGGGAGCTGTAATCATAATGTG		40 cycles: 98°C: 10 sec, 62°C: 3 min; 68°C: 5 min	2002)
	NCYBINF (inner)	TAAGAGAAATTATGGAGTGGATGGTG	822	94°C: 5 min	(Templeton et
	NCYBINR (inner)	CTTGTGGTAATTGACATCCAATCC		40 cycles: 98°C: 10 sec, 62°C: 3 min; 68°C: 5 min	al., 2016a)

Note: The letters in bold indicate amplification steps in 40 cycles that included denaturation, annealing, and extension.

Table 3 (cont). Primer sequences for identification of mosquito species, *Plasmodium* spp. detection, blood meal analysis, and PCR conditions

Parasite	Primer	Primer sequence (5'-3')	Expect	PCR condition	Reference
(Target gene)	name		size (bp)		
<i>P. caprae</i>	rPLU6 (outer)	TTAAAATTGTTGCAGTTAAAACG	1,200	94°C: 5 min	(Snounou et
(18S rRNA)	rPLU5 (outer)	CCGTTGTTGCCTTAAACTTC		40 cycles: 98°C: 10 sec, 55°C: 30 sec; 68°C: 1 min 30 sec 68°C: 5 min	al., 1993)
	PlaSSUF1 (inner)	CTTAGTTACGATTAATAGGAGTAG	420	94°C: 5 min	(Nugraheni
	PlaSSUR1 (inner)	TCCTACTCTTGTCCTAAACTAG		40 cycles: 98°C: 10 sec, 49°C: 30 sec; 68°C: 30 sec 68°C: 5 min	et al., 2022)

Note: The letters in bold indicate amplification steps in 40 cycles that included denaturation, annealing, and extension.

Table 3 (cont). Primer sequences for identification of mosquito species, *Plasmodium* spp. detection, blood meal analysis, and PCR conditions

Primer name	Primer sequence (5'-3')	Product size with UNREV1025 (bp)	PCR condition	Reference
UNFOR403	TGAGGACAAATATCATTCTGAGG	623	94°C: 5 min	(Kent et al., 2005)
UNREV1025	GGTTGTCTCCTCCAATTCATGTTA		40 cycles: 95°C: 1 min, 58°C: 1 min; 68°C: 40 sec 68°C: 10 min	
Cow121F	CATCGGCACAAAATTTAGTCG	561	94°C: 5 min	(Kent et al., 2005)
Dog368F	GGAATTGTACTATTATTCGCAACCAT	680	40 cycles: 95°C: 1 min, 58°C: 1 min; 68°C: 40 sec	
Pig573F	CCTCGCAGCCGTAGATCTC	453	40 sec	
Human741F	GGCTTACTTCTCTTCATTCTCCT	334	68°C: 10 min	
Goat894F	CCTAATCTTAGTACTTGTACCCTTCCTC	132		

CHAPTER 4

RESULTS

4.1 Experiment 1: Natural infection of *Plasmodium caprae* and its co-infections

4.1.1 Goats' gender, age, and pregnancy status

Between June 2020 and March 2022, 401 blood samples were collected from goat farms in three Thai provinces. There were three collection periods in Kanchanaburi Province, with (i) 55 samples collected in June 2020, (ii) 70 samples collected in November 2021, and (iii) 60 samples collected in March 2022. In Nan province, there were two collection periods in three districts, (iv) 99 samples collected in August 2020 and (v) 50 samples collected in August 2021. Furthermore, in October 2021, 67 blood samples were collected in Phetchaburi province. There were 401 goats in total, 38 males and 363 females. Furthermore, 119 goats were one year old or younger, while 167 goats were older than one year. The sex, age, and pregnancy status of the other remaining goats were unknown. Because we were not allowed to collect goat blood in Ratchaburi in June 2021, we included a collection of 22 goat blood samples collected in June 2018 at the same farm in this study. However, gender and age information were missing.

4.1.2 Natural infection of *P. caprae* and its clinical outcomes

In the present study, the prevalence of *Plasmodium caprae* in goats in four provinces of Thailand was 1.42% (6 out of 423 samples), which was found in Nan (3 out of 149 samples), Phetchaburi (1 out of 67 samples) and Ratchaburi (2 out of 22 samples). However, none of the 185 samples collected in Kanchanaburi was found to be positive to *P. caprae*. We tracked a pregnant goat in Nan Province for 14 days out

of six *P. caprae* positive goats found in Ratchaburi 2018, Nan 2020, and Phetchaburi 2021. The other five goats were unable to be tracked due to far distance between goat farms and the human power deficiency. During that time, the body condition and temperature of an infected goat were recorded every morning. The parasite burden in the malaria-infected goat was investigated using quantitative real-time PCR. The parasite burden in naturally infected goats was as low as 5 copies per microliter of blood sample until day 15, with the highest parasite load on the first day of blood collection (4,510 copies/ μ l blood) then declined significantly before being undetected since day 16 after infection (**Figure 4**). The body temperature of a naturally infected goat fluctuated within the normal range (38.6 - 39.7 ° C) during the 14-day observation period, except for three days when the values exceeded 40 ° C and the goat was observed to have diarrhea. The goat's body temperature was not taken on the first day of blood collection (**Figure 5**). The early stage of trophozoites has only been found in the blood smear of naturally infected goat (THGoat20-101) on the first day of blood collection for microscopic examination, then went undetected for the next 14 days.

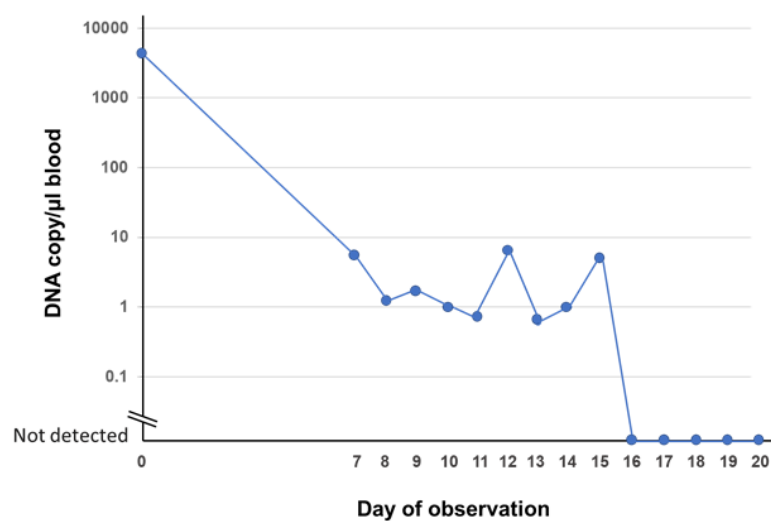


Figure 4. Malaria parasite's copy number in goat blood as measured by qPCR during the observation period in naturally infected goat ID THGoat20-101 in Nan Province.

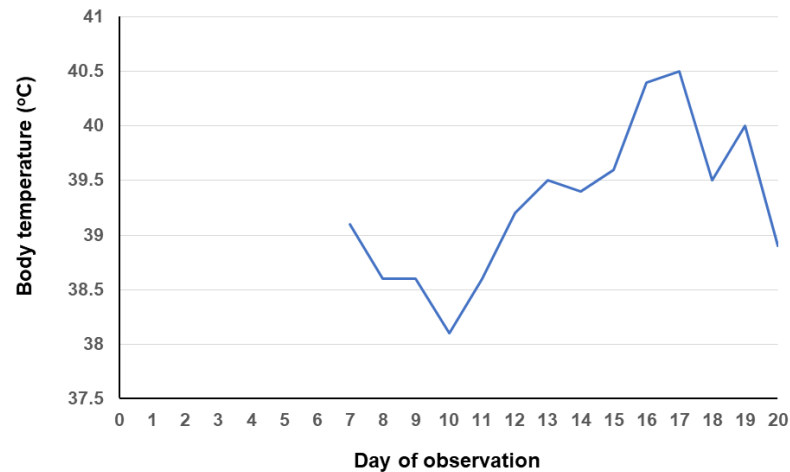


Figure 5. Body temperature of malaria in naturally infected goat ID THGoat20-101 in Nan Province during observation period.

4.1.3 Co-infection of goat with other protozoa parasites

Six *P. caprae*-positive goats were screened for the presence of other blood protozoa parasites using multiplex nested PCR to detect co-infections. The results revealed no co-infections of *Babesia* spp. and *Theileria luwenshuni* in any samples; however, four of them (three samples in Nan and one in Phetchaburi) were co-infected with *Anaplasma bovis* (accounted for 66.67%) based on the *groEL* gene. Except for malaria parasites, two samples collected in Ratchaburi in 2018 were not co-infected with any other blood parasites.

4.1.4 Association between season and malaria infection rate

The odds ratio showed that goats were 4.43 times more likely to be infected with *P. caprae* in the rainy season than in the dry season (**Table 4**). However, the

malaria infection rate in goats did not have a statistically significant difference between two seasons ($P > 0.05$) according to Fisher's exact test (**supplementary data 1**).

Table 4. Association between season and malaria infection rate

Season	Malaria infection		Odds ratio	95% confidential interval	P-value
	Positive	Negative			
Rainy	5	221	4.43	0.0065 – 0.0306	0.143
Dry	1	196			

4.2 Experiment 2: Multi-gene analysis of *Plasmodium caprae* and its related genera

4.2.1 *Plasmodium* identification based on nuclear genes

The sequencing results of four nuclear genes, ETIF2, Sec24a, RuvB, and RDR obtained in this study were all identified as *Plasmodium* species using searches by BLASTN in the PlasmoDB (<https://plasmodb.org/plasmo/app>) and the GenBank database. All sequences had between 80.41 and 94.79% identity with *Plasmodium* species genes previously deposited in the PlasmoDB and GenBank databases (**Table 5**). It is worth noting that no nuclear gene sequences of *P. caprae* or other ungulates have been previously deposited in GenBank. As a result, the percentage of identity in the BLASTN search results would be less than 95%. However, all BLASTN results revealed the correct genes within *Plasmodium* genera.

Table 5. BLASTN searches for *Plasmodium caprae* based on four nuclear genes.

Gene target	Size (bp)	Identification	Reference
1. Eukaryotic translation initiation factor 2 gamma subunit	578	94.79% with <i>P. odocoilei</i>	MF508338
2. Ribonucleoside-diphosphate reductase, large subunit	510	93.14% with <i>P. odocoilei</i>	MF508492
3. RuvB-like helicase 3	451	92.60% with <i>P. odocoilei</i>	MF775893
4. Protein transport protein Sec24a	410	80.41% with <i>P. lacertiliae</i>	MF775857

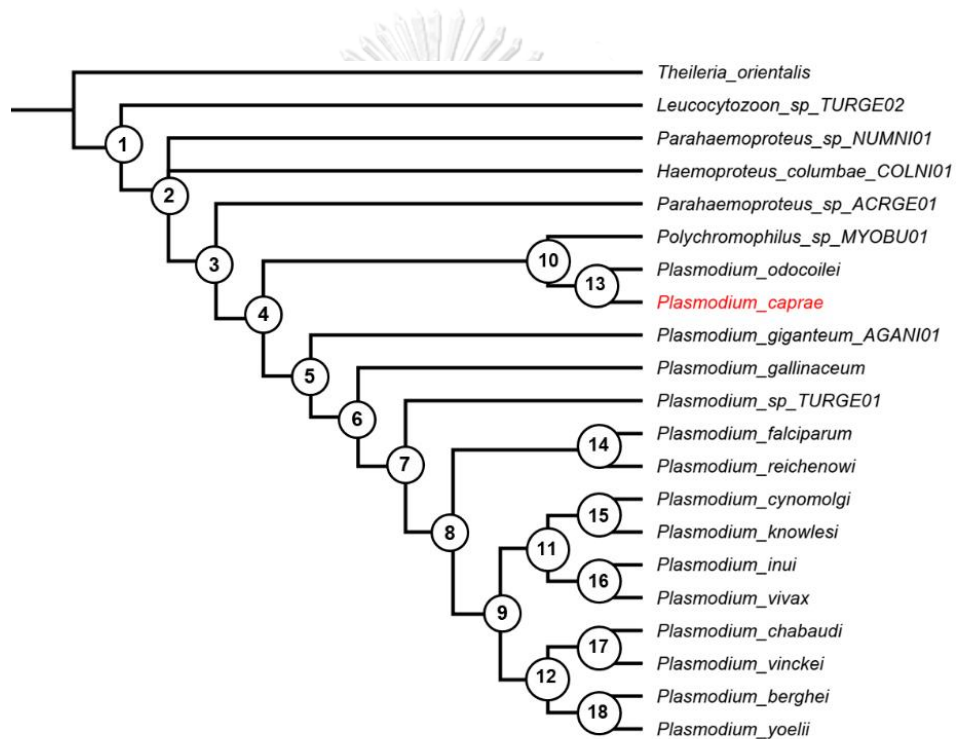
4.2.2 Molecular phylogeny of *Plasmodium caprae* based on four concatenated nuclear genes

Phylogenetic analyzes of all BI and ML methods were based on nucleotide, codon, and amino acid sequences. Posterior probabilities and bootstrap values are presented in **Figure 6a**. The analyses using Bayesian inference produced trees with the same topologies (**Figure 6b**), while the maximum likelihood analyses also resulted in similar trees (**Figure 6c**). *Plasmodium caprae* shared the 13th node with *Plasmodium odocoilei* in cervids. Only the tree derived from the BI nucleotide analysis had high support values and was highly congruent between the BI and the ML. Although they had slightly different topologies at the *Haemoproteus columbae* COLNI01, phylogenetic trees based on BI and ML (codons and amino acids) remained in agreement. According to nuclear gene analysis, *P. caprae* was a sister lineage of *P. odocoilei* (deer parasite) and had a close relationship with *Polychromophilus* sp. (bat parasite), as shown in **Figures 7 - 9**.

(a)

Node	1	2	3	4	5	6	7	8	9	10	11	12	13	14	15	16	17	18
Method																		
Bayes nucleotides	0.8	0.78	0.8	0.79	0.8	0.8	0.8	0.76	0.78	0.79	1	1	1	1	1	1	1	1
Bayes codons	1	0.77	0.58	0.91	0.62	0.99	0.99	1	1	0.66	1	1	1	1	1	0.99	1	1
Bayes proteins	1	0.52	0.65	0.88	0.91	0.97	0.96	1	1	0.64	1	1	1	1	0.94	0.77	0.97	0.96
ML nucleotides	77	77	77	74	80	80	80	60	84	77	92	98	100	100	92	92	86	99
ML codons	70	70	52	68	70	70	70	90	91	68	100	100	99	100	100	98	97	94
ML proteins	82	67	49	87	57	79	81	92	92	42	100	100	96	100	80	91	88	70

(b)



2.0

(c)

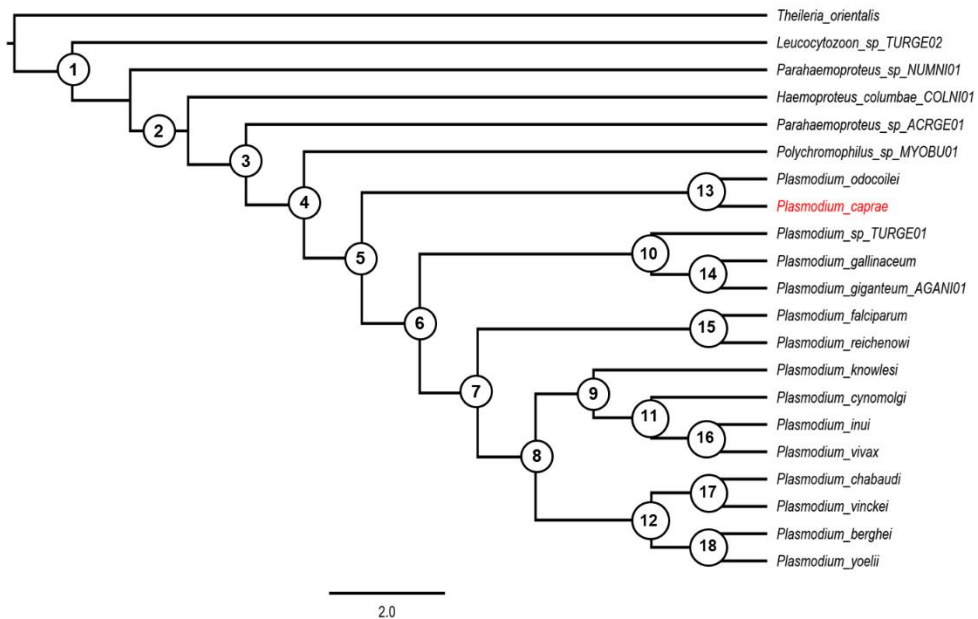


Figure 6. Bayesian posterior probabilities and Maximum likelihood bootstrap values from analysis of four concatenated nuclear genes (a). Consensus cladogram of the analysis using Bayesian inference (b). Consensus cladogram of analysis using Maximum likelihood (c). The non-haemosporidian parasite (*Theileria orientalis*) as an outgroup was displayed. Taxa recovered in this study were highlighted in red letters. The length (2.0) indicated the number of substitutions per site.

จุฬาลงกรณ์มหาวิทยาลัย

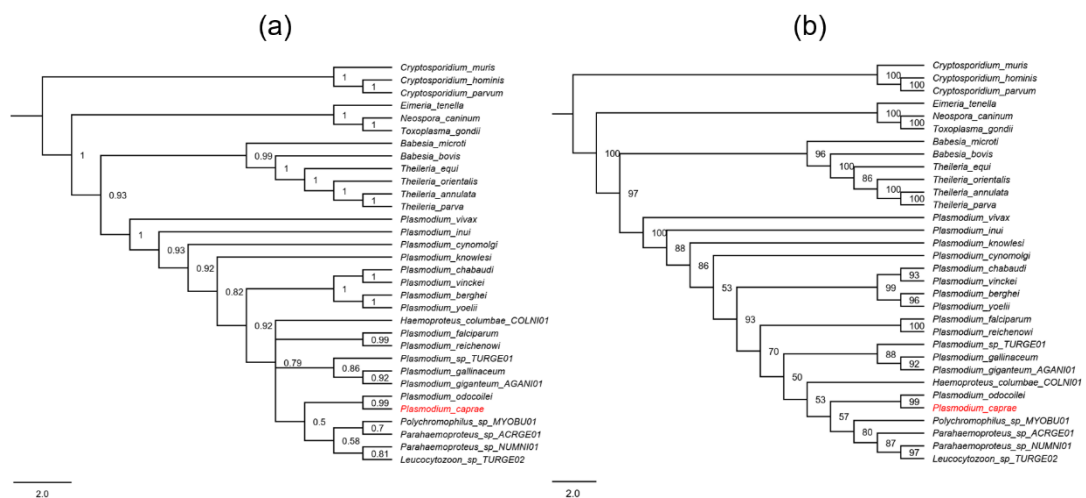


Figure 7. Phylogenetic trees of four concatenated nuclear genes based on nucleotides. Bayesian inference **(a)** and Maximum likelihood **(b)**. Bayesian posterior probabilities and bootstrap values were shown at the nodes. All trees were rooted with *Cryptosporidium* as an outgroup. The concatenated sequence of *P. caprae* obtained from this study is colored red. The length (2.0) indicated the number of substitutions per site.

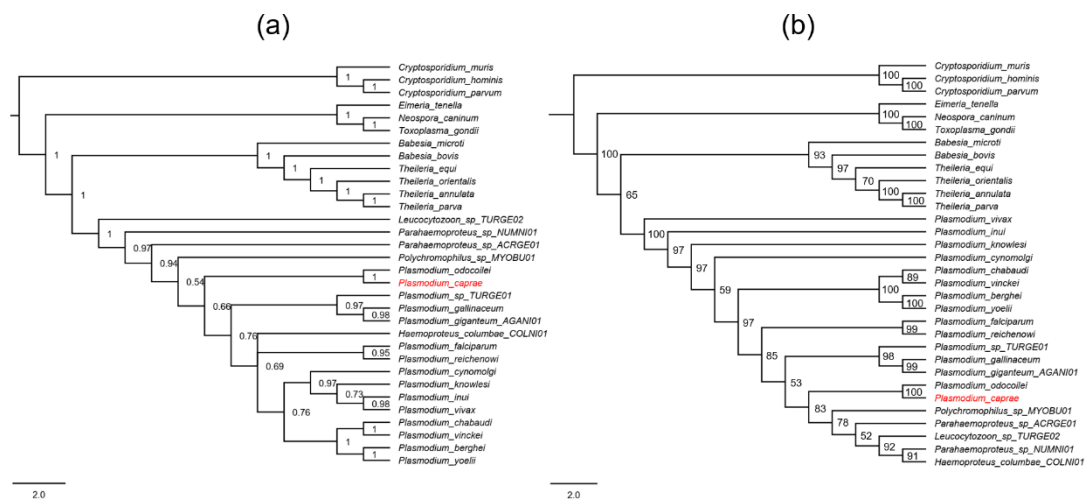


Figure 8. Phylogenetic trees of four concatenated nuclear genes based on codons. Bayesian inference **(a)** Maximum likelihood **(b)**. Bayesian posterior probabilities and bootstrap values were shown at the nodes. All trees were rooted with *Cryptosporidium* as an outgroup. The concatenated sequence of *P. caprae* obtained from this study is colored red. The length (2.0) indicated the number of substitutions per site.

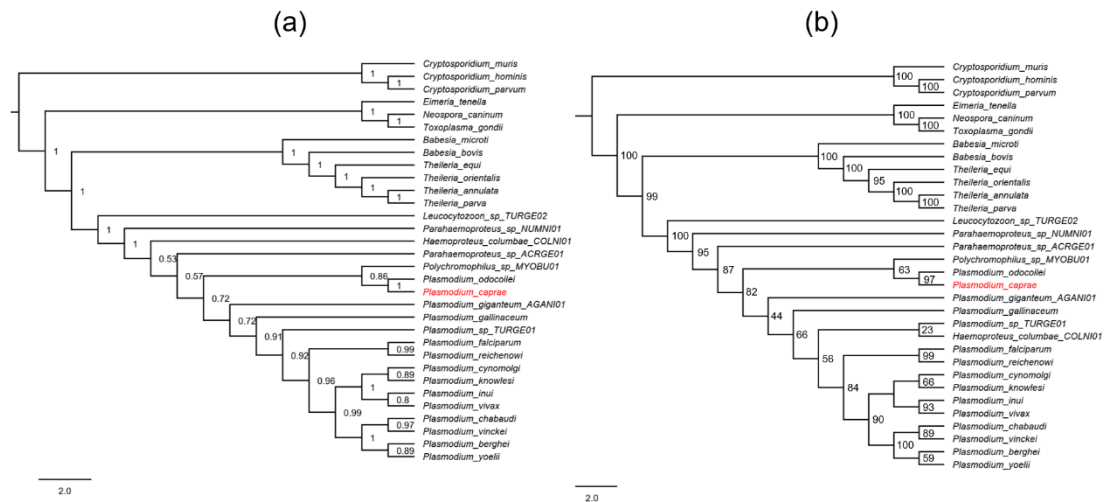


Figure 9. Phylogenetic trees of four concatenated nuclear genes based on amino acids. Bayesian inference (a) and Maximum likelihood (b). Bayesian posterior probabilities and bootstrap values were shown at the nodes. All trees were rooted with *Cryptosporidium* as an outgroup. The concatenated sequence of *P. caprae* obtained from this study is colored red. The length (2.0) indicated the number of substitutions per site.

4.2.3 Molecular phylogeny of *Plasmodium caprae* based on concatenated *cox1*, *cytb*, *clpC*, and four nuclear genes

The four nuclear genes obtained from this study were concatenated together with two mitochondrial genes (*cox1* and *cytb*) and one apicoplast gene (*clpC*) recovered from the public databases (GenBank and PlasmoDB) to investigate more about the phylo-genetic position and relationship among *Plasmodium* and other hemopodidian parasites. Bayesian inference (BI) and maximum likelihood (ML) were employed to construct the phylogenetic tree using our four nuclear genes and orthologous genes retrieved from the GenBank and PlasmoDB databases, with a total length of 4,044 bp. The topology of both BI and ML revealed that *Plasmodium caprae*

was clustered in the same clade with other Artiodactyla even-toed ungulate parasites (*P. bubalis* in water buffaloes and *P. odocoilei* in cervids and mosquitoes) and had close relationship with the bat parasite of the genus *Polychromophilus*. The consensus tree of BI and ML was represented in Figure 10.

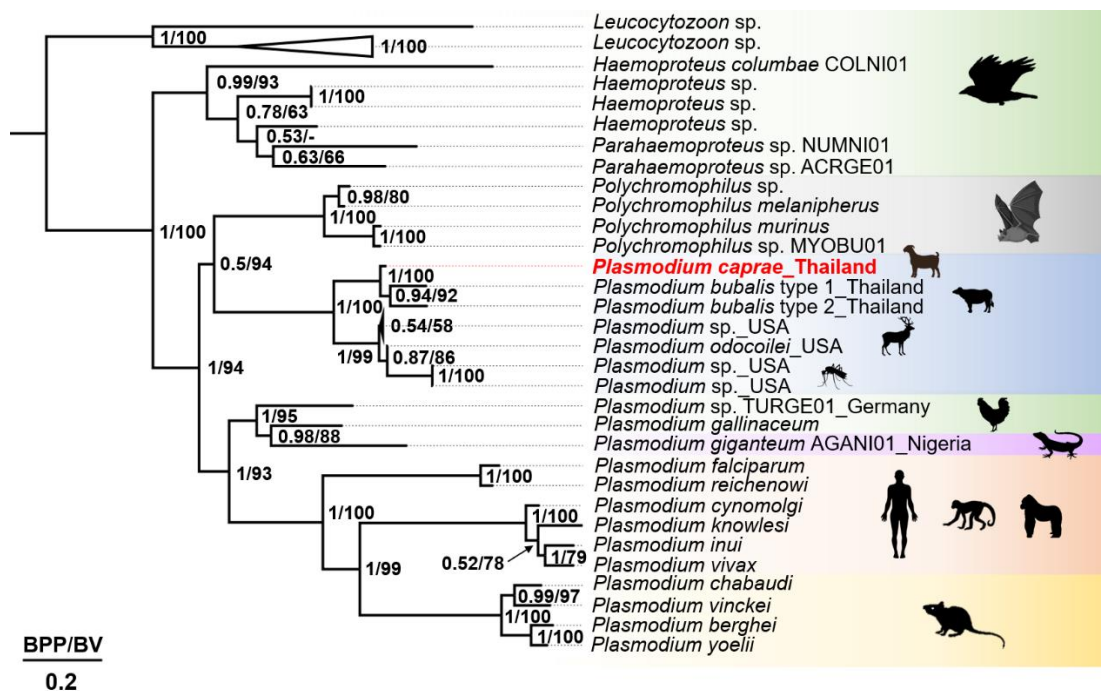


Figure 10. Consensus tree based on BI and ML analyzes using concatenated nucleotides (4,044 bp) of two mtDNA (*cox1*, *cytb*), one apDNA (*clpC*) and four novel nuDNA genes (ETIF2, Sec24a, RuvB and RDR). Bayesian posterior probabilities (BPP) and Maximum likelihood bootstrap values (BV) more than 0.5/58 were given at the nodes. A bootstrap value less than 50 was presented as '-'. The length (0.2) indicated the number of substitutions per site. The sequence of the goat malaria parasite *P. caprae* obtained from this study is highlighted in red. The icons in black represented the animal hosts of haemosporidian parasites.

4.3 Experiment 3: Mosquito composition and identification of the possible mosquito vector of *P. caprae* from goat farms

4.3.1 Mosquito species composition collected from goat farms based on morphological and molecular identifications

A total of 1,152 female mosquitoes were collected by mouth aspirator (n = 951), and CDC light trap (n = 201) from six goat farms in Kanchanaburi, Phetchaburi, Ratchaburi, and Nan. Morphological examination of mosquitoes collected by CDC light trap showed that *Culex* spp. accounted for 61.2% (n = 123), while *Anopheles* spp. accounted for 33.8% (n = 68), *Mansonia* spp. accounted for 2.0% (n = 4), and unidentified species due to wing and/or leg destruction constituted 3.0% (n = 6) (**Figure 11a**). The number of adult female anopheline mosquitoes collected in goat farms were as follows: Kanchanaburi (n = 534), Ratchaburi (n = 285), Phetchaburi (n = 86) and Nan (n = 114) during June 2020 to March 2022. The following species were found in the current study: *An. peditaeniatus* (n = 493) and *An. pursati* (n = 15) (Hyrcanus), *An. barbirostris* (n = 36) and *An. campestris* (n = 12) (Barbirostris), *An. subpictus* (n = 296) and *An. vagus* (n = 83) (Subpictus), *An. aconitus* (n = 72) (Funestus), *An. tessellatus* (n = 9) (Tessellatus), and *An. philippinensis* (n = 3) (Annularis). Five species were found in three western provinces (Kanchanaburi, Ratchaburi, and Phetchaburi), while six species were detected in northern Nan province. The most dominant mosquito species in Kanchanaburi and Nan belong to Hyrcanus Group (*An. peditaeniatus*) while the Subpictus group (*An. subpictus* and *An. vagus*) was the most prevalent in Ratchaburi and Phetchaburi, respectively (**Figure 11b**).

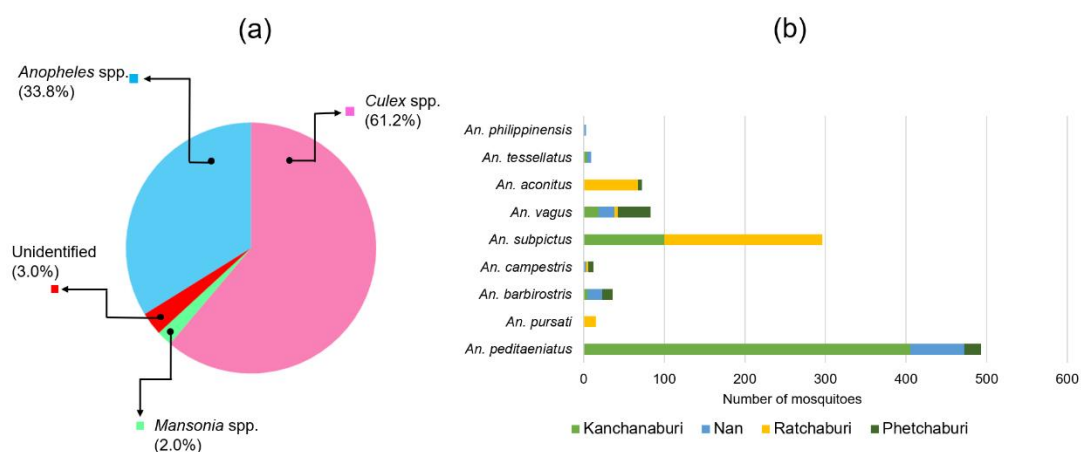


Figure 11. Chart illustrating the percentage and number of mosquitoes collected according to morphological identification. Percentages of each genus collected by the CDC light trap at goat farms **(a)**. Anopheline mosquitoes collected from goat farms by mouth aspirator according to the species in this study **(b)**.

The four different types of gonotrophic status of anopheline mosquitoes are shown in **Table 6**. Most of mosquitoes collected were unfed (44.85%), followed by gravid mosquitoes, which accounted for 33.86%. Approximately 12.37% of the collected mosquitoes were blood-engorged, and half-gravid mosquitoes accounting for 8.93% of the total collection.

Table 6. Number of anopheline mosquitoes collected in the present study according to gonotrophic status.

Status	Sampling site				Total
	Kanchanaburi	Nan	Ratchaburi	Phetchaburi	
Unfed	195	83	146	33	457
Blood-fed	52	20	41	13	126
Half-gravid	59	0	24	8	91
Gravid	228	11	74	32	345

Total	534	114	285	86	1,019
--------------	-----	-----	-----	----	--------------

A total of 363 sequences representing nine species were successfully obtained from direct sequencing of 126 mosquito pools in this study, including 120 *cox1*, 119 *cox2*, and 124 ITS2 sequences. The remaining 15 sequences were excluded from analysis because the chromatograms were ambiguous. The high similarity (97%) of each sequence with deposited sequences in GenBank or BOLD databases was considered to be within the same species. In general, the search results were consistent across three genetic markers, except for *cox1* sequences from five different species. Using *cox1* as a query for the BLASTN search against the GenBank database, the results indicate closely related species of anopheline mosquitoes within the same group. *Cox2* and ITS2 queries against the GenBank and BOLD databases revealed consistent results (Table 7).

Table 7. Overview of search results using *cox1*, *cox2* and ITS2 sequences in the BOLD and GenBank database.

BOLD ID	GenBank ID	Designated ID		
<i>cox1</i> (%)	<i>cox1</i> (%)	<i>cox2</i> (%)	ITS2 (%)	
<i>An. peditaeniatus</i>	<i>An. peditaeniatus</i>	<i>An. peditaeniatus</i>	<i>An. peditaeniatus</i>	<i>An. peditaeniatus</i>
99.45 – 100%	98.60 – 99.39%	99.56 – 100%	99.83 – 100%	
	(MT669948)	(JX070691)	(MF535198)	
<i>An. vagus</i>	<i>An. vagus</i>	<i>An. vagus</i>	<i>An. vagus</i>	<i>An. vagus</i>
98.74 – 100%	97.80 – 98.31%	95.35 – 100%	99.85 – 100%	
	(MT669956)	(JX070730)	(AB731658)	
<i>An. aconitus</i>	<i>An. aconitus</i>	<i>An. aconitus</i>	<i>An. aconitus</i>	<i>An. aconitus</i>

97.92 – 98.62%	97.03 – 99.4%	99.49 – 100%	100%	
	(HQ877378)	(JX070686)	(MF535233)	
<i>An. tessellatus</i>	<i>An. tessellatus</i>	<i>An. tessellatus</i>	<i>An. tessellatus</i>	<i>An. tessellatus</i>
99.54 – 100%	93.59 – 93.98%	99.13 – 100%	97.59 – 99.63%	
	(MT669953)	(EU620674)	(AB731657)	
<i>An. subpictus</i>	<i>An. epiroticus</i>	<i>An. subpictus</i>	<i>An. subpictus</i>	<i>An. subpictus</i>
97.82 – 100%	91.85 – 93.32%	93.61 – 96.38%	99.16 – 100%	
	(KT382821)	(KX669656)	(GQ870330)	
<i>An. barbirostris</i>	<i>An. donaldi</i>	<i>An. barbirostris</i>	<i>An. barbirostris</i>	<i>An. barbirostris</i>
99.54 – 100%	97.12 – 97.29%	99.45 – 100%	98.89 – 99.53%	
	(MT669935)	(AB331591)	(AB435985)	
<i>An. campestris</i>	<i>An. donaldi</i>	<i>An. campestris</i>	<i>An. campestris</i>	<i>An. campestris</i>
99.39 – 100%	97.07 – 97.12%	99.32 – 100%	98.47 – 100%	
	(MT669938)	(AB331601)	(AB436084)	
<i>An. philippinensis</i>	<i>An. maculatus</i>	<i>An. philippinensis</i>	<i>An. philippinensis</i>	<i>An. philippinensis</i>
94.67 – 94.83%	90.27 – 90.33%	99.69 – 100%	99.79%	
	(KT382822)	(AM396698)	(FJ526619)	
<i>An. pursati</i>	<i>An. sinensis</i>	<i>An. pursati</i>	<i>An. pursati</i>	<i>An. pursati</i>
98.77 – 99.08%	92.88 – 93.32%	99.32 – 99.59%	100%	
	(MG816554)	(AB826103)	(AB826062)	

Note: ID refers to identification; search results are shown only the highest hit target with ranges of % identity to the closest reference sequence (accession number in parentheses). Contradictory BLASTN results are highlighted in blue and subsequently ignored on the ground that a divergence of 2 to 3% is a threshold for intraspecific variation (Hebert et al., 2003).

4.3.2 Molecular detection and phylogenetic analysis of *P. caprae* from mosquito samples

On the one hand, a total of 322 anopheline mosquitoes were dissected to separate their salivary glands with head and thorax from the abdomen part. The salivary glands were then stained with 0.1% mercurochrome dye and examined under a microscope. However, no sporozoites were not found. Then, depending on the groups and species, one to three samples including salivary gland, head, and thorax were pooled for DNA extraction; finally, 358 mosquito pools were prepared. DNA was extracted from the pooled samples and PCR was performed for *Plasmodium cytb*, *cox1*, and *18S rRNA* genes. The number of each pool was as follows: Hyrcanus (n = 508, 175 pools), Barbirostris (n = 48, 19 pools), Subpictus (n = 379, 130 pools), Aconitus (n = 72, 27 pools) Tessellatus (n = 9, 5 pools), and Annularis (n = 3, 2 pools). Of 358 pools of anopheline mosquitoes, three pools (which account for 0.84% of the entire collection) were PCR positive for *Plasmodium caprae*. These samples were from the Aconitus group (ID THMosGoat21-02_P11) and the Subpictus group (IDs THMosGoat21-01_P18 and THMosGoat21-01_P38) collected from Ratchaburi in 2021. Minimum infection rates (MIR) were 1.4% (0.25 – 7.46) in the mosquito of the Aconitus group and 0.9% (0.25 – 3.24) in the mosquito of the Subpictus group (Table 8).

Table 8. Minimum infection rates (MIR) of *P. caprae* in collected mosquitoes

Species	Total no. of mosquitoes	Pool size (range)	No. of tested	No. of positive pools	MIR (%) (95% CI)
<i>An. aconitus</i>	72	1-3	72	1	1.4 (0.25 – 7.46)
<i>An. subpictus</i>	296	1-3	221	2	0.9 (0.25 – 3.24)

On the other hand, a total of 133 non-anopheline mosquitoes were collected by CDC light traps in Kanchanaburi in 2020, and Phetchaburi in 2021 including 123 *Culex* spp. mosquitoes, 4 *Mansonia* spp. mosquitoes, and 6 unidentified mosquitoes due to wing and leg damage. Among them, 11 pools consisting of (*Culex* spp. n = 25, 8 pools) and *Mansonia* spp. n = 4, 3 pools) were tested. However, *P. caprae* was not detected in any *Culex* spp. or *Mansonia* spp. pools.

BLASTN searches of *Plasmodium* spp. obtained from two pools of *An. subpictus* mosquitoes using *cytb* sequences (THMosGoat21-01_P18 & THMosGoat21-01_P38) showed 99.88% identity, while *An. aconitus* pool (THMosGoat21-02_P11) revealed 99.75% similarity with *P. caprae* (accession nos. LC090215 & LC326032) in goats from Zambia and Thailand; 98.02% and 97.93% similarity to *P. odocoilei* (accession nos. MK502145 & LC326035) in pampas deer from Brazil; 96.19% and 96.05% similarity with *P. bubalis* (accession nos. LC090213 & LC090214) from water buffalo in Thailand, respectively. The phylogenetic tree inferred from *cytb* sequences showed that *Plasmodium* sequences derived from *An. subpictus* (Subpictus group) and *An. aconitus* (Funestus group) were clustered together with *P. caprae* from Thailand and Zambia (**Figure 12**). BLASTN searches of partial *P. caprae*'s *cox1* sequences from *An. subpictus* and *An. aconitus* showed 99.3% and 98.94% similarity to *P. caprae* (accession nos. LC090215 & LC326032); 98.94% and 97.89% similarity with *P. bubalis* (accession no. LC090213); 97.54% and 96.48% similarity with *P. odocoilei* (accession no. LC326034), respectively. Meanwhile, the *P. caprae*'s *18S rRNA* sequences revealed a similarity of 92.6% with *P. bubalis* (accession nos. OL624705 – OL624709) and 92.2% similarity with *P. falciparum* (accession no. LR131366). The *18S rRNA* sequences from other ungulate malaria parasites are not available in the database. The BI phylogenetic

tree inferred from *cox1* and *18S rRNA* sequences were shown in **Figure 13**. Similar to the *cytb* gene, sequences of *cox1* gene from *P. caprae* found in *An. subpictus* and *An. aconitus* mosquitoes were grouped in the same clade with *P. caprae* in Zambia and Thailand and had closer relationship with *P. bubalis* type II (accession nos. LC090214 & MK518339) than *P. bubalis* type I. Regarding the *18S rRNA* phylogenetic tree, since there have not been many available sequences of ungulate malaria parasites in the GenBank except for *P. bubalis*, our *P. caprae* were therefore clustered in the same clade with *P. bubalis* in water buffaloes and mosquitoes with a high posterior probability of 0.97 (Nugraheni et al., 2022).

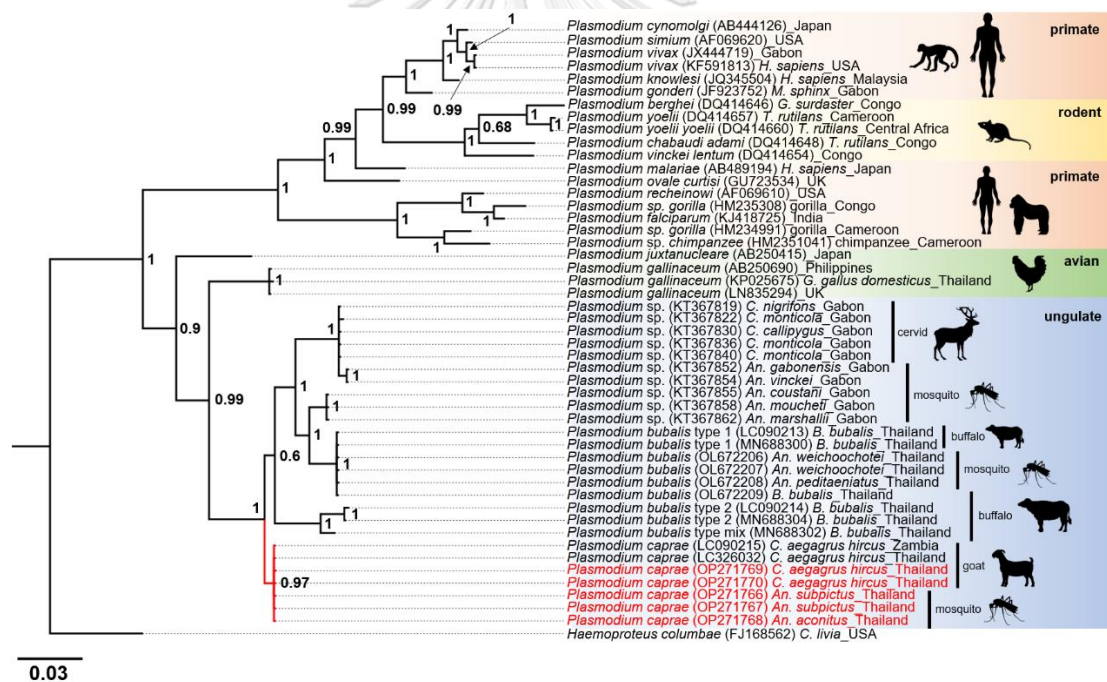


Figure 12. Phylogenetic position of *Plasmodium caprae* that infects *Anopheles* mosquitoes in this study. Phylogenetic tree inferred by BI based on the partial *cytb* gene (632 bp). All sequences were rooted with *Haemoproteus columbae*. Bayesian posterior probabilities values (≥ 0.60) were given in the nodes. The *P. caprae* sequences obtained in this study were highlighted in red and reference sequences retrieved from

the GenBank database in black. The length (0.03) indicated the number of substitutions per site.

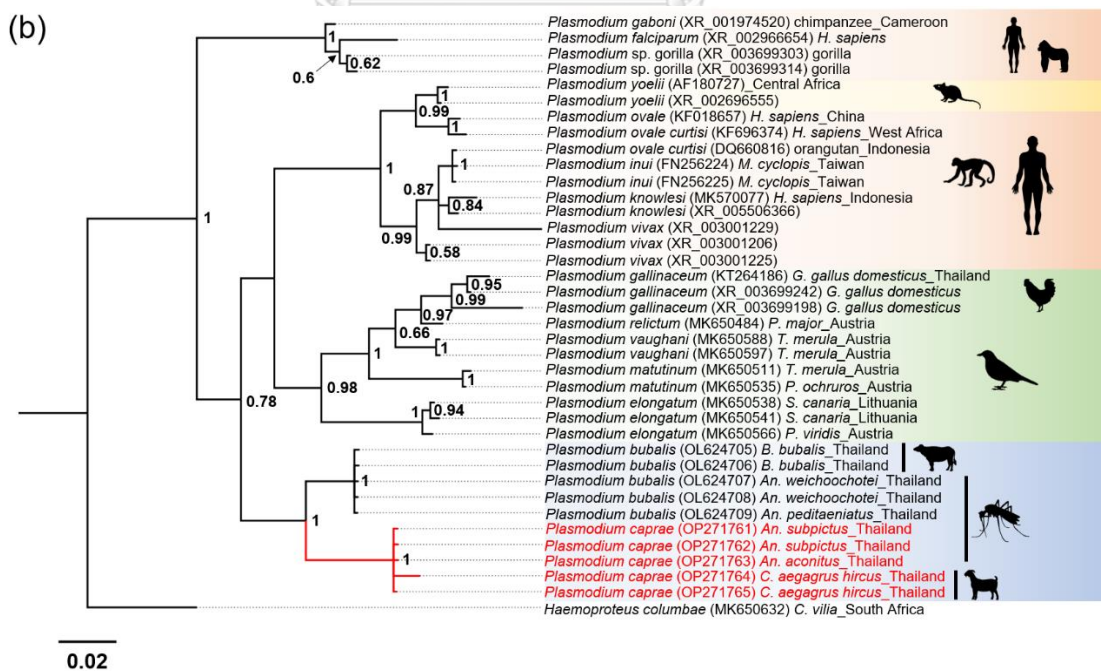
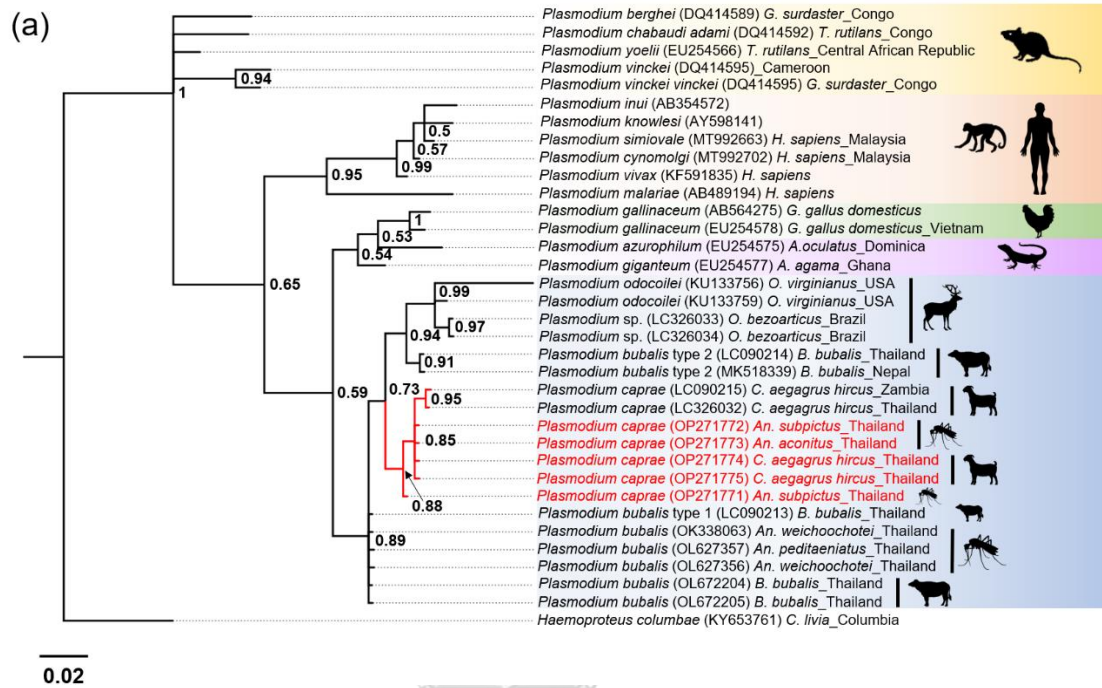


Figure 13. Phylogenetic position of *Plasmodium caprae* obtained in this study. The phylogenetic tree was constructed using partial *cox1* gene (231 bp) **(a)**. Phylogenetic tree was constructed using partial *18S rRNA* gene (335 bp) **(b)**. The length (0.02) indicated the number of substitutions per site.

4.3.3 Molecular determination of the source of host blood meal in anopheline mosquito

The abdomen of 38 blood-fed mosquitoes of *An. peditaeniatus* (n = 19), *An. barbirostris* (n = 7), *An. subpictus* (n = 10) and *An. aconitus* (n = 2) was carefully separated from the head and thorax, followed by individual DNA extraction. Then, the gDNA was amplified by nested multiplex PCR targeting the *cytochrome b* gene. Our result showed that the majority of blood meal sources in the abdomen came from one host, either human, cattle, dog, or goat (29 of 38 samples, accounted for 76.3%). Eight mosquitoes harbored the blood from two hosts (accounted for 21.1%), while only one mosquito *An. subpictus* fed the blood from three hosts, including human, cattle, and goat blood (accounted for 2.6%) **(Table 9)**.

Table 9. Host blood meal source of female anopheline mosquitoes collected from goat farms in Thailand

Blood source	<i>An. peditaeniatus</i>	<i>An. barbirostris</i>	<i>An. subpictus</i>	<i>An. aconitus</i>	Total
Human	1	0	0	0	1
Cattle	10	2	6	0	18
Dog	4	2	1	0	7
Goat	2	0	1	0	3

Human + cattle	2	3	0	1	6
Cattle + goat	0	0	1	0	1
Dog + goat	0	0	0	1	1
Human + cattle + goat	0	0	1	0	1
Total	19	7	10	2	38

4.3.4 Intraspecific and interspecific variations of dominant mosquito species

Among the *cox1* sequences, the haplotype diversity (Hd) was high in all species, ranging from 0.929 in *An. subpictus* to 0.985 in *An. vagus*. The nucleotide diversity (π) was quite low for all species, ranging between 0.005 in *An. peditaeniatus* and 0.015 in *An. subpictus*. The values of all the neutrality tests were not statistically significant with $p > 0.1$, indicating that *An. peditaeniatus*, *An. vagus*, and *An. aconitus* collected in four provinces of Thailand were in genetic equilibrium. Only Fu and Li's test of *An. subpictus-cox1* showed a significant positive value, indicating evolution population (Table 10).

Regarding the *cox2* sequences, the haplotype diversity (Hd) was relatively high, while the nucleotide diversity (π) was low in all sequences analyzed. According to the neutrality tests, the estimated values of Tajima D and Fu & Li's were accordant and not statistically significant with $p > 0.1$ (Table 10). In contrast, analysis of *An. subpictus-cox2* sequences revealed a negative selection that implies population expansion with $p < 0.02$. However, the neutrality tests of the results of *An. subpictus cox1* and *cox2* were discordant. The low number of sequenced samples and different lengths of DNA fragments in the *cox1* and *cox2* genes may explain the variability in genetic diversity

and opposite values estimated by neutrality tests. *An. subpictus-cox2* revealed higher % homology compared to GenBank, and an absolute agreement between Tajima's D and Fu & Li's tests may provide a more reliable estimation about the natural selection of the mosquito population than *An. subpictus-cox1*.

Collectively, *An. subpictus* showed the highest number of polymorphic sites, but the second most abundant number of haplotypes, followed by *An. vagus*, *An. peditaeniatus* and *An. aconitus*. Haplotype diversity values were significantly high, while nucleotide diversities were relatively low. Neutrality tests of concatenated *cox1* and *cox2* agreed with the *cox2* analysis, suggesting population expansion in *An. subpictus* with $p < 0.05$. On the contrary, *An. peditaeniatus*, *An. vagus*, and *An. aconitus* showed positive selection, but all values were not statistically significant ($p > 0.1$).

Table 10. Genetic diversity indices and neutrality test values of *cox1*, *cox2*, and concatenated sequences within and among the four dominant anopheline mosquitoes in the present study.

Species (Series)	Marker	N	Size (bp)	S	h	Hd (\pm SD)	π (\pm SD)	D	D*
<i>An. peditaeniatus</i>	<i>cox1</i>	37	1,449	22	21	0.959 \pm 0.016	0.005 \pm 0.000	0.875	0.751
(<i>Myzorrhynchus</i>)	<i>cox2</i>	35	763	6	5	0.627 \pm 0.063	0.002 \pm 0.000	-0.517	-0.401
	<i>cox1 + cox2</i>	35	2,212	28	23	0.968 \pm 0.015	0.003 \pm 0.000	0.473	0.498
<i>An. subpictus</i>	<i>cox1</i>	30	1,485	122	20	0.929 \pm 0.039	0.015 \pm 0.006	-1.178	1.871*
(<i>Pyretophorus</i>)	<i>cox2</i>	25	623	42	9	0.597 \pm 0.115	0.008 \pm 0.004	-2.189*	-3.130*
	<i>cox1 + cox2</i>	25	2,108	164	19	0.930 \pm 0.046	0.011 \pm 0.005	-1.996*	-2.701*
<i>An. vagus</i>	<i>cox1</i>	17	1,461	31	15	0.985 \pm 0.025	0.007 \pm 0.000	-0.0170	0.217
(<i>Pyretophorus</i>)	<i>cox2</i>	20	764	8	7	0.800 \pm 0.068	0.002 \pm 0.000	-1.435	-1.485
	<i>cox1 + cox2</i>	17	2,225	37	15	0.985 \pm 0.025	0.005 \pm 0.000	-0.255	0.035
<i>An. aconitus</i>	<i>cox1</i>	10	1,508	17	8	0.933 \pm 0.077	0.005 \pm 0.001	0.767	0.847
(<i>Myzomyia</i>)	<i>cox2</i>	12	740	4	4	0.682 \pm 0.102	0.002 \pm 0.000	-0.419	-0.459
	<i>cox1 + cox2</i>	10	2,248	24	10	0.982 \pm 0.046	0.004 \pm 0.001	0.156	0.351

Note: Values in bold and with asterisks indicate statistically significant ($p < 0.02$). N: no. of sequences analyzed, S: no. of polymorphic sites, h: number of haplotypes, Hd: haplotype diversity, π : nucleotide diversity, SD: Standard Deviation, D: Tajima's D, D*: Fu & Li's.

4.3.5 Population genetic structure of the four dominant mosquito species

The pairwise comparison of population differentiation of *An. peditaeniatus*, *An. subpictus*, *An. vagus*, and *An. aconitus* based on separated *cox1*, *cox2*, and concatenated *cox1* and *cox2* of four mosquito species showed similar patterns. The general genetic differentiation based on F_{ST} values was relatively low among populations, ranging from -0.019 to 0.228 (*cox1* gene, $p < 0.05$), and from -0.047 to 0.348 (*cox2* gene, $p < 0.05$). The negative F_{ST} value of *An. subpictus-cox1* can be considered zero and be further explained by a significant low F_{ST} value of the *cox2* gene, meaning there were considerable gene flows and no genetic differences among *An. subpictus* populations ($p < 0.05$). Additionally, *An. aconitus* has undergone the same pattern with *An. subpictus-cox2* while *An. aconitus-cox1* sequences among populations were not available for analysis. The high level of migrants (N_m) in the range of 1.689 to 5.345 for *An. vagus-cox1* and *An. peditaeniatus-cox1* and 4.988 to 13.565 for *An. vagus-cox2* and *An. subpictus-cox2*, respectively, indicates substantial allele flows among different geographic mosquito populations. A high level of genetic variation of more than 65% was observed within populations of four species, while a low level of genetic variation (-4 to 34%) was found between populations.

Similarly, the combined *cox1* and *cox2* sequences also had greater variance within populations compared to between populations (61-96% vs 3-38%, $p < 0.05$). Pairwise F_{ST} values ranged from 0.03335 (*An. subpictus* populations) to 0.385 (*An. aconitus* populations) with gene flow between populations varying between 0.799 and 14.493. All the F_{ST} values of the anopheline populations were statistically significant (Table 11).

Table 11. Analysis of molecular variance (AMOVA), Wright's fixation index and gene flow based on the *cox1*, *cox2* and concatenated sequences within and between the four dominant anopheline mosquitoes found in the present study.

Genetic variation	Marker	<i>An. peditaeniatus</i>	<i>An. subpictus</i>	<i>An. vagus</i>	<i>An. aconitus</i>
Among populations	<i>cox1</i>	8.554	-1.908	22.833	NA
	<i>cox2</i>	34.758	3.555	9.110	-4.689
	<i>cox1</i> + <i>cox2</i>	13.550	3.335	21.916	38.503
Within populations	<i>cox1</i>	91.446	101.907	77.167	NA
	<i>cox2</i>	65.242	96.445	90.890	104.689
	<i>cox1</i> + <i>cox2</i>	86.450	96.665	78.084	61.497
Wright's fixation index (F_{ST})	<i>cox1</i>	0.0855*	-0.019*	0.228*	NA
	<i>cox2</i>	0.348*	0.0356*	0.091*	-0.047*
	<i>cox1</i> + <i>cox2</i>	0.136*	0.03335*	0.219*	0.385*
Gene flow (Nm)	<i>cox1</i>	5.345	-26.705	1.689	NA
	<i>cox2</i>	0.939	13.565	4.988	-11.163
	<i>cox1</i> + <i>cox2</i>	3.190	14.493	1.781	0.799

Note: * indicates statistically significant ($p < 0.05$). NA: not applicable.

4.3.6 Haplotype network of the four dominant mosquito species

The nucleotide sequence lengths of the *cox1* gene used for haplotype network analyzes in *An. peditaeniatus*, *An. subpictus*, and *An. vagus* were 1,449, 1,485, and 1,461 bp, respectively. The *An. aconitus* mosquitoes in this study were found in Ratchaburi and Phetchaburi provinces. However, the sequencing results of the Phetchaburi samples were excluded from further analysis due to poor quality. Therefore, the reference sequences (accession no. DQ000254) in Phetchaburi were retrieved from the GenBank and their length was shorter than ours (504 bp). *Anopheles peditaeniatus* was collected in three (Nan, Kanchanaburi, and Phetchaburi) of four provinces, and showed the highest number of haplotypes sharing among three locations (4 shared haplotypes), followed by *An. subpictus* (3 shared haplotypes) between Kanchanaburi and Ratchaburi, except Phetchaburi, and *An. vagus* (1 shared haplotype) between Nan and Phetchaburi. Most *An. aconitus* mosquitoes were captured in Ratchaburi, where they could be grouped into six haplotypes. The haplotypes found in Ban Kha District, Ratchaburi were exclusively for this sampling site and did not share with any haplotypes from the neighboring province Phetchaburi (Supplementary data 2).

The lengths of the *cox2* nucleotide sequences used for haplotype network analyses in *An. peditaeniatus*, *An. subpictus*, *An. vagus*, and *An. aconitus* were 763, 623, 764, and 740 bp, respectively. In general, the longer the sequences that were analyzed, the greater the number of haplotypes obtained. The *cox2* haplotype networks revealed that *An. subpictus* had the most diverse number of haplotypes, with only one shared by Kanchanaburi and Ratchaburi. However, *An. vagus* and *An.*

peditaeniatus shared three haplotypes across localities, while a single haplotype of *An. aconitus* was shared in Ratchaburi and Phetchaburi (**Supplementary data 3**).

Based on the concatenated sequences of the *An. peditaeniatus*, *An. subpictus*, *An. vagus* and *An. aconitus* *cox1* and *cox2* genes, we observed a total of 23, 19, 15, and 9 haplotypes, respectively. These mosquitoes shared four haplotypes between Nan, Kanchanaburi, and Phetchaburi. Only one haplotype was found to be shared by Kanchanaburi and Ratchaburi (*An. subpictus*), Nan and Phetchaburi (*An. vagus*). *Anopheles aconitus* had nine distinct haplotypes, eight of which were found in Ratchaburi, and one in Phetchaburi (**Figure 14**).

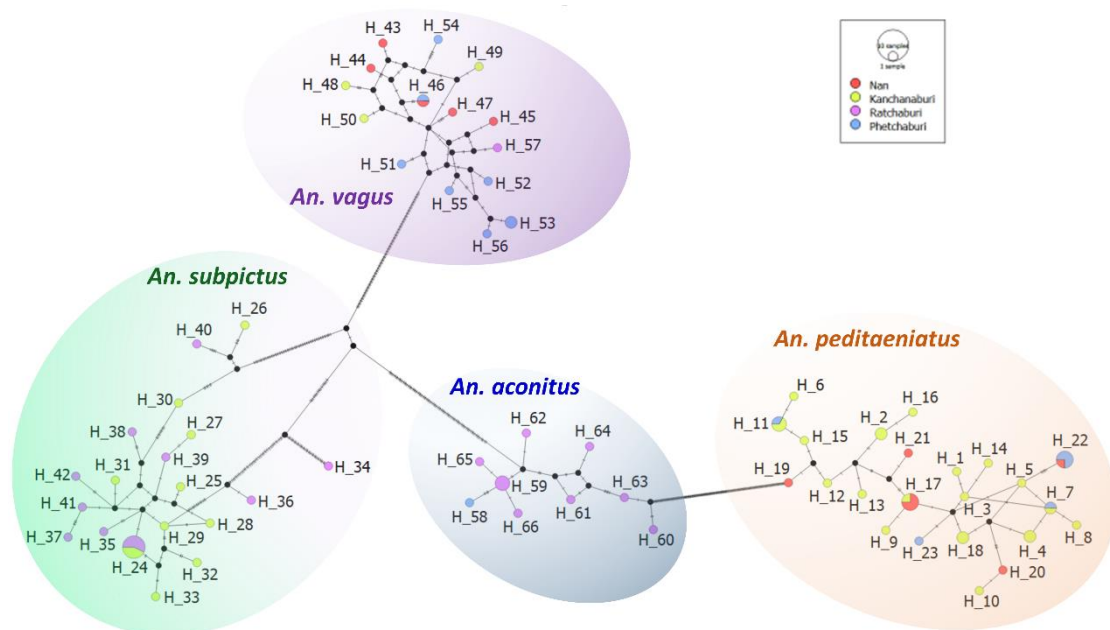


Figure 14. TCS network of the concatenated *cox1* and *cox2* sequences of the dominant mosquito species collected from four provinces in Thailand. The brown, green, purple, and blue shadows indicated four different mosquito species, *An. peditaeniatus*, *An. subpictus*, *An. vagus*, and *An. aconitus*, respectively. Each haplotype was represented by a cycle, and the size of the cycle was proportional to the number

of individuals in each haplotype. The number of nucleotide differences between haplotypes was presented by lines indicating mutations from the common haplotype. The colors of four provinces were annotated in the box.

4.3.7 Phylogenetic analysis of anopheline mosquitoes collected from goat farms

Anopheline mosquitoes in this study were classified into six distinct groups, according to phylo-genetic trees: Hyrcanus (n = 40), Barbirostris (n = 15), Subpictus (n = 52), Tessellatus (n = 7), Annularis (n = 2), and Aconitus (n = 12). The Hyrcanus group consisted of *An. peditaeniatus* (n = 37) and *An. pursati* (n = 3). The Barbirostris complex comprised *An. barbirostris* (n = 10), and *An. campestris* (n = 5). The Subpictus group included *An. subpictus* (n = 32) and *An. vagus* (n = 20). Meanwhile, the mosquito species of the remaining three groups were *An. tessellatus*, *An. philippinensis*, and *An. aconitus*, respectively. In the *cox1* sequence-based tree, *An. peditaeniatus* clustered with isolates from Sri Lanka (accession no. MH330207), India (MZ088143), Vietnam (MT380489), Malaysia (MT669948) and Thailand (AB715048), and had a close relationship with *An. pursati* previously found in Thailand (AB826088). The other five groups formed a separate branch from the Hyrcanus group (*An. peditaeniatus*, *An. pursati*, and *An. sinensis*). Among these, Barbirostris and Tessellatus were placed in one clade, while Annularis and Aconitus were placed in another. The subpictus group observed in this study included two members: *An. vagus* and *An. subpictus*. However, *An. vagus* was grouped with *An. barbirostris* and *An. tessellatus*, while *An. subpictus* was closely related to *An. philippinensis* and *An. maculatus* (Figure 15).

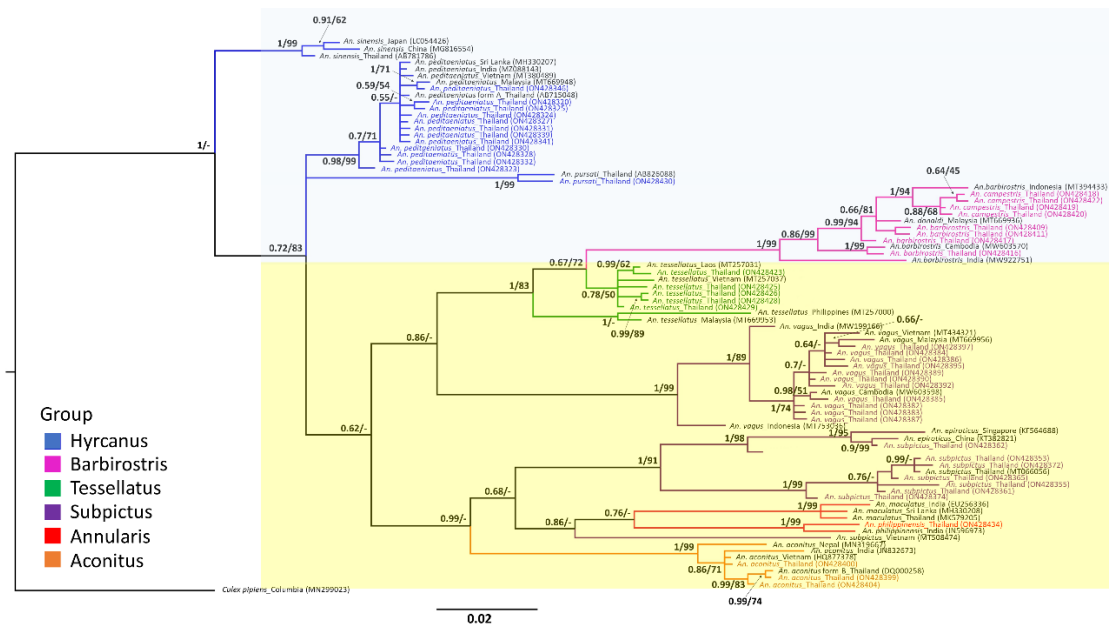


Figure 15. Consensus phylogenetic tree of *Anopheles* spp. based on the *cox1* gene using the BI and ML method. The posterior probability and the bootstrap value were shown at the nodes. Bootstrap values less than 50 were presented as “-”. The reference taxa retrieved from GenBank were in black, the color codes were from the present study. The subgenus *Anopheles* and *Cellia* was highlighted in blue and yellow shadows, respectively.

With high posterior probabilities and bootstrap support, the *cox2* phylogenetic tree was divided into 4 clades representing six different groups of mosquitoes. The Barbirostris complex (*An. barbirostris* and the *An. campestris*) and Tessellatus group (*An. tessellatus*) were classified as distinct clades. Hyrcanus was found in the same cluster as Annularis and Subpictus, indicating a close relationship. All *An. vagus* and *An. subpictus* mosquitoes found in this study were considered to belong to the same clade and were closely related to *An. subpictus* isolated from India (KX669652), Australia (U94314) and Thailand (AF417747). However, *An. vagus* from China (AY953356) and the *An. aconitus* subgroup were separated into a different clade (Figure 16).

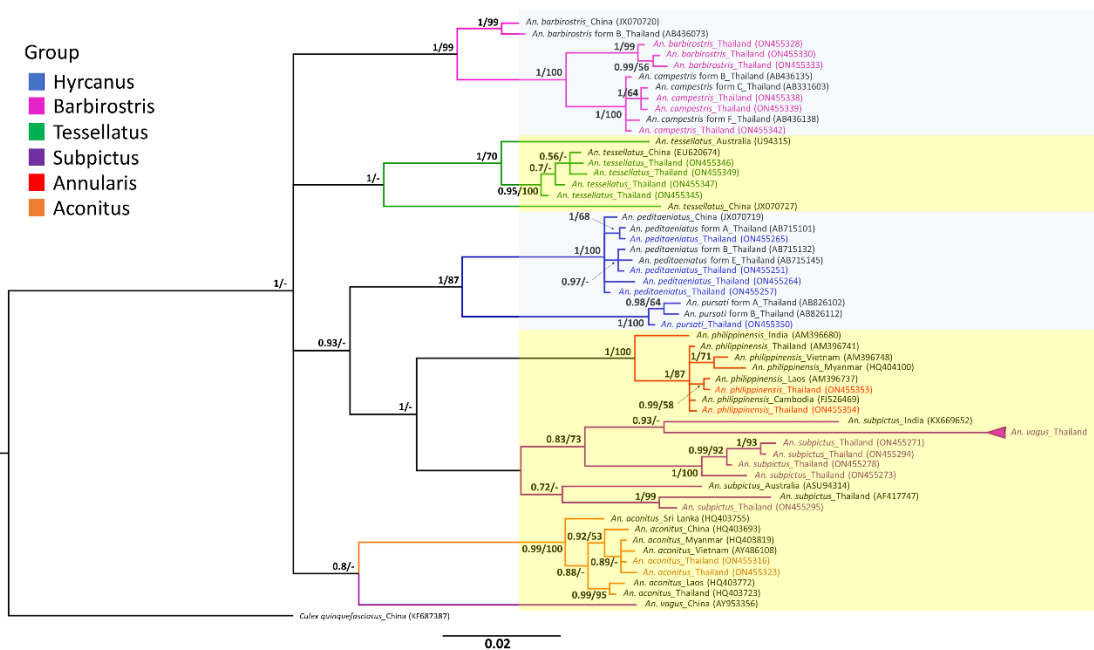


Figure 16. The BI and ML methods were used to construct a consensus phylogenetic tree of *Anopheles* spp. based on the *cox2* gene. Posterior probability and bootstrap values were presented at the nodes. Bootstrap values less than 50 were denoted by a “-”. The GenBank reference taxa were in black and the color codes are from the current study. *Anopheles* and *Celia* subgenera were highlighted in blue and yellow shadow, respectively.

Cox1 reference sequences from GenBank varied in length and position along the *cox1* protein-coding sequences; thus, 407 bp-*cox1* sequences were used, while *cox2* fragments were 547 bp in length. We created an alignment of 954 bp of concatenated *cox1* and *cox2* sequences from our 88 nucleotide sequences to minimize bias in the selection and analyses. In general, the topology of the concatenated *cox1* and *cox2* tree was similar to that of the other two single genes (Figure 17). As a result, the combined tree improved the consistency and robustness of phylogenetic relationships among different anopheline mosquito species.

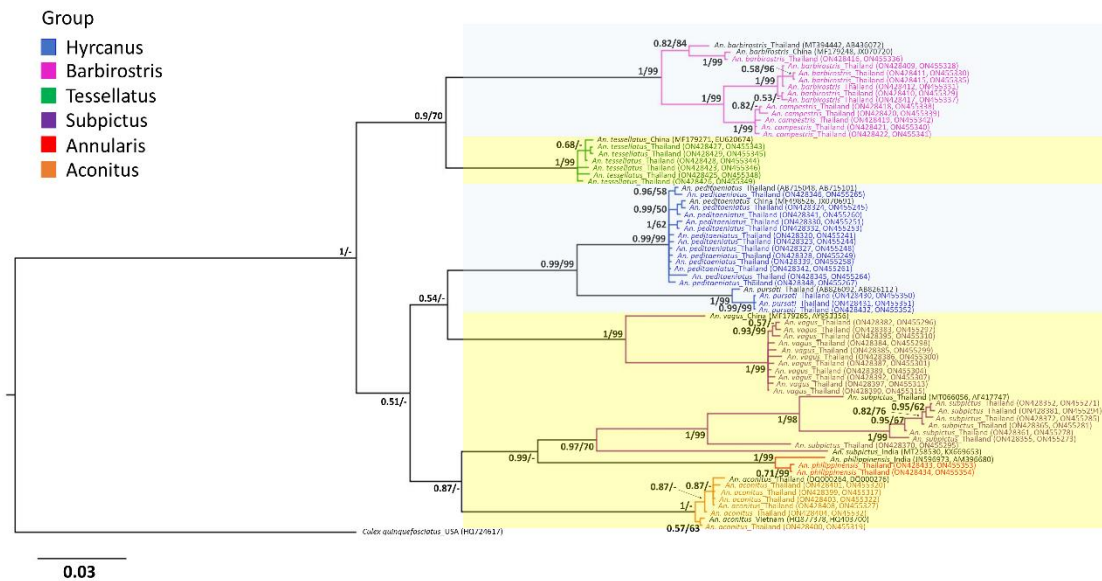


Figure 17. Consensus phylogenetic tree of *Anopheles* spp. based on concatenated *cox1* and *cox2* sequences (954 bp) using the BI and ML method. The posterior probability and the bootstrap value were shown at the nodes. Bootstrap values less than 50 are presented as “-”. The GenBank accession numbers and the reference species names were given in black. Blue, pink, green, purple, red, and orange represent the Hyrcanus, Barbirostris, Tessellatus, Subpictus, Annularis groups, and Aconitus subgroup, respectively. The subgenus *Anopheles* and *Cellia* was highlighted in blue and yellow shadows, respectively. Accession numbers in brackets represented for *cox1* and *cox2* sequences, respectively.

The phylogenetic tree inferred from the ITS2 sequence had the same topology as the two genetic markers shown earlier. The subgenus *Anopheles* is divided into two branches: the Hyrcanus group (*An. peditaeniatus* and *An. pursati*) and the Barbirostris complex (*An. barbirostris* and *An. campestris*). With high posterior probabilities and bootstrap supports, *An. aconitus* and *An. philippinensis* shared the same ancestor in the subgenus *Cellia*. Furthermore, the Subpictus group, which included *An. vagus* and

An. subpictus, formed two subclades in a clade with *An. tessellatus* in Myanmar and China (OM060231 and EU650425) (Figure 18).

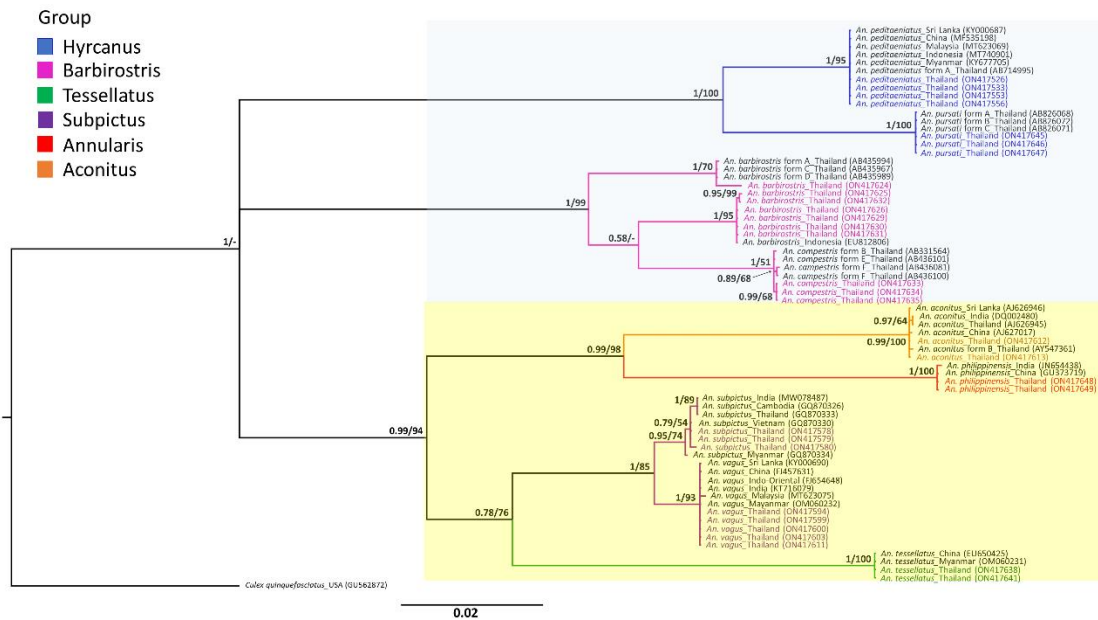


Figure 18. Consensus phylogenetic tree of anopheline mosquitoes in the genera *Anopheles* and *Cellia* of the present study based on the ITS2 region using the BI and ML methods. The subgenus *Anopheles* and *Cellia* was in light blue and yellow shades, respectively. The reference taxa retrieved from GenBank were in black, and taxa in colors were from the present study.

CHAPTER 5

DISCUSSION

5.1 Experiment 1: Natural infection of *Plasmodium caprae* and its co-infections

In this study, the prevalence of *P. caprae* was extremely low with only 1.42% found in the blood samples collected in rainy season from June 2018 to early October 2021. Among the samples collected in dry season, the malaria parasite was not found. In Thailand, the previous study in 2018 reported the malaria positive goat in Phetchaburi Province only with an overall prevalence of 1.12% (Kaewthamasom et al., 2018). They also stated that the prevalence of *P. caprae* in Thai goats was sporadic, ranging from 0 to 5% and much lower than that of *P. bubalis* in Thai water buffalo (16 to 45%) (Templeton et al., 2016a, Nguyen et al., 2020), and *P. odocoilei* in white-tailed deer (25%) (Guggisberg et al., 2018). However, the result of this study revealed the expansion of the existence of malaria in Nan Province, northern Thailand. An adult naturally infected goat in Nan Province has been followed up in two weeks. The goat was pregnant while infected with malaria parasite. During the observation period, the goat did not express specific clinical signs, except for three days with diarrhea and a slight fever. The malaria parasite loads were detected by qPCR until day 15, however, the goat was recorded to have fever and diarrhea on day 16, 17, and 19 of observation. Hence, the fever and diarrheal status may be due to other infections. Furthermore, the malaria-infected goat in our study was also co-infected with the bacteria *A. bovis* on the first day of blood collection. So far there have been limited research studies on the goat malaria parasite so far. A study in 1923 showed that the malaria-infected goat had a submandibular abscess with bacterial infection but no anemia (de Mello et al., 1923). Other studies focused mainly on the prevalence and genetic information of

P. caprae based on the mitochondrial gene, but not on the clinical signs of infected goats.

Parasite loads of infected goats were determined by quantitative PCR (qPCR) using primers targeting the *cox1* partial sequence of mitochondrial genes. The mitochondrial genes such as *cox1* and *cytochrome b* are known to have multi-copy in a cell. The number of mitochondria in animal cells varies widely depending on the organism, tissue, cell type, and functions they perform. For example, a mature eukaryotic red blood cell has no mitochondria (Ney, 2011) whereas a hepatocyte can have more than 2,000 (Alberts et al., 2008). In the phylum Apicomplexa, *Plasmodium* mtDNA is approximately 6 kb in length and arranged in head-to-tail tandem arrays with multiple copies, ranging from about 30 in human malaria *P. falciparum* to about 100 in rodent malaria parasite *P. yoelii*, and 20 in *P. gallinaceum* (Vaidya and Mather, 2005). However, the ungulate malaria parasite in general and *P. caprae* in particular remain unclarified. Recently, Nugraheni et al have described the primers targeting the *cox1* region (283 bp) for ungulate malaria *P. bubalis* detection (Nugraheni et al., 2022). Using primers targeting multi-copy genes may help improve the detection limit and efficiency of diagnostic assay. This study also used previously published primers for qPCR detection and parasite burdens were confirmed to last until day 15 in naturally infected adult goats with 5 copies per microliter of blood sample. In a previous study, the highest parasite loads in Kenya and Thailand goats were 91,000 and 23,000 copies per microliter of blood, respectively. However, most of the samples were estimated ranging between 1 and 100 copies per microliter of blood (Kaewthamasorn et al., 2018). Another study revealed that malaria-infected buffaloes were quantitatively tested

positive with 150,000 copies per microliter of blood sample until day 28, then remained positive until day 49 of observation.

In terms of co-infection with other blood protozoa parasites, previous studies found that goats were infected with several blood parasites, including *Babesia* spp. (Naderi et al., 2017, Kage et al., 2019); *Theileria luwenshuni* (Tu et al., 2021, Aung et al., 2022); *Theileria lestoquardi* and *T. ovis* (Hakimi et al., 2019); *Anaplasma bovis*, *A. marginale* and *A. ovis* (Hakimi et al., 2019, Aung et al., 2022). Furthermore, a study was conducted in Iran that revealed that there was a negative correlation between *P. caprae* and *A. ovis* infections (Hakimi et al., 2019). In the present study, we have found that the goats were co-infected with *P. caprae* and *A. bovis*.

Regarding the natural infection of *P. caprae* and its co-infections, our study has several shortcomings, consisting of a small number of blood samples collected that resulted in a low percentage of *P. caprae* positive, a sparse sampling frequency, and lack of hematological tests in the infected goats. Therefore, further research should be carried out to appropriately investigate the natural infection and co-infections in ungulates, as these could impact animal health and welfare.

5.2 Experiment 2: Multigene analysis of *Plasmodium caprae* and its related genera

There has been significant conflict about the evolutionary history of haemosporidian parasites, especially on how many times that the parasites have switched and used mammals as vertebrate hosts (Galen et al., 2018). The very first phylogenetic study has concluded that the virulent human malaria parasite *Plasmodium falciparum* was a sister to the avian malaria parasites and this was a result

of host switch between domesticated chickens and human (Waters et al., 1991). More and more later research studies utilizing broader taxonomic sampling and multiple gene targets have revealed that the genus *Plasmodium* has consistently been found to be paraphyletic or polyphyletic with *Haemoproteus*, *Parahaemoproteus*, and *Hepatocystis* (Galen et al., 2018). In this study, we combined our four nuclear gene analyzes with the dataset from Borner et al. (2016) for constructing the phylogenetic trees based on nucleotides, codons, and amino acids using Bayesian inference and Maximum likelihood. Our phylogenetic trees showed that *P. caprae* was consistently recovered as a monophyletic taxon, forming a sister group with the bat parasite of *Polychromophilus*. These results were consistent with findings from previous studies on multigene analyses of haemosporidian parasites (Borner et al., 2016, Perkins and Schaer, 2016). *Plasmodium caprae* and *Polychromophilus* have different life cycles and invertebrate host vectors for transmission (Gamham, 1966). So far, there has been limited information on ungulate malaria parasites so far, and it has not been clear whether they have hypnozoite stage in their life cycle (Templeton et al., 2016b). In particular, the position of *P. caprae* in this study had relatively high bootstrap value in Maximum likelihood based on codons and strong posterior probability in Bayesian inference based on amino acid analyzes (83 and 0.86, respectively) while both Bayesian inference and maximum likelihood based on nucleotides showed quite low support values. It would probably be related to the parasite genome. The genome of *Plasmodium* species was known to have a higher amount of AT content than other organisms, especially *P. falciparum*, which is an AT-rich species of about 82% (Weber, 1987). Base composition bias may affect the precision of molecular phylogenetic inference (Galen et al., 2018). In this study, the low support values in the maximum

likelihood tree based on nucleotides were most likely due to the high AT content of *P. caprae* and the missing gene sequences in the *Polychromophilus* and other organism data set.

Besides, four nuclear genes from this study were also concatenated with two mitochondrial genes (*cox1* and *cytb*) and apicoplast (*clpC*) gene to reconstruct the phylogenetic tree for comparison and confirmation of the position of *P. caprae* among haemosporidian parasites. Due to the limited taxon sampling and to minimize the influence of missing data on phylogenetic inference, *Haepatocystis*, *Nycteria*, *Plasmodium cephalophi* and *P. brucei* were excluded from our analysis. Several studies have shown that outgroup selection may have effect on tree topology (Holland et al., 2003, Martinsen et al., 2008). However, those subsequent studies have revealed that the choice of outgroup had no effect on the accuracy of the phylogenetic tree (Borner et al., 2016, Galen et al., 2018). According to the result of our combined dataset, *P. caprae* in goat was grouped in the same clade with other ungulate malaria parasites (*P. bubalis* in water buffalo, *P. odocoilei* in white-tailed deer and pampas deer), and formed a sister clade with a bat parasite of *Polychromophilus*. Our results were in agreement with the findings of previous studies (Borner et al., 2016, Galen et al., 2018, Rasoanoro et al., 2021). Ungulate malaria parasites were proven to branch before other *Plasmodium* species that infect rodent, bird, reptile, apes, monkey, human, and form a monophyletic clade within the hemosporida (Templeton et al., 2016a, Templeton et al., 2016b, Asada et al., 2018). Therefore, our results are consistent with those of previous studies and provide more supporting evidence for Borner's findings that nuclear gene markers are reliable and capable of providing a stronger tree for phylogenetic inference, since the result of concatenated nuclear

genes was consistent with the combined data set of mitochondrial, apicoplast, and nuclear genes. Our consensus tree was rooted in *Leucocytozoon* and supported the basal position of *Haemoproteus columbae* among the remaining haemosporidian (0.99/93 posterior probability and bootstrap value, respectively). *Haemoproteus*, *Parahaemoproteus*, *Hepatocystis*, and *Nycteria* were recovered as paraphyletic groups with *Plasmodium* sp. (Martinsen et al., 2008, Borner et al., 2016, Galen et al., 2018). However, in our current study, *Hepatocystis* and *Nycteria* were not included due to missing sequence data.

The evolutionary history among haemosporidian parasites has remained controversy for a long time. The analysis based on the mitochondrial *cytb* gene of *Plasmodium* has shown that there was heterogeneity in the protein evolution in the *cytb* gene of the malaria parasite, especially in the transition of *Plasmodium* lineages between mammalian and sauropsid hosts (Outlaw and Ricklefs, 2010). The relatively high rates of nucleotide substitution resulted in long branches in phylogenetic inference, likely placing *Leucocytozoon* to a basal position in previous studies of the remaining haemosporidian parasites (Escalante et al., 1998, Perkins et al., 2002). Later, Borner et al. found that *Leucocytozoon* was the deepest branching taxon among Haemosporida and support *Plasmodium* as a monophyletic group based on a combined dataset of 21 nuclear genes (Borner et al., 2016).

Additionally, life history traits including blood schizogony and hemozoin pigment were also used to define the species and genera of blood parasites (Martinsen et al., 2008). Gain or loss of blood schizogony was suggested to support the tree topology. In detail, the parsimonious reconstruction suggested that a gain of schizogony at the transition to mammalian hosts, and three losses in the lineages

leading to *Polychromophilus*, *Hepatocystis* and *Nycteria* although the causes for the blood schizogony loss remain unknown. Therefore, a clade between *P. caprae* and *Polychromophilus* in this study seems to be supported by the gain or loss of blood schizogony at the transition of haemosporidian to mammalian hosts (Galen et al., 2018).

To our knowledge, this study is the first report on the phylogenetic reconstruction of *P. caprae* based on combined nuclear, apicoplast and mitochondrial genes. We have successfully amplified four nuclear genes based on previous data, a small number of nuclear genes in comparison to the previous study (Borner et al., 2016). Furthermore, due to the extremely low parasitemia of *P. caprae*, we face many challenges in the amplification of parasite DNA, as well as the limited reference sequences from the GenBank and PlasmoDB databases. More research should be conducted to overcome this dilemma in the future.

5.3 Experiment 3: Mosquito composition and identification of the possible mosquito vector of *P. caprae* from goat farms

The purpose of this study is to investigate possible vectors of *P. caprae* and to evaluate the species diversity and genetic characterization of goat anopheline mosquitoes in malaria-endemic areas in Thailand. We found a diverse composition of mosquitoes, in which the majority of mosquitoes on goat farms were *Culex* spp. (61.2%), followed by *Anopheles* spp. (33.8%), unidentified species (3%), and *Mansonia* spp. (2%). A total of nine anopheline species belonging to six groups/subgroups were observed in these goat farms. Among them, four of the most dominant mosquito species including *An. peditaeniatus*, *An. subpictus*, *An. vagus* and *An. aconitus* were

captured from goat farms in Kanchanaburi and Ratchaburi provinces. These mosquito species have previously been reported in several districts in Thailand, Southeast Asia, and Asian countries (Rattanarithikul et al., 2006). *An. peditaeniatus*, *An. subpictus*, and *An. vagus* are distributed in Thailand, Vietnam, Cambodia, Indonesia, Malaysia, India, and Sri Lanka, while *An. aconitus*, *An. barbirostris*, *An. campestris*, *An. tessellatus*, and *An. philippinensis* are present in Thailand, Vietnam, and Cambodia (Tainchum et al., 2014, Maquart et al., 2021). *Anopheles peditaeniatus*, *An. subpictus*, *An. vagus* and *An. aconitus* were previously implicated as human malaria vectors among the nine species found in the current study (Vantaux et al., 2021). These four species were also the most abundant species found in this study. As a result, we analyzed and characterized their genetic diversity, population structure, and phylogeny to gain insight into the mosquito populations that share the common living environment with goats and farm owners.

In this study, we collected the mosquitoes from goat farms in four provinces comprising Kanchanaburi, Nan, Ratchaburi, and Phetchaburi between 2020 and 2021. Unfortunately, we were not allowed to collect goat blood in Ratchaburi province in 2021 where *P. caprae*-positive mosquitoes were detected. Therefore, a total of 22 previous goat blood samples collected at the same goat farm in 2018 was used to screen for the presence of goat malaria parasite. The results revealed that there was malaria infection in goats in 2018. Then, we have also detected the DNA of *P. caprae* in *An. aconitus* and *An. subpictus* mosquitoes from Ratchaburi Province in 2021 with a minimum infection rate (MIR) of 1.4 and 0.9%, respectively. Therefore, there may be a relationship between the malaria parasite detected in goats and two mosquito species, *An. subpictus* and *An. aconitus*. However, no sporozoites were observed in these

mosquito salivary glands, so this problem requires further investigations. However, our results were in agreement with the findings in previous studies on vector of ungulate malaria parasites. As an example, the sporozoites and oocysts of the mouse deer malaria parasite *P. traguli* were found in salivary glands of experimentally infected mosquitoes *An. umbrosus* and *An. letifer* (Wharton et al., 1963). *An. umbrosus* was also found in a high-risk malaria area of Ranong Province, southern Thailand (Chookaew et al., 2020). However, none of these species was recorded in our study. In another study, the white-tailed deer malaria parasite *P. odocoilei* sporozoite was isolated from the mosquito *An. punctipennis* in North America (Martinsen et al., 2016). Elsewhere, hemsporidian parasites of antelopes and other vertebrates (family Plasmodiidae) were observed in sylvatic anopheline mosquitoes in Gabon, Central Africa (Boundenga et al., 2016). These reports, along with our results, may provide more supporting evidence for the hypothesis that anopheline mosquitoes are possible vectors for ungulate malaria. However, many criteria are needed to conclude that one mosquito species is a vector for transmitting the malaria parasite. As stated by Makanga et al. (2016), the presence of *Plasmodium* sporozoites in salivary glands and oocysts in the midgut are prerequisite for malaria vectors conclusion (Makanga et al., 2016). In addition, an experimental design should be conducted to confirm whether anopheline mosquitoes could transmit *Plasmodium* by letting those mosquitoes bite *Plasmodium*-infected vertebrate animals. Subsequently, the sporozoites and oocysts in the mosquito midgut should be microscopically examined 1-2 weeks after infection. After that, infected mosquitoes to feed another naive vertebrate animal and observed the *Plasmodium* positive rate at least 10-14 days after infection (Wharton et al., 1963). In our study, two pools of *An. subpictus* and one pool of *An. aconitus* collected from

goat farms were molecularly found to be positive for *P. caprae* and confirmed by DNA sequencing. Since no sporozoites were observed in the salivary glands, we were unable to conclude that two species are competent vectors for goat malaria transmission. However, our findings suggested the possibility and role of *An. subpictus* and *An. aconitus* mosquitoes in the transmission of *P. caprae*. Additionally, more investigations are required to find the sporozoites in the salivary glands of these two species. Then, experimentally infected mosquitoes with *P. caprae* should also be conducted in *An. subpictus* and *An. aconitus* for the conclusion of vector competence.

Although collected in goat farms in western and northern Thailand, most of the blood meals in mosquitoes came from cattle and humans rather than goats. This finding could be explained by the fact that cattle, goats, and dogs are raised in close proximity to human households. Cattle have shorter and thinner hair on their bodies than goats and dogs, making them more vulnerable to mosquito bites. Several previous studies also reported that most of the mosquito blood sources came from cattle, despite the fact that the mosquitoes were collected in urban and semi-urban human residences, highland and lowland sites (Gyawali et al., 2019), highland and lowland sites (Zhong et al., 2020).

The morphological identification method is time-consuming and requires the expertise of entomologists. Furthermore, if the sample collection and storage processes are not carried out properly, there may be a problem with species identification. On the other hand, many species complexes or sibling species are isomorphic and morphologically indistinguishable (Beebe, 2018). As a result, molecular approaches that target mitochondrial genes or ribosomal DNA internal transcribed spacers appear to overcome these issues. In the early 2000s, DNA barcoding was

initiated and applied for accurate species identification using mitochondrial DNA *cox1* sequences against the Barcode of Life Database (BOLD) (Beebe, 2018), and since then it has been continued to expand for the barcode reference library of mosquito fauna in Singapore, Sri Lanka, and Portugal (Chan et al., 2014, Madeira et al., 2021). DNA barcoding has been shown to be more effective, reliable, time-saving, and cost-effective than traditional morphological identification (Grant et al., 2021). Based on search results through the GenBank and BOLD databases, using three markers including *cox1*, *cox2*, and ITS2 confirms four mosquito species: *An. peditaeniatus*, *An. vagus*, *An. aconitus*, and *An. tessellatus* in the present study. However, *cox1* sequence searches against the GenBank database for *An. subpictus*, *An. barbirostris*, *An. campestris*, *An. philippinensis* and *An. pursati* reveal another species in the same group with low homology (90 – 97%). The reason for this finding could be the incompleteness of the *cox1* sequences of varying length deposited in GenBank. When the same *cox1* sequences are searched in the BOLD database, the identification results match completely those of *cox2* and ITS2 with a higher percentage of similarity. As a result, we ignored these contradictory results from BLASTN because the divergence of 2 – 3% is considered a threshold for intraspecific variation (Hebert et al., 2003).

Mitochondrial DNA, especially *cox1* and *cox2* genes, possess several benefits for molecular taxonomy, demographic history, genetic diversity, and phylogenetic evolutionary studies due to their high copy number in the cell, comparatively higher substitution rates than nuclear genes, no or rare recombination in mosquitoes, and give a single evolutionary history (Beebe, 2018). The genetic diversity of *An. peditaeniatus*, *An. subpictus*, *An. vagus* and *An. aconitus* based on *cox1* is generally higher than those of the *cox2* gene, implied by high haplotype diversity and low genetic

diversity. This is probably explained by the longer the sequences analyzed, the higher the genetic diversity obtained (*cox1* 1,400 bp, *cox2* 700 bp in length). Therefore, *cox1* is a more suitable gene marker to explore the genetic variation and population structure of mosquitoes. A similar result on genetic diversity was also reported in *An. balabacensis* in Sabah, Malaysia (Manin et al., 2018). Demographic inference tests based on Tajima's D and Fu & Li's D* show that *An. subpictus* experienced population expansion ($p < 0.05$) whereas the neutrality test of *An. peditaeniatus*, *An. vagus*, and *An. aconitus* are not statistically significant. The relatively high haplotype diversity and low nucleotide diversity detected also reflect population expansion, implying that recent populations diverged from one another due to rapid demographic expansion (Bunmee et al., 2021). Furthermore, the negative Tajima D and Fu & Li's D* values found in all subpopulations indicate that DNA sequences are evolving nonrandomly and many uncommon alleles are present in subpopulations that are demographically expanding (Tajima, 1989). The demographic history of other malaria vectors also experienced similar patterns of population expansion under substantial negative selection, including *An. aconitus* and *An. dirus* in Southeast Asia (Walton et al., 2000), and *An. baimaii* in north-eastern India (Sarma et al., 2012).

Our results provide some basic information about the population genetic structure as well as evidence of gene flow among anopheline mosquitoes in three northern and western provinces. The low to moderate F_{ST} values obtained from pairwise comparisons reveal that the genetic variations in four dominant species exist within populations rather than between populations. These observations suggest that gene flow occurred between *An. peditaeniatus*, *An. subpictus*, *An. vagus*, and *An. aconitus* populations without geographic distance between northern and western

Thailand. However, using an unequal number of mosquito samples from different geographical locations may have an effect on the findings of population genetic structures. Some DNA sequences do not fairly reflect the genetic structure of the entire mosquito population. Although the provinces of Nan, Kanchanaburi and Phetchaburi are separated by a distance of 800 kilometers, they still share common haplotypes. Other studies found that geographic distance and barriers did not impede gene flows and population genetic structures of mosquitoes in distant locations (Bunmee et al., 2021).

The phylogenetic trees are constructed based on both separate *cox1*, *cox2*, concatenated *cox1* and *cox2* genes and the ITS2 region to provide a more robust and reliable phylogenetic relationship among five series in the subgenus *Anopheles* and *Cellia* of anopheline mosquitoes. The contradictory results of *An. subpictus*, *An. barbirostris*, *An. campestris*, *An. philippinensis*, and *An. pursati* among *cox1*, *cox2*, and ITS2 presented in **Table 7** are elucidated in our three phylogenetic trees. The *An. epiroticus-cox1* sequences are placed together with *An. subpictus* in Thailand (accession no. MT066056). *An. donaldi-cox1* are classified in the same clade as *An. barbirostris* in Indonesia (MT394433), India (MW922751), and *An. donaldi* in Malaysia (MT669936). The sequences of *An. campestris-cox1* retrieved from GenBank are varied in length and do not overlap with other sequences; therefore, they are excluded from further phylogenetic analysis. *An. barbirostris*, *An. campestris*, and *An. donaldi* belong to the Barbirostris Complex Group, which is indistinguishable solely depending on morphology. Previous studies have suggested that *cox1*, *cox2*, and ITS2 are reliable genetic markers for resolving this problem, but *cox1* seems to be more useful for distinguishing sibling and cryptic species within the complex group of anopheline

mosquitoes (Wang et al., 2017). *An. maculatus-cox1* in this study is placed in the same clade as *An. philippinensis* in India (JN596973) but different clade with *An. maculatus* in India, Sri Lanka and Thailand (EU256336, MH330208, and MK579205), respectively, indicating that *An. philippinensis-cox1* found in this study completely agrees with *cox2* and ITS2 results. Similarly, our *An. sinensis-cox1* sequence is placed with *An. pursati* previously isolated in Thailand (AB826088) and is distinct from the *An. sinensis* clade. Regarding the *cox2* and ITS2 trees, each species is represented as a monophyletic group, while they form paraphyletic branches within the *Anopheles* and *Cellia* subgenera.

The analysis of the molecular variance of *An. aconitus-cox1* among different localities is still incomplete. The majority of this species are found in Ratchaburi, and a minority in Phetchaburi. In addition, the *cox1* sequences of Phetchaburi samples are ambiguous and not of good quality for molecular analysis. This study has limitations in collecting representative populations of each mosquito species in each province. The small sample size may not be exactly representative of the population's genetic structure. Further studies should be carried out to increase the sample sizes and sampling coverage to provide more accurate results on species composition, genetic diversity, population growth and dynamics of mosquito fauna in Thailand.

CHAPTER 6

CONCLUSIONS AND SUGGESTIONS

The parasite burdens obtained from goats during a particular follow-up period were extremely low and dramatically reduced over two weeks, but they could still be quantified using qPCR. Except for diarrhea and a slight fever in a few days, the goat infected with *P. caprae* showed no specific clinical signs. Due to farm distances and logistics issues, we have only followed up on one out of six infected goats. Furthermore, the DNA of *P. caprae* was found in *An. subpictus* and *An. aconitus* mosquitoes in this study. As an invertebrate host, these mosquito species may contribute to goat malaria transmission. However, more mosquitoes of the species *An. subpictus* and *An. aconitus* should be continuously collected for salivary gland dissection and sporozoite detection under light microscope in order to draw a conclusion about the malaria vector. In addition, nine different mosquito species were found in goat farms. Despite their geographical distance, there was evidence of gene flow in mosquito populations from one northern and three western provinces. Furthermore, multiple nuclear gene analyzes of *P. caprae* produced congruent tree topology, indicating that in addition to mitochondrial and apicoplast genes, nuclear genes are reliable and robust markers for phylogenetic inference.

More malaria-infected goats should be monitored and followed in the future to gain an overall assessment of the malaria infection dynamic of malaria, as well as the biology of the parasite in mosquitoes and the goat hosts, to gain more advanced knowledge about the goat malaria parasite *P. caprae*. Alternatively, experimental inoculation of *P. caprae* in splenectomized disease-free naive goats may increase the

probability of malaria infection and parasite burden. As a result, whole genome sequencing of goat malaria parasites would be feasible using this method.

Advantages of The Study

1. This study provided preliminary findings on the infection dynamics of goat malaria parasites. This may give a basis for further investigation in the future.
2. For the first time, the current study reveals that *P. caprae* nuclear genes are shared by the *Plasmodium* genus. This may improve our understanding of the origin and evolutionary history of *Plasmodium* parasites together with mitochondrial genes.
3. This study advances our understanding of mosquito composition, population genetic structure, gene flow, and probable mosquito vectors for goat malaria transmission.

REFERENCES

- Alberts B, Johnson A, Wilson J, Lewis J, Hunt T, Roberts K, Raff M and Walter P. 2008. Molecular Biology of the Cell. In: Garland Science.
- Amills M, Capote J and Tosser-Klopp G. 2017. Goat domestication and breeding: a jigsaw of historical, biological and molecular data with missing pieces. *Anim Genet.* 48(6): 631-644.
- Anothaisinthawee S, Nomura K, Oishi T and Amano T. 2010. Goat genetic resources and breeding strategies in Thailand. *J Anim Genet.* 38(1): 41-48.
- Ariey F, Gay F and Ménard R. 2020. Malaria control and elimination. In: Springer New York.
- Asada M, Takeda M, Tomas WM, Pellegrin A, de Oliveira CHS, Barbosa JD, da Silveira JAG, Braga ÉM and Kaneko O. 2018. Close relationship of *Plasmodium* sequences detected from South American pampas deer (*Ozotoceros bezoarticus*) to *Plasmodium* spp. in North American white-tailed deer. *International journal for parasitology. Parasites and wildlife* 7(1): 44-47.
- Aung A, Kaewlamun W, Narapakdeesakul D, Poofery J and Kaewthamasorn M. 2022. Molecular detection and characterization of tick-borne parasites in goats and ticks from Thailand. *Ticks Tick Borne Dis.* 13(3): 101938.
- Beebe NW. 2018. DNA barcoding mosquitoes: advice for potential prospectors. *Parasitology.* 145(5): 622-633.
- Beebe NW and Saul A. 1995. Discrimination of all members of the *Anopheles punctulatus* complex by polymerase chain reaction-restriction fragment length polymorphism analysis. *Am J Trop Med Hyg.* 53(5): 478-481.
- Borner J, Pick C, Thiede J, Kolawole OM, Kingsley MT, Schulze J, Cottontail VM, Wellinghausen N, Schmidt-Chanasit J, Bruchhaus I and Burmester T. 2016. Phylogeny of haemosporidian blood parasites revealed by a multi-gene approach. *Mol Phylogen Evol.* 94(2016): 221-231.
- Boundenga L, Makanga B, Ollomo B, Gilabert A, Rougeron V, Mve-Ondo B, Arnathau C, Durand P, Moukodoum ND, Okouga A-P, Delicat-Loembet L, Yacka-Mouele L,

- Rahola N, Leroy E, Ba CT, Renaud F, Prugnolle F and Paupy C. 2016. Haemosporidian parasites of antelopes and other vertebrates from Gabon, Central Africa. *Plos One*. 11(2): e0148958.
- Bruce D, Harvey D, Hamerton AE and Bruce L. 1913. *Plasmodium cephalophi*, sp. nov. *Proc Royal Soc B*. 87(592): 45-47.
- Bunmee K, Thaenkham U, Saralamba N, Ponlawat A, Zhong D, Cui L, Sattabongkot J and Sriwichai P. 2021. Population genetic structure of the malaria vector *Anopheles minimus* in Thailand based on mitochondrial DNA markers. *Parasit Vectors*. 14(1): 496.
- Caraballo H and King K. 2014. Emergency department management of mosquito-borne illness: malaria, dengue, and West Nile virus. *Emerg Med Pract*. 16 (5): 1-23.
- CDC. 2019. "Subject: Centers for Disease Control and Prevention " (online). Available: <https://www.cdc.gov/malaria/about/disease.html>
- Chan A, Chiang LP, Hapuarachchi HC, Tan CH, Pang SC, Lee R, Lee KS, Ng LC and Lam-Phua SG. 2014. DNA barcoding: complementing morphological identification of mosquito species in Singapore. *Parasit Vectors*. 7: 569.
- Chookaew S, Atta Y, Thongkhao K, Kaewmanee P, Ninsaeng U, Jidkaew T and Sranglean P. 2020. *Anopheles* species composition in malaria high-risk areas in Ranong Province. *Dis Control J*. 46(4): 483-493.
- Daniel WW. 1999. *Biostatistics: A foundation for analysis in the health sciences*. 7th Edition ed. In: John Wiley & Sons, Inc., Hoboken.
- de Mello F and Paes S. 1923. Sur une plasmodiae du sang des chèvres. *C.r. séanc. Soc. Biol*. 88: 829-830.
- Dhanda JS, Taylor DG, Murray PJ, Pegg RB and Shand PJ. 2003. Goat meat production: Present status and future possibilities. *Asian-Australasian Journal of Animal Sciences*. 16(12): 1842-1852.
- Escalante AA and Ayala FJ. 1994. Phylogeny of the malarial genus *Plasmodium*, derived from *rRNA* gene sequences. *Proceedings of the National Academy of Sciences of the United States of America*. 91(24): 11373-11377.
- Escalante AA, Freeland DE, Collins WE and Lal AA. 1998. The evolution of primate malaria parasites based on the gene encoding *cytochrome b* from the linear

- mitochondrial genome. Proceedings of the National Academy of Sciences of the United States of America. 95(14): 8124-8129.
- Excoffier L, Laval G and Schneider S. 2005. Arlequin ver. 3.0: An integrated software package for population genetics data analysis. *Evolutionary Bioinformatics*. 1: 47-50.
- Fang J. 2010. Ecology: A world without mosquitoes. *Nature*. 466(7305): 432-434.
- FAO. 2021. "Subject: Food and Agriculture Organization of the United Nations" (online). Available: <http://www.fao.org/faostat/en/#data/OCL>.
- Feistkorn G, Ritter P and Jessen C. 1983. Cardiovascular responses to thermal stress in conscious goats. *J Therm Biol*. 8: 241-246.
- Galen SC, Borner J, Martinsen ES, Schaer J, Austin CC, West CJ and Perkins SL. 2018. The polyphyly of *Plasmodium*: comprehensive phylogenetic analyses of the malaria parasites (order Haemosporida) reveal widespread taxonomic conflict. *Royal Soc Open Sci*. 5(5): 171780.
- Garnham PC. 2007. A malaria parasite of the hippopotamus. *J Eukaryot Microbiol*. 5(2): 149-151.
- Garnham PC and Edeson JF. 1962. Two new malaria parasites of the Malayan mousedeer. *Rivista di Malariologica*. 41: 1-8.
- Garnham PC and Kuttler KL. 1980. A malaria parasite of the white-tailed deer (*Odocoileus virginianus*) and its relation with known species of *Plasmodium* in other ungulates. *Proc R Soc Lond, Ser B: Biol Sci*. 206(1165): 395-402.
- Garnham PCC. 1966. Malaria parasites and other Haemosporidia. In: Blackwell Scientific Publications, Oxford. 494-498 pp.
- Govindaraju DR. 2009. Estimates of gene flow in forest trees. *Biol J Linn Soc*. 37(4): 345-357.
- Grant DM, Brodnicke OB, Evankow AM, Ferreira AO, Fontes JT, Hansen AK, Jensen MR, Kalaycı TE, Leeper A, Patil SK, Prati S, Reunamo A, Roberts AJ, Shigdel R, Tyukosova V, Bendiksby M, Blaallid R, Costa FO, Hollingsworth PM, Stur E and Ekrem T. 2021. The future of DNA barcoding: Reflections from early career researchers. *Diversity*. 13(7): 313.

- Guggisberg AM, Sayler KA, Wisely SM and Odom John AR. 2018. Natural history of *Plasmodium odocoilei* malaria infection in farmed white-tailed deer. mSphere. 3(2).
- Gyawali N, Taylor-Robinson AW, Bradbury RS, Huggins DW, Hugo LE, Lowry K and Askov JG. 2019. Identification of the source of blood meals in mosquitoes collected from north-eastern Australia. Parasit Vectors. 12(1): 198.
- Hagner SC, Misof B, Maier WA and Kampen H. 2007. Bayesian analysis of new and old malaria parasite DNA sequence data demonstrates the need for more phylogenetic signal to clarify the descent of *Plasmodium falciparum*. Parasitol Res. 101(3): 493-503.
- Hakimi H, Sarani A, Takeda M, Kaneko O and Asada M. 2019. Epidemiology, risk factors, and co-infection of vector-borne pathogens in goats from Sistan and Baluchestan province, Iran. Plos One. 14(6): e0218609.
- Hall TA. 1999. BioEdit: A user-friendly biological sequence alignment editor and analysis program for Windows 95/98/NT. Nucleic Acids Symp Ser. 41: 95-98.
- Harbach RE. 2011. Genus Anopheles Meigen, 1818. Mosquito taxonomic. In: Inventory City.
- Hebert PD, Cywinska A, Ball SL and deWaard JR. 2003. Biological identifications through DNA barcodes. Proc R Soc Lond, Ser B: Biol Sci. 270(1512): 313-321.
- Holland BR, Penny D and Hendy MD. 2003. Outgroup misplacement and phylogenetic inaccuracy under a molecular clock-a simulation study. Syst Biol. 52(2): 229-238.
- Hudson RR, Slatkin M and Maddison WP. 1992. Estimation of levels of gene flow from DNA sequence data. Genetics. 132(2): 583-589.
- Huelsenbeck JP and Ronquist F. 2001. MRBAYES: Bayesian inference of phylogenetic trees. Bioinformatics. 17(8): 754-755.
- Junsiri W, Watthanadirek A, Poolsawat N, Kaewmongkol S, Jittapalapong S, Chawengkirttikul R and Anuracpreeda P. 2020. Molecular detection and genetic diversity of *Anaplasma marginale* based on the major surface protein genes in Thailand. Acta Trop. 205: 105338.
- Kaewthamasorn M, Takeda M, Saiwichai T, Gitaka JN, Tiawsirisup S, Imasato Y, Mossaad E, Sarani A, Kaewlamun W, Channumsin M, Chaiworakul S, Katepongpun W,

- Teeveerapunya S, Panthong J, Mureithi DK, Bawm S, Htun LL, Win MM, Ismail AA, Ibrahim AM, Suganuma K, Hakimi H, Nakao R, Katakura K, Asada M and Kaneko O. 2018. Genetic homogeneity of goat malaria parasites in Asia and Africa suggests their expansion with domestic goat host. *Sci Rep.* 8(1): 5827.
- Kage S, Mamatha GS, Lakkundi JN, Shivashankar BP and D'Souza PE. 2019. Detection of incidence of *Babesia* spp. in sheep and goats by parasitological diagnostic techniques. *J Parasit Dis.* 43(3): 452-457.
- Kent RJ and Norris DE. 2005. Identification of mammalian blood meals in mosquitoes by a multiplexed polymerase chain reaction targeting *cytochrome b*. *Am J Trop Med Hyg.* 73(2): 336-342.
- Khamseekhiew B and Pompei O. 2016. Goats production system in upper southern Thailand. *Proc Int Seminar Livestock Prod Vet Tech.* P 336-340.
- Kumar S, Stecher G, Li M, Knyaz C and Tamura K. 2018. MEGA X: Molecular evolutionary genetics analysis across computing platforms. *Mol Biol Evol.* 35(6): 1547-1549.
- Lanfear R, Calcott B, Ho SY and Guindon S. 2012. Partitionfinder: combined selection of partitioning schemes and substitution models for phylogenetic analyses. *Mol Biol Evol.* 29(6): 1695-1701.
- Leigh J and Bryant D. 2015. Popart: full-feature software for haplotype network construction. *Methods Ecol Evol.* 6: 1110-1116.
- Madeira S, Duarte A, Boinas F and Costa Osório H. 2021. A DNA barcode reference library of Portuguese mosquitoes. *Zoonoses Public Health.* 68(8): 926-936.
- Makanga B, Yangari P, Rahola N, Rougeron V, Elguero E, Boundenga L, Moukodoum ND, Okouga AP, Arnathau C, Durand P, Willaume E, Ayala D, Fontenille D, Ayala FJ, Renaud F, Ollomo B, Prugnolle F and Paupy C. 2016. Ape malaria transmission and potential for ape-to-human transfers in Africa. *Proceedings of the National Academy of Sciences of the United States of America.* 113(19): 5329-5334.
- Manin BO, Drakeley CJ and Chua TH. 2018. Mitochondrial variation in subpopulations of *Anopheles balabacensis* Baisas in Sabah, Malaysia (Diptera: Culicidae). *PLOS ONE.* 13(8): e0202905.
- Maquart PO, Fontenille D, Rahola N, Yean S and Boyer S. 2021. Checklist of the mosquito fauna (Diptera, Culicidae) of Cambodia. *Parasite.* 28: 60.

- Martinsen E, McInerney N, Brightman H, Ferebee K, Walsh T, McShea W, Forrester TD, Ware LH, Joyner P, Perkins S, Latch EK, Yabsley M, Schall J and Fleischer R. 2016. Hidden in plain sight: Cryptic and endemic malaria parasites in North American white-tailed deer (*Odocoileus virginianus*). *Sci Adv.* 2(2): e1501486.
- Martinsen ES, Perkins SL and Schall JJ. 2008. A three-genome phylogeny of malaria parasites (*Plasmodium* and closely related genera): evolution of life-history traits and host switches. *Mol Phylogen Evol.* 47(1): 261-273.
- McKenzie FE, Jeffery GM and Collins WE. 2002. *Plasmodium vivax* blood-stage dynamics. *J Parasitol.* 88(3): 521-535.
- Merrick CJ. 2021. Hypnozoites in *Plasmodium*: Do parasites parallel plants? *Trends Parasitol.* 37(4): 273-282.
- Minh BQ, Schmidt HA, Chernomor O, Schrempf D, Woodhams MD, von Haeseler A and Lanfear R. 2020. IQ-TREE 2: New models and efficient methods for phylogenetic inference in the genomic era. *Mol Biol Evol.* 37(5): 1530-1534.
- Naderi A, Nayebzadeh H and Gholami S. 2017. Detection of *Babesia* infection among human, goats and sheep using microscopic and molecular methods in the city of Kuhdasht in Lorestan Province, West of Iran. *J Parasit Dis.* 41(3): 837-842.
- Nakavisut S and Anothaisinthawee S. 2014. Dairy goat production in Thailand. The 2nd Asian-Australasian Dairy Goat Conference. P.
- Ney PA. 2011. Normal and disordered reticulocyte maturation. *Current Opinion in Hematology.* 18(3): 152-157.
- Nguyen AHL, Tiawsirisup S and Kaewthamasom M. 2020. Low level of genetic diversity and high occurrence of vector-borne protozoa in water buffaloes in Thailand based on *18S ribosomal RNA* and mitochondrial *cytochrome b* genes. *Infect Genet Evol.* 82: 104304.
- Nugraheni YR, Amuphappasert A, Nguyen TT, Narapakdeesakul D, Nguyen HLA, Poofery J, Kaneko O, Asada M and Kaewthamasom M. 2022. Myzorhynchus series of Anopheles mosquitoes as potential vectors of *Plasmodium bubalis* in Thailand. *Sci Rep.* 12(1): 5747.
- Outlaw DC and Ricklefs RE. 2010. Comparative gene evolution in haemosporidian (apicomplexa) parasites of birds and mammals. *Mol Biol Evol.* 27(3): 537-542.

- Outlaw DC and Ricklefs RE. 2011. Rerooting the evolutionary tree of malaria parasites. *Proceedings of the National Academy of Sciences of the United States of America*. 108(32): 13183-13187.
- Perkins SL. 2014. Malaria's many mates: past, present, and future of the systematics of the order Haemosporida. *J Parasitol*. 100(1): 11-25.
- Perkins SL and Schaer J. 2016. A modern menagerie of mammalian malaria. *Trends Parasitol*. 32(10): 772-782.
- Perkins SL and Schall JJ. 2002. A molecular phylogeny of malarial parasites recovered from *cytochrome b* gene sequences. *J Parasitol*. 88(5): 972-978.
- Quartermain AR and Broadbent MP. 1974. Some patterns of response to climate by the Zambian goat. *East Afr Agric For J*. 40(1): 115-124.
- Rao MAN. 1938. A note on *Plasmodium bubalis* Sheather, 1919. *Indian J Vet Sci Anim Husbandry*. 8: 387-389.
- Rasoanoro M, Goodman SM, Randrianarivelosia M, Rakotondratsimba M, Dellagi K, Tortosa P and Ramasindrazana B. 2021. Diversity, distribution, and drivers of *Polychromophilus* infection in Malagasy bats. *Malar J*. 20(1): 157.
- Rattanarithikul R, Harrison BA, Harbach RE, Panthusiri P, Coleman RE and Panthusiri P. 2006. Illustrated keys to the mosquitoes of Thailand. IV. *Anopheles*. *Southeast Asian J Trop Med Public Health*. 37: 1-128.
- Robertshaw D. 1968. The pattern and control of sweating in the sheep and the goat. *J Physiol*. 198(3): 531-539.
- Rozas J, Ferrer-Mata A, Sánchez-DelBarrio JC, Guirao-Rico S, Librado P, Ramos-Onsins SE and Sánchez-Gracia A. 2017. DnaSP 6: DNA sequence polymorphism analysis of large data sets. *Molecular Biology and Evolution* 34(12): 3299-3302.
- Sarma DK, Prakash A, O'Loughlin SM, Bhattacharyya DR, Mohapatra PK, Bhattacharjee K, Das K, Singh S, Sarma NP, Ahmed GU, Walton C and Mahanta J. 2012. Genetic population structure of the malaria vector *Anopheles baimaii* in north-east India using mitochondrial DNA. *Malar J*. 11(1): 76.
- Shastri SR, Shastri UV and Deshapande PD. 1985. Haematozoan infections in buffalo, *Bubalus bubalis* in Maharashtra. *Indian J Parasitol*. 9: 183-185.

- Sheather AL. 1919. A malarial parasite in the blood of a buffalo. *J Comp Pathol.* 32(4): 223-229.
- Shinde P, Maske DK, Samradhni D, Kolte S and Banubakode S. 2005. Some observations on bovine malaria associated with developing phases of *Plasmodium bubalis* in Vidarbha region of Maharashtra. *J Vet Parasitol.* 19: 61-62.
- Sinka ME, Bangs MJ, Manguin S, Rubio-Palis Y, Chareonviriyaphap T, Coetzee M, Mbogo CM, Hemingway J, Patil AP and Temperley WH. 2012. A global map of dominant malaria vectors. *Parasit Vectors.* 5(69): 1-11.
- Snounou G, Viriyakosol S, Xin Ping Z, Jarra W, Pinheiro L, do Rosario VE, Thaithong S and Brown KN. 1993. High sensitivity of detection of human malaria parasites by the use of nested polymerase chain reaction. *Mol Biochem Parasitol.* 61(2): 315-320.
- Tainchum K, Ritthison W, Chuaycharoensuk T, Bangs MJ, Manguin S and Chareonviriyaphap T. 2014. Diversity of *Anopheles* species and trophic behavior of putative malaria vectors in two malaria endemic areas of northwestern Thailand. *J Vector Ecol.* 39(2): 424-436.
- Tajima F. 1989. Statistical method for testing the neutral mutation hypothesis by DNA polymorphism. *Genetics.* 123(3): 585-595.
- Templeton TJ, Asada M, Jiratanh M, Ishikawa SA, Tiawsirisup S, Sivakumar T, Namangala B, Takeda M, Mohkaew K, Ngamjituea S, Inoue N, Sugimoto C, Inagaki Y, Suzuki Y, Yokoyama N, Kaewthamasorn M and Kaneko O. 2016a. Ungulate malaria parasites. *Sci Rep.* 6(1): 23230.
- Templeton TJ, Martinsen E, Kaewthamasorn M and Kaneko O. 2016b. The rediscovery of malaria parasites of ungulates. *Parasitology.* 143(12): 1501-1508.
- Tu HLC, Nugraheni YR, Tiawsirisup S, Saiwichai T, Thiptara A and Kaewthamasorn M. 2021. Development of a novel multiplex PCR assay for the detection and differentiation of *Plasmodium caprae* from *Theileria luwenshuni* and *Babesia* spp. in goats. *Acta Trop.* 220: 105957.
- Vaidya AB and Mather MW. 2005. A post-genomic view of the mitochondrion in malaria parasites. *Curr Top Microbiol Immunol.* 295: 233-250.

- van den Berghe L. 1937. *Plasmodium limnotragi* n. sp., d'une antilope *Limnotragus spekei*. Bulletin de la Société de Pathologie Exotique et de ses Filiales. 30: 272-274.
- Vantaux A, Riehle MM, Piv E, Farley EJ, Chy S, Kim S, Corbett AG, Fehrman RL, Pepey A, Eglmeier K, Lek D, Siv S, Mueller I, Vernick KD and Witkowski B. 2021. *Anopheles* ecology, genetics and malaria transmission in northern Cambodia. Sci Rep. 11(1): 6458.
- Ventim R, Ramos JA, Osório H, Lopes RJ, Pérez-Tris J and Mendes L. 2012. Avian malaria infections in western European mosquitoes. Parasitol Res. 111(2): 637-645.
- Venugopal K, Hentzschel F, Valkiūnas G and Marti M. 2020. *Plasmodium* asexual growth and sexual development in the haematopoietic niche of the host. Nat Rev Microbiol. 18(3): 177-189.
- Walton C, Handley JM, Tun-Lin† W, Collins FH, Harbach RE, Baimai V and Butlin RK. 2000. Population structure and population history of *Anopheles dirus* mosquitoes in Southeast Asia. Mol Biol Evol. 17(6): 962-974.
- Wang G, Li C, Zheng W, Song F, Guo X, Wu Z, Luo P, Yang Y, He L and Zhao T. 2017. An evaluation of the suitability of *COI* and *COII* gene variation for reconstructing the phylogeny of, and identifying cryptic species in, anopheline mosquitoes (Diptera Culicidae). Mitochondrial DNA. Part A, DNA Mapping, Sequencing and Analysis. 28(5): 769-777.
- Waters AP, Higgins DG and McCutchan TF. 1991. *Plasmodium falciparum* appears to have arisen as a result of lateral transfer between avian and human hosts. The Proceedings of the National Academy of Sciences. 88(8): 3140-3144.
- Weber JL. 1987. Analysis of sequences from the extremely A + T-rich genome of *Plasmodium falciparum*. Gene. 52(1): 103-109.
- Wharton RH, Eyles DE, Warren M, Moorhouse DE and Sandosham AA. 1963. Investigations leading to the identification of members of the *Anopheles umbrosus* group as the probable vectors of mouse deer malaria. Bull WHO. 29(3): 357-374.

WHO. 2015. "Subject: Microscopy for the detection, identification and quantification of malaria parasites on stained thick and thin blood films in research settings" (online). Available: <https://apps.who.int/iris/handle/10665/163782>.

Williams J and Pinto J. 2012. Training Manual on Malaria Entomology. In.

Wright S. 1978. Evolution and the genetics of populations. Vol. Vol. 4. In: Variability within and among Natural Populations, University of Chicago Press, Chicago, IL, USA.

Zhong D, Hemming-Schroeder E, Wang X, Kibret S, Zhou G, Atieli H, Lee M-C, Afrane YA, Githeko AK and Yan G. 2020. Extensive new *Anopheles* cryptic species involved in human malaria transmission in western Kenya. Sci Rep. 10(1): 16139.



APPENDIX

Supplementary data 1. Fisher's exact test for the association between rainy and dry seasons with the malaria infection rate

Case Processing Summary

	Cases					
	Valid		Missing		Total	
	N	Percent	N	Percent	N	Percent
Season * Result	423	100.0%	0	0.0%	423	100.0%

Season * Result Crosstabulation

		Result		Total
		Negative	Positive	
Season	Rainy	221	5	226
	Dry	196	1	197
Total		417	6	423

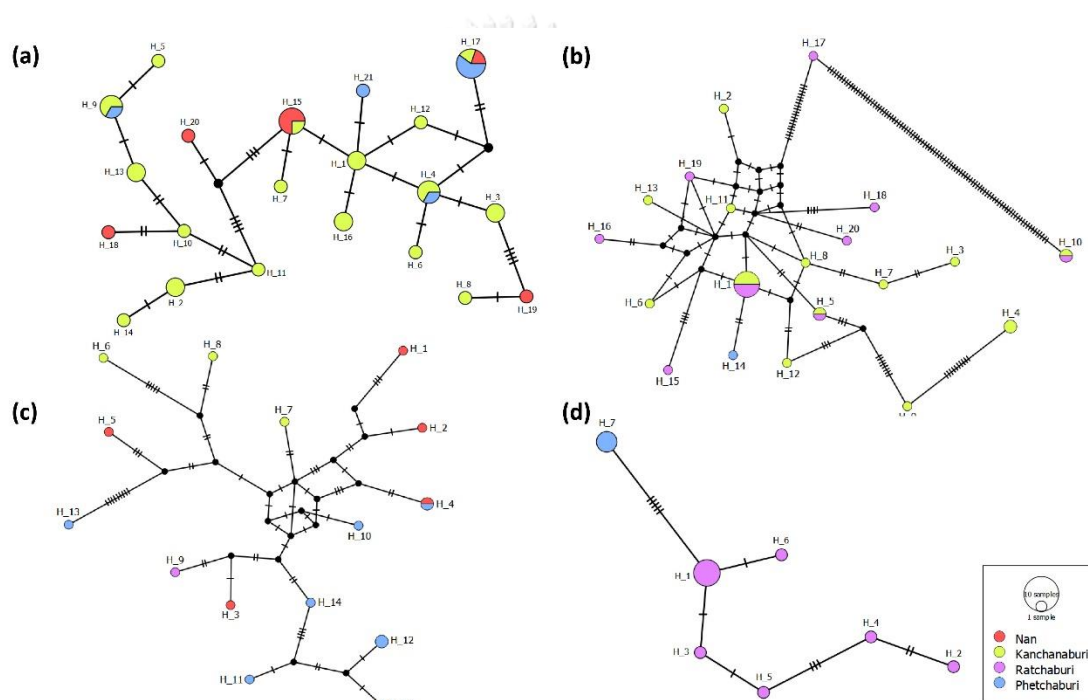
Chi-Square Tests

	Value	df	Asymp. Sig. (2-sided)	Exact Sig. (2-sided)	Exact Sig. (1-sided)
Pearson Chi-Square	2.188 ^a	1	.139		
Continuity Correction ^b	1.138	1	.286		
Likelihood Ratio	2.421	1	.120		
Fisher's Exact Test				.222	.143
Linear-by-Linear Association	2.182	1	.140		
N of Valid Cases	423				

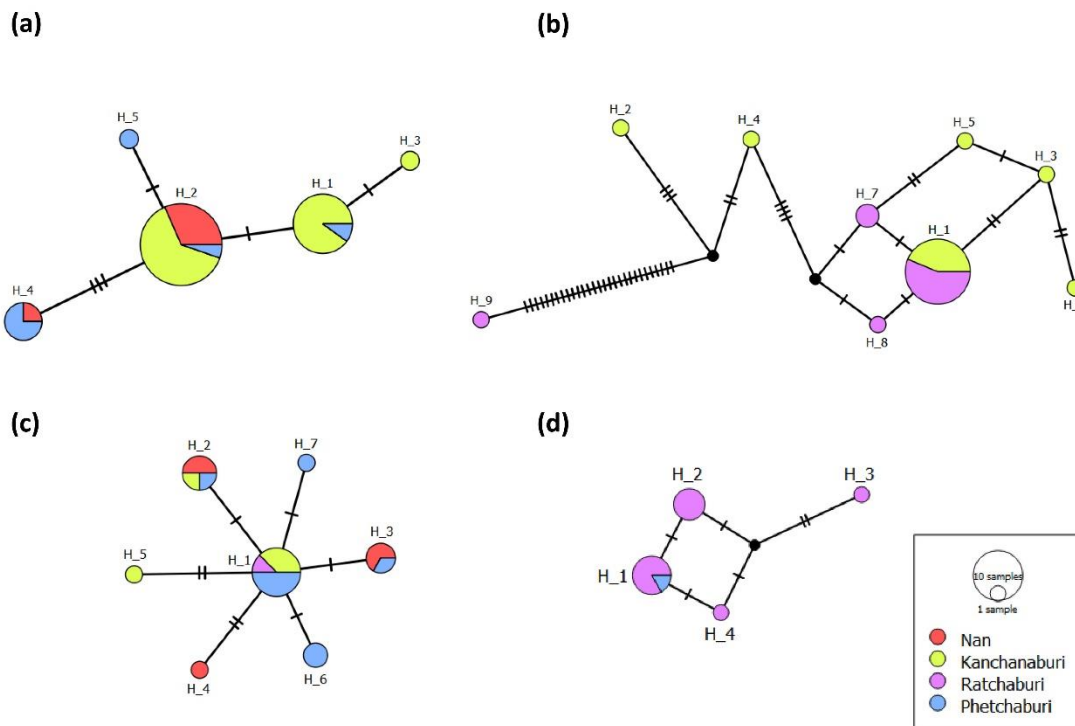
a. 2 cells (50.0%) have an expected count of less than 5. The minimum expected count is 2.79.

b. Computed only for a 2 x 2 table

Supplementary data 2. Median-joining haplotype network of the *cox1* sequences of the dominant mosquito species collected from four provinces in Thailand: *An. peditaeniatus* (a), *An. subpictus* (b), *An. vagus* (c), and *An. aconitus* (d).



Supplementary data 3. Median-joining haplotype network of the *cox2* sequences of the dominant mosquito species collected from four provinces of Thailand: *An. peditaeniatus* (a), *An. subpictus* (b), *An. vagus* (c), and *An. aconitus* (d).



VITA

NAME Hoang Lan Anh Nguyen

DATE OF BIRTH 04 March 1993

PLACE OF BIRTH Ho Chi Minh City, Vietnam

INSTITUTIONS ATTENDED + Doctor of Veterinary Medicine, Nong Lam University, Vietnam.
+ Master of Veterinary Science and Technology, Chulalongkorn University, Thailand.

PUBLICATION

1. Nguyen, A.H.L., Nugraheni, Y.R., Nguyen, T.T., Aung, A., Narapakdeesakul, D., Kaewlamun, W., Asada, M., & Kaewthamasorn, M. Molecular characterization of anopheline mosquitoes from the goat malaria-endemic areas of Thailand. *Med. Vet. Entomol.* Submitted – 27-06-2022, Revised – 26-09-2022.
2. Nugraheni, Y.R., Arnuphapprasert, A., Nguyen, T.T., Narapakdeesakul, D., Nguyen, H.L.A., Poofery, J., Kaneko, O., Asada, M., & Kaewthamasorn, M. Myzorrhynchus series of Anopheles mosquitoes as potential vectors of Plasmodium bubalis in Thailand. *Sci Rep* 12, 5747 (2022). <https://doi.org/10.1038/s41598-022-09686-9>
3. Nguyen, A.H.L., Tiawsirisup, S., Kaewthamasorn, M. Molecular detection and genetic characterization of Anaplasma marginale and Anaplasma platys-like (Rickettsiales: Anaplasmataceae) in water buffalo from eight provinces of Thailand (2020) *BMC Veterinary Research*, 16 (1), art. no. 380.

4. Nguyen, A.H.L., Tiawsirisup, S., Kaewthamasom, M. Low level of genetic diversity and high occurrence of vector-borne protozoa in water buffaloes in Thailand based on 18S ribosomal RNA and mitochondrial cytochrome b genes (2020) *Infection, Genetics and Evolution*, 82, art. no. 104304.

